



NTNU – Trondheim
Norwegian University of
Science and Technology

Robustness of support structures for offshore wind turbines

Dynamics, fatigue damage and extreme loads
with a damaged foundation

Konrad Robert Hryniewicki

Coastal and Marine Civil Engineering

Submission date: June 2015

Supervisor: Michael Muskulus, BAT

Co-supervisor: Sebastian Schafhirt, BAT

Norwegian University of Science and Technology
Department of Civil and Transport Engineering

Konrad Hryniewicki

Robustness of support structures for offshore wind turbines

Master of Science in Marine Civil Engineering

Submission date : June 2015

Supervisor: Prof. Dr. Michael Muskulus

Assistant Professor D. Sc. Waldemar Magda

Co-supervisor : Sebastian Schafhirt

Norwegian University of Science and Technology

Faculty of Engineering Science and Technology

Department of Civil and Transport Engineering



NTNU – Trondheim
Norwegian University of
Science and Technology



Division: Marine Civil Engineering

Postal address:

Høgskoleringen 7A

7491 Trondheim

Phone: 73 59 46 40

Telefax: 73 59 70 21

Master thesis TBA4920

Spring 2015

Student: *Konrad Hryniewicki*

working title:

“Robustness of support structures for offshore wind turbines”

Dynamics, fatigue damage and extreme loads with a damaged foundation

Background:

Support structures for offshore wind turbines are expensive, and current designs are conservative, with a certain potential for cost reduction. It is important to explore different ways of reducing the cost through better design. The design of support structures is typically driven by fatigue damage, since the turbine rotor is a significant source of vibrations. A better understanding of fatigue damage can lead to cheaper designs.

Objective:

The topic of the thesis is to investigate in detail what happens when a modern jacket support structure is damaged or fails in a structural member. In particular it is of interest how the fatigue damage accumulation in the remaining members is affected, but also the effect on ultimate loads should be investigated. Although current standards do not allow such a situation, it could be the case that the loss of one structural member is not critical for the survival of the structure, even under full

operational loads from the turbine. Alternatively, the turbine could be down-regulated for the (often significant) time needed for repair, leading to less loads (but also less electricity production).

Approach:

Time-domain simulations of the complete wind turbine (including support structure and piled foundations) in special analysis software: FEDEM Windpower, a flexible multibody / finite-elementsolver will be used. A standard turbine (NREL 5MW) and support structure model (OC4 jacket) will be analyzed, if time permits a commercial design (OWEC Quattropod Jacket) can be looked at, too. Damage will be simulated by loss of stiffness (reduction of Young's modulus) and/or splitting of the member in question into two unconnected beams.

Work plan

-Literature study: load simulations for offshore wind turbines, IEC 61400-3 and DNV OS-J101standard [2 weeks]

-Familiarization with FEDEM Windpower simulation software and the simulation models [3 weeks]

-Investigating dynamics, fatigue and extreme loads with a damaged member [6 weeks]

-Implementation of a down-regulated turbine by adjusting the controller constants and investigation of fatigue loads [6 weeks]

-Writing of the thesis [3 weeks]

Supervisor(s):

Sebastian Schafhirt (sebastian.schafhirt@ntnu.no)

Prof. Dr. Michael Muskulus (michael.muskulus@ntnu.no)

Professor in charge:

Michael Muskulus

Preface

This thesis is a result of the well spent spring semester at the Norwegian University of Science and Technology in Trondheim, Norway. The topic of the thesis has been proposed by Professor Michael Muskulus and the research is a part of my Master of Science degree in Marine Civil Engineering.

I would like to thank Professor Michael Muskulus for his introduction into the interesting but yet not thoroughly explored discipline of marine civil engineering i.e. the fatigue in damaged jacket support structure and for his guidance to proper conclusions.

My great gratitude goes to my co-supervisor Sebastian Schafhirt for his time and patience in answering my infinite number of questions. I would also like to thank him for performing simulations in Fedem Windpower software at the departmental workstations.

Special thanks to my whole family for their understanding and limitless help.

I want to dedicate this thesis to my parents to express my gratitude for their support from heaven in the moments of my weakness.

Abstract

This master thesis considers the strength analysis of the offshore wind turbine's jacket support structure with one structural member damaged or weakened, not capable of transferring the loads. A wind turbine and its substructure are usually exposed to environmental loadings (i.e. wind, waves) and described by computer simulations. FEDEM Windpower environment is used to analyse the model of the offshore wind turbine.

Firstly, the thesis is to indicate the areas of the largest fatigue damage accumulation in the remaining structure members and to estimate their ultimate strength. The fatigue evaluation of the steel structure elements is based on the Palmgren-Miner linear damage hypothesis. The steel brace member damage has been modelled by reducing the elastic modulus (Young's modulus) or inserting a free-joint mechanism in the middle of the element. Then the results of structure strength calculations before and after damage are collected and compared.

Secondly, the analysis assumes a reduction in the fatigue loads applied to the support structure by changing the wind turbine control system. These changes are aimed at decreasing mainly the rotor revolution frequency and generator torque at the same time. The adjustment is achieved by varying a turbine blade pitch. The controller has also been modified to avoid continuous turbine operation at frequencies close to resonance.

Abstrakt

Masteroppgaven omhandler styrkeanalyse av offshore vindturbin jakke understell med et konstruksjonselement som er skadet eller svekket og ikke i stand til å overføre lasten. Vindmøller og dets understell er utsatt for miljøbelastninger, (dvs. vind, bølger) illustrert og beskrevet av datasimuleringer. FEDEM Windpower miljø brukes til å analysere modellen av OWT.

For det første går oppgaven ut på å indikere de områdene med de største utmattingsskadene og opphopning i de resterende konstruksjonselementene og å anslå deres ultimate styrke. Tretthetsvaluering av stålstrukturelementer er basert på Palmgren-Miners lineære skade hypotese. Stål støtteorgansskade har blitt modellert ved å redusere elastisitetsmodulen (Youngs modulus) og innføre en free-joint mekanisme i midten av elementet. Derneft har resultatene av styrkeberegninger av strukturen før og etter skaden blitt samlet inn og sammenlignet.

I tillegg vil analysen gå ut ifra reduksjon av utmatteleseslast påført støttestrukturen ved å endre på kontrollsystemet til vindturbinen. Disse forandringen har som mål å redusere i hovedsak rotorens omdreiningfrekvens og generatormoment samtidig. Dette oppnås ved å endre vinkelen på turbinbladene. Kontrolleren har også blitt endret for å unngå kontinuerlig turbindrift på frekvenser nær resonans.

TABLE OF CONTENT

1. INTRODUCTION	1
1.1. General.....	1
1.2. Motivation	1
1.3. Scope of work.....	2
2. DESCRIPTION OF THE OFFSHORE WIND TURBINE	5
2.1. Model.....	5
2.1.1. Wind turbine	5
2.1.2. Jacket support structure [6].....	5
2.1.3. Transition piece	6
2.1.4. Tower	6
2.2. Location.....	7
2.3. Material properties.....	8
2.4. Environmental conditions	8
2.4.1. Sea water	8
2.4.2. Water depths.....	8
2.4.3. Water levels	8
2.4.4. Currents	9
2.4.5. Wave parameters.....	9
2.4.6. Wind parameters.....	9
3. BACKGROUND.....	11
3.1. Available wind power/ Wind turbine Energy Production	11
3.1.1. Betz's law and power coefficient	11
3.1.2. Tip speed ratio	13
3.2. Wind Turbine Terminology	14
3.3. Fatigue assessment	16
3.3.1. General	16
3.3.2. Loads time series	17
3.3.3. Sectional time series	18
3.3.4. Hot spot stress analysis	20
3.3.5. Rainflow counting.....	22
3.3.6. Damage Equivalent Load, DEL	23
3.3.7. Equivalent Fatigue Load, EFL	24
3.4. Ultimate strength analysis	25
3.4.1. General	25
3.5. Modal analysis.....	26
3.5.1. Free vibrations of discrete multi degrees of freedom system	27
3.6. Software implementation	30
3.6.1. FEDEM Windpower.....	30

3.6.2.	AeroDyn	31
3.6.3.	TurbSim.....	31
4.	FATIGUE, ULTIMATE STRENGTH AND DYNAMIC ANALYSIS	33
4.1.	Introduction.....	33
4.2.	Design Load Cases	33
4.3.	Model preparation.....	34
4.3.1.	Wind and wave input	34
4.3.2.	Wind speed distributions	36
4.3.3.	State structure cases.....	36
4.4.	Fatigue analysis	39
4.4.1.	Loading time series	40
4.4.2.	Sectional stress time series and HSS time series	40
4.4.3.	Rainflow counting method	40
4.4.4.	Equivalent fatigue load, EFL	41
4.5.	Ultimate strength analysis.	43
4.5.1.	General	43
4.5.2.	Load time series.....	43
4.5.3.	Yield check.....	44
4.6.	Modal analysis.....	56
4.6.1.	Allowable rotor frequency range.....	56
4.6.2.	Campbell diagram and Modal analysis.....	57
5.	RESULTS	63
5.1.	Fatigue analysis results	63
5.1.1.	General	63
5.1.2.	More detailed analysis.....	67
6.	ADJUSTING THE CONTROLLER CONSTANTS AND INVESTIGATION OF FATIGUE LOADS	71
6.1.	Introduction.....	71
6.2.	Control system	71
6.3.	Steady-state response of the offshore wind turbine	72
6.4.	Controller modification.....	74
6.4.1.	Rotor frequency analysis.....	74
6.4.2.	Rated wind speed.....	75

7. RESULTS SUMMARY	77
8. CONCLUSIONS	81
9. DISCUSSION.....	83
10. BIBLIOGRAPHY	85
11. APPENDICES.....	89
APPENDIX A.....	91
APPENDIX B.....	93
APPENDIX C	103
APPENDIX D	113
APPENDIX E.....	125
APPENDIX F	141

LIST OF FIGURES

Fig. 1.1. Jacket support structures 2

Fig. 2.1. Schematic dimensions of the Offshore Wind Turbine [6] 7

Fig. 2.2. Location of the offshore wind turbine K13 provided by Google Maps [19] 7

Fig. 2.3. Measured water levels at the OWT location [8] 9

Fig. 3.1. Speed and pressure variation in an ideal model of a wind turbine [35]..... 11

Fig. 3.2. Power coefficient C_p as a function of the axial interference factor a 13

Fig. 3.3. Power output curve for typical wind turbine 14

Fig. 3.4. Definition of Blade pitch angle and angle of attack [26] 16

Fig. 3.5. Example of load time series 18

Fig. 3.6. Hollow cylindrical cross section 19

Fig. 3.7. Model of jacket support structure with selected geometrical configurations of joints 20

Fig. 3.8. Geometrical definitions for tubular joints [18] 20

Fig. 3.9. Superposition of stresses [18] 22

Fig. 3.10. Stress time series 22

Fig. 3.11. Example of fatigue assessment according to Palmgren-Miner rule..... 24

Fig. 3.12. Diagram of fatigue assessment procedure. 25

Fig. 3.13. Fedem’s main window with an offshore wind turbine model in workspace area .. 30

Fig. 4.1. Wind speed distribution for the measurement location 36

Fig. 4.2. Jacket support structure model with marked damaged members 38

Fig. 4.3. Scheme of free-joint mechanism 39

Fig. 4.4. Load range histogram 41

Fig. 4.5. EFL diagrams in force and moment units 42

Fig. 4.6. Sample of sectional loads at the jacket cross-brace 44

Fig. 4.7. Allowable rotor frequency range [8]..... 57

Fig. 4.8. Campbell diagram of the OWT model [38]..... 58

Fig. 4.9. 1st and 2nd Tower Eigenmodes 59

Fig. 4.10. Displacement power spectral density for X-brace 103 60

Fig. 4.11. Summary of eigenfrequencies in different structure states – beam 86 61

Fig. 4.12. Summary of eigenfrequencies in different structure states – beam 45 61

Fig. 5.1. Representative view of fatigue damage distribution..... 64

Fig. 5.2. Diagrams presenting EFL ratio in cross-braces considering different cases 66

Fig. 5.3. Fatigue damage distribution showed in one side of jacket support structure by: 67

Fig. 5.4. Normalized summary of force and equivalent moment EFL ratio change 68

Fig. 5.5. Summary of Force and equivalent moment DEL ratios 69

Fig. 5.6. EFL_F stacked column chart consists of wind speed distribution 69

Fig. 6.1. Steady-state responses as a function of wind speed [4]	73
Fig. 6.2. Allowable ranges of rotor frequencies	75
Fig. 6.3. Allowable ranges of wind speed	75
Fig. 6.4. Modified steady-state responses as a function of wind speed	76
Appendixes	
Fig. A.1. Member properties	91

LIST OF TABLES

Table 2.1. Turbine parameters for NREL 5MW [8] 5

Table 2.2. Steel properties for whole structure[4]..... 8

Table 2.3. Properties of sea water [8]..... 8

Table 2.4. Properties of sea currents [8]..... 9

Table 4.1. Overview of design load cases 34

Table 4.2. Lumped environmental loads of the offshore wind turbine site 35

Table 4.3. Extreme conditions..... 35

Table 4.4. Weibull distribution parameters obtained from Matlab Curve Fitting Tool 36

Table 4.5. Overview of performed simulations..... 37

Table 4.6. Denotation of structural damage cases..... 39

Table 4.7. Tubular member properties 44

Table 4.8. Geometrical characteristics of sections 45

Table 4.9. Design load – DLC 1.3, Set 1 45

Table 4.10. Design load – DLC 1.3, Set 3 48

Table 4.11. Design load – DLC 6.1a, Set 1 51

Table 4.12. Design load – DLC 6.1a, Set 3..... 53

Table 5.1. Overview of extreme EFL and DEL ratio values..... 65

Table 7.7.1. Overview of extreme EFL and DEL ratio values..... 78

Appendixes

Table A. 1. Nodal coordinates..... 91

Table A.2. Property sets for jacket members 91

Table A.3. Members..... 92

1. INTRODUCTION

1.1. General

Scarcity of available land, environmental restrictions, prejudice local society and tax benefits induce significant interest in offshore wind turbine development.

According to report conducted by European Wind Energy Association [27] by the end of year 2014 there has been already built 2488 offshore wind turbines in 11 European countries, making a cumulative total of 8045,3 MW. Energy produced by offshore wind turbines in 2014 is enough to cover 1% of European Union's total consumption. Fast-growing market of wind farms impose a detailed study on the possibility of reducing the cost of manufacture, transport, installation and commissioning of wind plants. Considerable part of the investment costs is related to the wind turbine's foundation and ranges up to 20%.

Offshore wind turbines (OWT) may be sited on monopiles or gravity-based substructures in shallow water, where the water depth is less than 30 meters. At transitional water depths between 30 and 60 meters, it is more economical to design fix-bottom substructures such as tripods or jackets. For water depth greater than 60 m, floating platforms may be considered.

Support structure design is extremely challenging due to non-linearity and time-history dependency of the various loads. Sea wave loadings, wind loadings, dynamic loadings due to turbine rotor are sources of continually changing stresses leading to fatigue damages. Fatigue is an important factor which affects durability i.e. shortens lifetime of support structure elements. In order to minimize repair costs and maintenance works, support structures are currently designed conservatively to prevent early failures. Therefore there is a large potential for cost reduction in design approach.

1.2. Motivation

The main objective of this thesis is to investigate fatigue accumulation in jacket support structure, when damage or failure occurs in a structural member. Analysis concerns of jacket substructure OC4 with wind turbine NREL 5MW (Vorpahl 2013, Jonkmann 2009). Model of offshore wind turbine is implemented in FEDEM Windpower (Version R7.1, Fedem Technology AS, Trondheim) using finite elements method.

Calculations of fatigue damages distribution on remaining jacket elements may lead us to more effective and cheaper design. Moreover it can result in conclusion that the loss of one structural

member is not critical for the power production suspension limitations shall be introduced to prevent further damage.

Current standards does not allow such operation due to the safety requirements. However more sophisticated calculations may result in new standards and safety procedures in the future.



a)



b)



c)

Fig. 1.1. Jacket support structures

- a) jacket support structures on transportation barge before installation [30]
- b) view of jacket support structure already mounted on seabed [29]
- c) supporting structure with the turbine already assembled at the top [42]

1.3. Scope of work

The scope of this work comprises following 7 design evaluation steps :

- Choose environmental conditions based on design load cases from guideline IEC 61400-3 [3]

- Prepare the turbine model in Fedem Windpower Software.
- Apply damage of substructure member to the OWT model
- Perform simulations to obtain load time series
- Carry out fatigue analysis and ultimate analysis
- Compare results between undamaged and damaged model
- Suggest modified controller to reduce loadings and extend structure's lifetime

2. DESCRIPTION OF THE OFFSHORE WIND TURBINE

2.1. Model

2.1.1. Wind turbine

The reference wind turbine in this thesis is adapted from the National Renewable Energy Laboratory(NREL) 5MW baseline turbine. The baseline turbine consists of an upwind, three-bladed turbine mounted at hub height 90.55m. The original hub height was 90m and it was increased due to a shifted tower top elevation[6]. Turbine has a variable speed system with blade-pitch controller to efficiently extract energy from wind and to better copy with stormy wind conditions [25]. The basic parameters of the turbine are listed in the Table 2.1. Turbine parameters for NREL 5MW [8].

The turbine is installed on a supporting system, which combines a tower, concrete transition piece, jacket substructure and four grouted piles.

Turbine parameter	Value	Unit
Rated power	5.0	MW
Rotor diameter	126	m
Mass of rotor and nacelle	350	ton
Cut-in wind speed	3	m/s
Rated wind speed	11.4	m/s
Cut-out wind speed	25	m/s
Nominal rotor speed	12.1	rpm
Lower bound rotor speed	6.9	rpm
Upper bound rotor speed	12.1	rpm

Table 2.1. Turbine parameters for NREL 5MW [8]

For the detailed characteristics of turbine NREL 5MW please refer to *Definition of a 5-MW reference wind turbine for offshore system development* (Jonkman,2009) [4].

2.1.2. Jacket support structure [6]

Generally ‘jacket’ is steel lattice frame consisting of tubular members connected to one another by welded joints. Tubular members are appropriate to guarantee high nondirectional buckling and bending strength of the jacket and its high strength-to-weight ratio [20]. Jacket support structure has four legs and four levels of X-braces. Jacket legs are fixed to the seabed by means of the grouted connection between bottom legs and piles. The structure is treated as cantilever at mudline i.e. all six degrees of freedom are set to zero[6]. The upper part of jacket penetrates the concrete transition piece. The total height of the substructure from sea bottom to the

transition piece is 70.15 meters. The properties of tubular members and node coordinates are described in Appendix A.

Comparing to the monopiles, the jacket structure idea seems to function very well in the transitional waters due to its definitely lower mass as well as much greater transparency to the wave forces, higher structural stiffness and lower soil dependency [5]. The X-bracings are designed according to the NORSOK recommendations i.e. the angle between the brace and the leg exceeds 30 degrees[44].

2.1.3. Transition piece

Transition piece (TP) is a rigid block of concrete between tower and jacket structure. It is in a shape of cuboid and a size of 4×9.6×9.6m. The mass of the transition piece is 666t. The connection between TP and jacket lies at MSL +16.15m whereas between TP and tower lies at MSL +20.15m (Fig. 2.1) [6].

The material for the transition piece has been chosen as reinforced concrete rather than steel, which is based on a cost benefit evaluation. The concrete transition piece has the weight as a disadvantage. However, it is neither as susceptible to fatigue damage nor as labour intensive compared to a steel transition piece [5].

2.1.4. Tower

Tower is in a shape of cone and its diameter and wall thickness linearly decreases with height. In the last upper section of tower the wall thickness is reincreased. Paint, bolts, welds, and flanges are not accounted in the tower thickness [4]. Tower is attached to concrete block transition piece at +20.15 MSL. The yaw bearing is mounted on the highest point of tower i.e. at 88.15m above MSL. The tower cross sectional properties are discussed in more detail in *Vorpahl (2013)*.

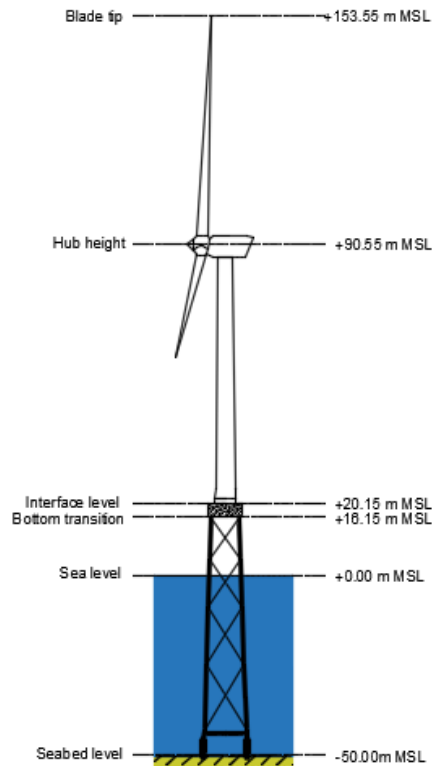


Fig. 2.1. Schematic dimensions of the Offshore Wind Turbine [6]

2.2. Location

According to the *UpWnd Design Basis* [8] offshore wind turbine is located in the Dutch North Sea. It is denoted as *K13-Alpha 3* (Fig. 2.2). The coordinates of K13 are $53^{\circ}13'04''$ north and $3^{\circ}13'13''$ east. It should be noted that K13 location is a reference for typical site conditions in the Dutch North Sea and constitutes basis for the calculation. The offshore wind turbine has not been built in this place.

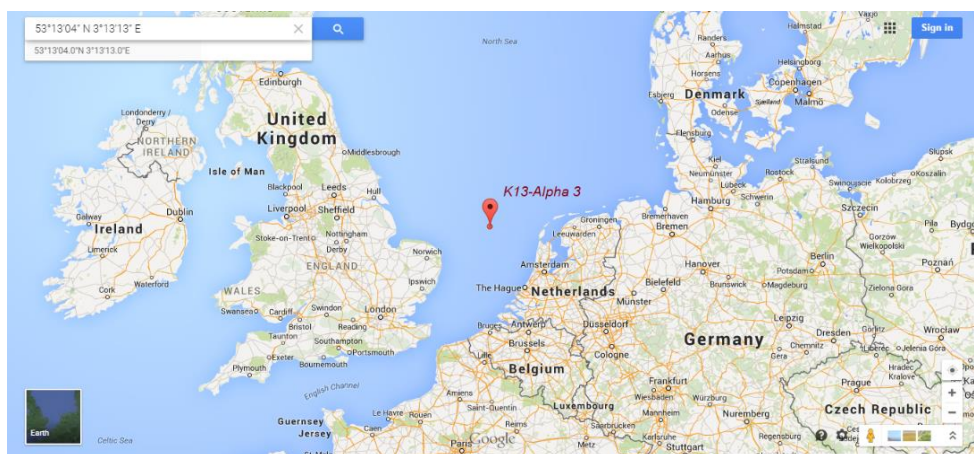


Fig. 2.2. Location of the offshore wind turbine K13 provided by Google Maps [19]

2.3. Material properties

Based on the IEC-guideline [4] material properties for steel are assumed identical for the wind turbine model NREL 5-MW and jacket support structure model OC4 (Table 2.2).

Description	Value	Unit
Young's modulus E_s	210	GPa
Density ρ_s	7850	kg/m ³
Poisson's ratio ν_s	0.3	-

Table 2.2. Steel properties for whole structure[4]

The critical structural-damping ratio ζ_s equals 1% and the corresponding logarithmic decrement δ_s is 6% for all modes of the support structure (without the rotor-nacelle assembly mass present).

2.4. Environmental conditions

The climate information is based on 22-years observations (January 1979 - December 2000) provided by Rijkswaterstaat [8].

2.4.1. Sea water

Properties of sea water are listed in Table 2.3.

Description	Value	Unit
Water density	1025	kg/m ³
Water salinity	3.5	%
Range of water temperature	0/22	°C

Table 2.3. Properties of sea water [8]

2.4.2. Water depths

The offshore wind turbine is sited on 50 m under the MSL level. This value does not take into account scour effect.

2.4.3. Water levels

Water levels and storm surges are settled for the K13 site based on 22 years measurements.

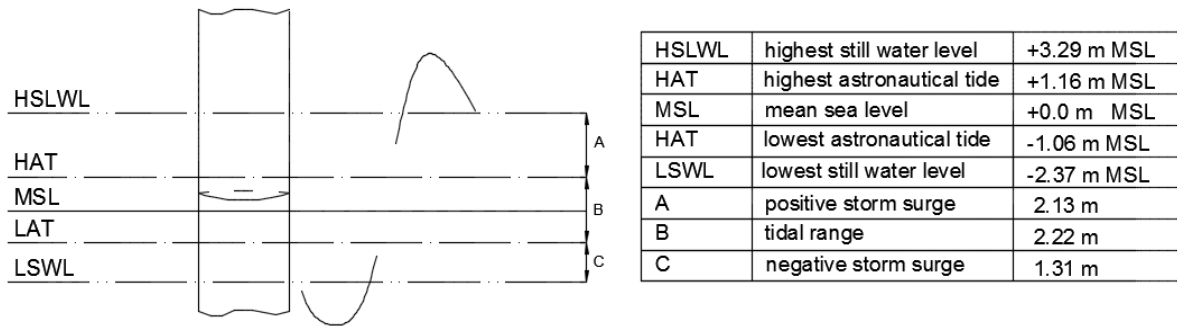


Fig. 2.3. Measured water levels at the OWT location [8]

2.4.4. Currents

Values of the currents in the studied location are listed in Table 2.4.

Load situation	Value	Unit
Normal current	0,6	m/s
Extreme current	1,2	m/s

Table 2.4. Properties of sea currents [8]

For the simplification of the computations no currents are assumed in this research, as their influence is negligible.

2.4.5. Wave parameters

All wave parameters implemented in calculations are taken from *Upwind Design Basis* [8]. For values see Chapter No. 4.3.

2.4.6. Wind parameters

Wind parameters implemented in calculations are taken from *Upwind Design Basis* [8].

For values see Chapter No. 4.3.

3. BACKGROUND

3.1. Available wind power/ Wind turbine Energy Production

3.1.1. Betz's law and power coefficient

In 1919 Albert Betz, a German physicist concluded that no wind turbine is capable to convert more than 16/27 (59.3%) of wind kinetic energy into mechanical energy propelling a rotor [36]. The factor 16/27 (59.3%) is known as Betz limit and it is valid independently of the wind turbine design.

The Betz limit is based on actuator disc model which represents idealized model of a wind turbine (Fig. 3.1).

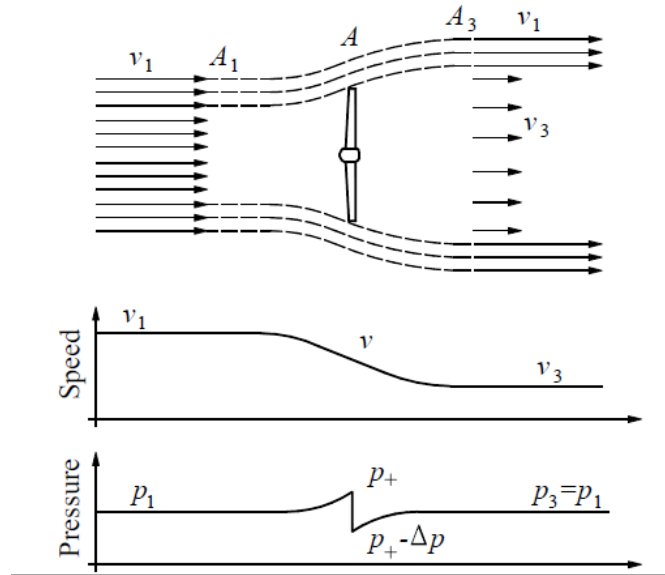


Fig. 3.1. Speed and pressure variation in an ideal model of a wind turbine [35]

In order to find relation between speed and pressure, Bernoulli's equation can be used. Assuming that the flow of the air is frictionless while moving towards the rotor plane, the following relation can be formed according to the Bernoulli's equation:

$$\frac{1}{2}\rho v^2 + p = p_{tot} \quad (3.1)$$

Thus for the flow up-stream of the rotor, we obtain :

$$p_1 + \frac{1}{2}\rho v_1^2 = p_+ + \frac{1}{2}\rho v^2 \quad (3.2)$$

For the flow down-stream of the rotor, the equation (3.1) looks like :

$$p_+ - \Delta p + \frac{1}{2}\rho v^2 = p_+ + \frac{1}{2}\rho v_3^2 \quad (3.3)$$

Subtracting formulas (3.3) from (3.2) we get :

$$\Delta p = \frac{1}{2}\rho(v_1^2 - v_3^2) \quad (3.4)$$

The mass flow equals $\rho \cdot v$ per one square meter of the rotor plane. Momentum equals mass times velocity, with the unit N. Pressure is equal to the force per surface ratio and the differential pressure can be then calculated as :

$$\Delta p = \rho v(v_1 - v_3) \quad (3.5)$$

Equation (3.5) indicates that the speed of air in the rotor plan equals the average value of the flow speed upstream and downstream of the rotor

$$v = \frac{1}{2}(v_1 + v_3) \quad (3.6)$$

The power of the turbine is equal to the drop of the kinetic energy in the flowing air:

$$P = \frac{1}{2}\rho(v_1^2 - v_3^2)A \quad (3.7)$$

The speed of air in the rotor plane (3.8) and the speed of downstream of the rotor (3.9) are defined by the axial interference factor 'a' :

$$v = (1 - a)v_1 \quad (3.8)$$

$$v_3 = (1 - 2a)v_1 \quad (3.9)$$

Substituting formulas (3.8) and (3.9) into equation (3.7) leads to:

$$P = 2\rho a(1 - a)^2 v_1^3 A \quad (3.10)$$

Power coefficient C_p is defined by :

$$C_p = 4a(1 - a)^2 \quad (3.11)$$

The power coefficient of a wind turbine denotes efficiency how the wind turbine converts wind energy into electricity [32].

This formula may be inserted into (3.10) .The result is the following expression for power P:

$$P_{rotot} = \frac{1}{2}\rho v_1^3 A C_p \quad (3.12)$$

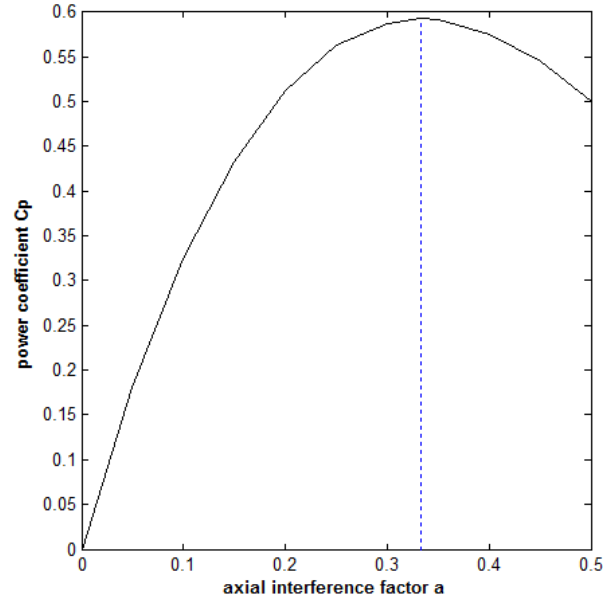


Fig. 3.2. Power coefficient C_p as a function of the axial interference factor a .

C_p extreme is reached at about 0.593 (16/27) as shown in Fig. 3.2. It refers to value 0.333 (1/3) of an axial interference factor.

$$P_{Betz} = C_{p,Betz} \frac{1}{2} \rho v_1^3 A \quad (3.13)$$

The power coefficient may be also expressed as ratio between rotor power from equation (3.12) and the total energy available in the wind:

$$C_p = \frac{P_{rotor}}{\frac{1}{2} \rho A v_1^3} \quad (3.14)$$

3.1.2. Tip speed ratio

Tip speed ratio (TSR) is the ratio between the tangential speed of the tip of a blade and the current velocity of the wind v_1 [33].

The optimal tip speed ratio depends on the number of blades. The smaller the number of blades, the faster the rotor has to spin to extract maximum power from the wind.

When TSR is too low, the turbine tends to slow down and to stall. On the contrary, if the tip speed ratio is too high, the turbine rotates very fast through turbulent air, and the power is not only extracted with large losses from the wind flow, but the turbine is also highly stressed with the risk of catastrophic damage [34]

A well designed typical three-bladed rotor has usually a tip speed ratio of around 6 to 7 [25].

$$TSR = \frac{V_{tip}}{V_1} = \frac{\omega R}{V_1} \quad (3.15)$$

where :

TSR – tip speed ratio [-]

V_{tip} – tangential speed of the tip of a blade $\left[\frac{m}{s}\right]$

ω – angular velocity of the rotor [rad/s]

R – distance between the axis of rotation and the tip of the blade [m]

V₁ – undisturbed wind speed [m/s]

3.2. Wind Turbine Terminology

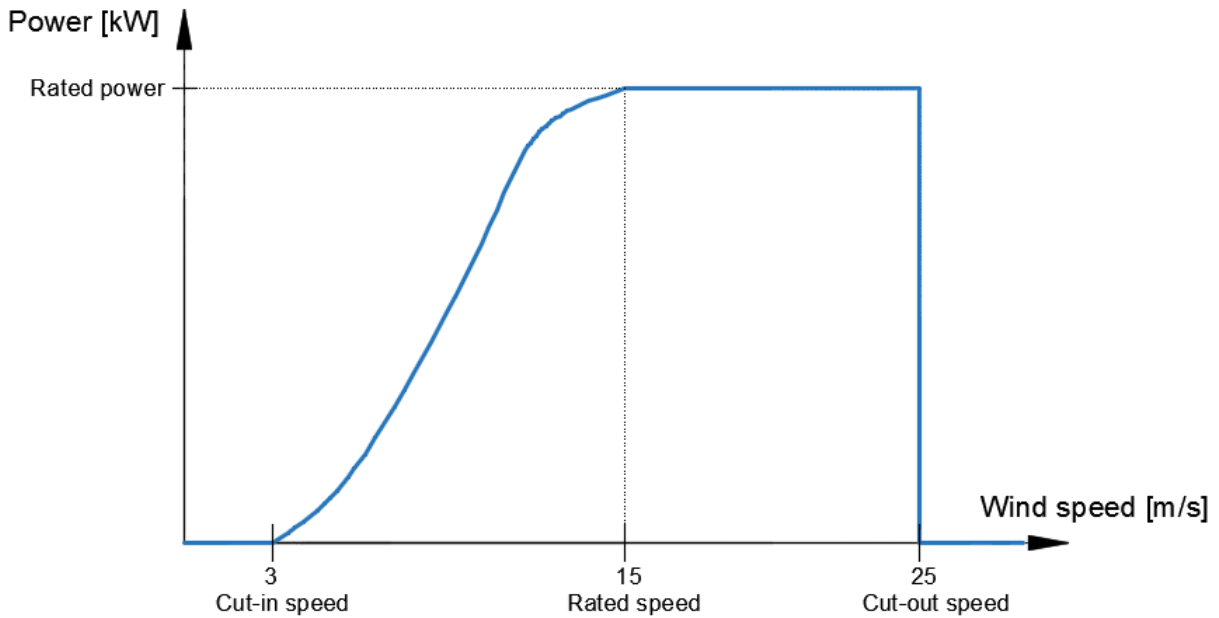


Fig. 3.3. Power output curve for typical wind turbine

Cut-in Wind Speed – the minimum wind speed below which no useful power output can be produced by wind turbine, typically between 3 and 4 m/s [25].

Rated power and Rated wind speed – as the wind speed rises above the cut-in speed, the power output rises exponentially until it reaches limit that generator is capable of (Fig. 3.3). The power output limit is called rated power and the corresponding wind speed is known as rated wind speed [39]. Once rated power is exceeded, the pitch controller starts to vary the pitch of the turbine blades which leads to rotor speed reduction. In consequence, the generator is subjected to less mechanical power while the electrical power output remains constant. The rated wind speed is typically somewhere between 12-15 m/s.

Cut-out speed – the maximum wind speed at which the turbine develops power output meeting safety requirements. A cut-out speed of 25 m/s is typical for very large turbine [25].

Torque – tendency of an air force applied by wind to blades to rotate the rotor about its axis. A torque can be perceived as a twist to the rotor. It appears when the wind power is transmitted to the rotor and is defined by the equation:

$$T = \frac{P}{\omega} \left[\frac{Nm}{rad} \right] \quad (3.16)$$

where:

P – is mechanical power [W]

ω – is angular velocity [rad/s]

Changing the rotor dimensions has a high impact to parameters achieved by the turbine. When the rotor's radius is doubled, the area of rotor plane and extracted power is quadrupled while the rotor speed drops by half to maintain same tip speed. The torque will be increased by a factor of 8. In general, the rotor torque will be proportional to cube of its radius. [31]

Blade pitch angle, angle of attack – angles referred to in the Blade Element Theory. Pitch angle is the angle between the turbine rotation plane and the blade chord (line connecting leading and trailing edge of the blade in its cross-section). This angle can be set by a pitch mechanism and can be visually observed while changing.

The attack angle is the angle between the blade chord (see above) and the apparent wind direction (direction of the vector sum resulted from adding the real wind velocity vector and the rotating blade tangential velocity vector). This angle differentiates from hub to blade tip as the blade tangential speed along the blade changes with the radius. For more information see the diagram below (Fig. 3.4).

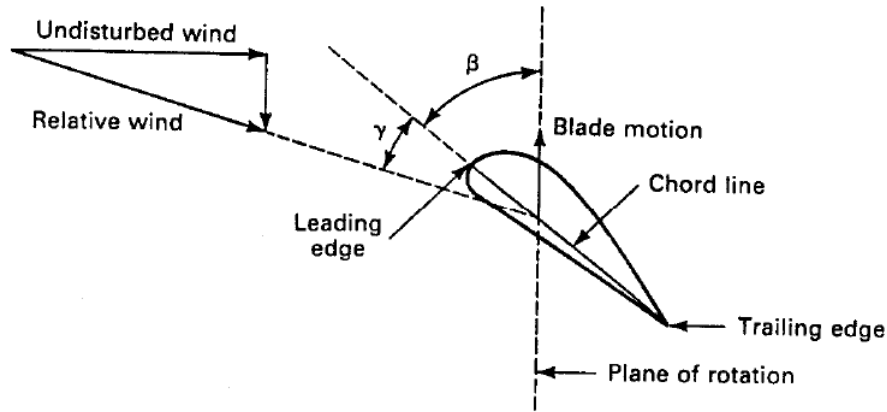


Fig. 3.4. Definition of Blade pitch angle and angle of attack [26]

Turbine downregulation - an operational state of the turbine allowing the active power output to be curtailed by pitching the blades, limiting thrust and power output this way

3.3. Fatigue assessment

3.3.1. General

Fatigue is the process of material degradation when imposed to continually changing stresses. These repeatedly changing stresses, cause slow deterioration of the material, initiate cracks which finally lead to eventual damage [41]. Fatigue damage occurs in the material due to the long term stress variation.

Offshore wind turbines are exposed to turbine, wind and waves loads varying in time throughout their lifetime. This leads to constantly varying in time stresses and making the support structure prone to fatigue [40]. In particular, tubular steel support structures such as monopiles, tripods or lattice frames should be investigated in terms of fatigue, because fatigue damage has been identified as a factor having destructive influence on welded tubular joints.

Fatigue damage accumulation in welded tubular joints is usually analyzed using hot spot stress method. This method mainly consist of solving set of equations comprising stress time series multiplied by factors reflecting different geometrical configuration of tubular members. As a result hot spot stress time series are determined, which are then post-processed basing on a rainflow counting algorithm. Subsequently, equivalent cycles of stress amplitudes are extracted from hot spot stress time series and sorted in bins forming a stress range histogram, which is further used to calculate cumulative fatigue damage based on Palmgren-Miner rule.

The total amount of cumulative fatigue damage generated over the examined period of time depends on the damage which comes into being in particular weather conditions and the share of a time that those conditions take place [31]. The wind loads may exceed 60% fatigue damage contribution of welded tubular joints [40]. An off-shore wind turbine with 20 years of estimated life time usually reaches more than 10^9 load cycles generated by the rotor [26]. Thus, the distribution of the wind speed is crucial and should be taken into account during fatigue assessment.

More detailed description of each computational step is presented in this section. The diagram of fatigue assessment procedure is shown in Fig. 3.12.

3.3.2. Loads time series

A common method to obtain loads acting on an offshore wind turbine is performing simulations with wave trains and turbulent wind fields in time domain. The calculation of wind loads are usually based on blade element momentum (BEM) whereas wave loads are modelled in accordance with Morison equation. Implementing wind and waves input in simulation software such as for instance Abaqus, Fedem or FAST enable to calculate the response of the structure and extract the loads time series (Fig. 3.5).

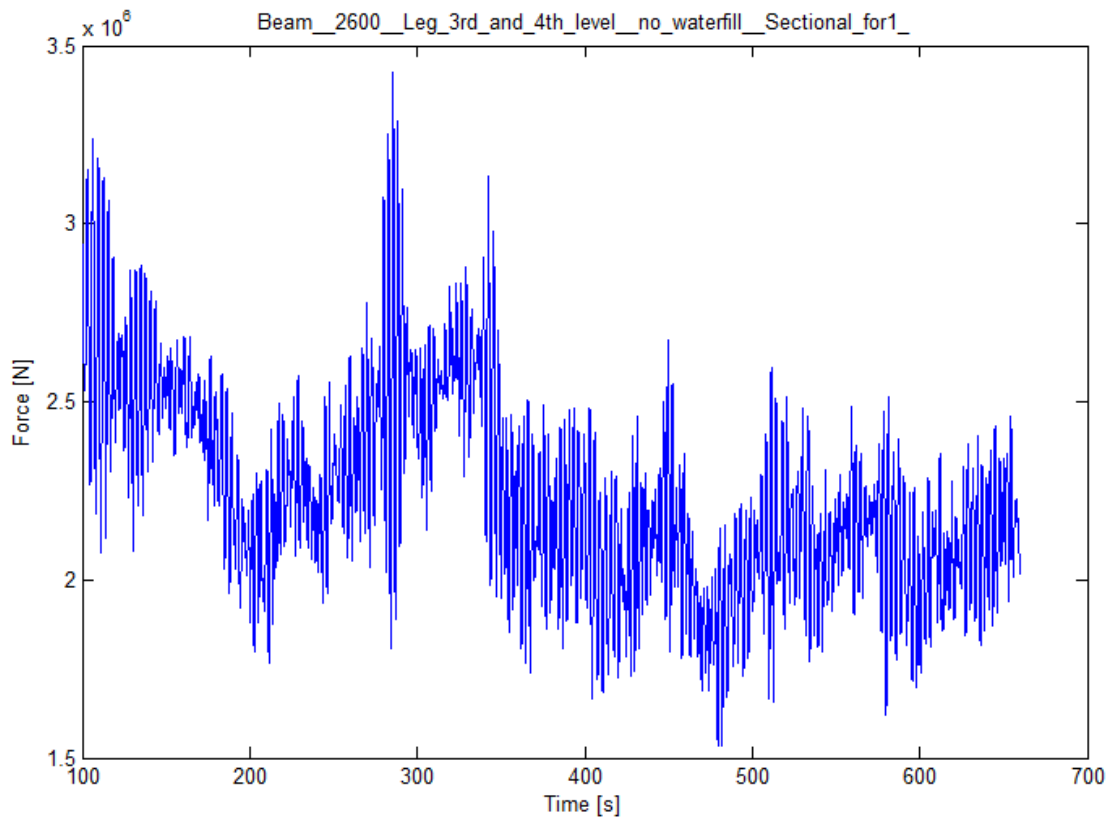


Fig. 3.5. Example of load time series

It should be noted that transient loads (due to start, stop or failure) are usually not taken into account in fatigue analysis and therefore part of raw load time series is cut off, from 60 to 200s depending on wind speed.

3.3.3. Sectional time series

Loads time series i.e. force and moment time series are converted afterwards to sectional time series, using proper cross-section area and moment of inertia for each beam. Sectional stresses are also known as nominal stresses.

Tubular structural element's cross-section is considered as hollow cylindrical cross-section (Fig. 3.6)

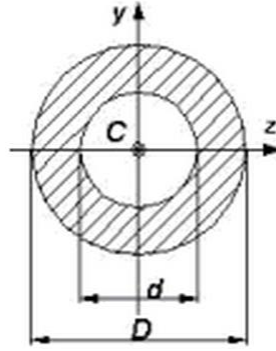


Fig. 3.6. Hollow cylindrical cross section

The math expressions describing cross-section area and moment of inertia are shown below, respectively:

$$A = \frac{\pi \times (D^2 - d^2)}{4} \quad (3.17)$$

$$I = \frac{\pi \times (D^4 - d^4)}{64} \quad (3.18)$$

where,

d- inner diameter [m]

D-outer diameter [m]

A-area of hollow cylindrical cross section [m^2]

I-area moment of inertia for hollow cylindrical cross section [m^4]

Sectional stresses are calculated from following formulas:

$$\sigma_x = \frac{F}{A} \quad (3.19)$$

$$\sigma_y = \frac{M_y}{I} \cdot \frac{1}{2}D \quad (3.20)$$

$$\sigma_z = \frac{M_z}{I} \cdot \frac{1}{2}D \quad (3.21)$$

where,

F – axial force [kN]

M_y – in-plane bending moment [kNm]

M_z – out-plane bending moment [kNm]

σ_x – nominal stress due to axial load [MPa]

σ_y – nominal stress due to in-plane bending [MPa]

σ_z – nominal stress due to out-of-plane bending [MPa]

3.3.4. Hot spot stress analysis

Hot spot stress analysis is widely used method to evaluate the fatigue life of offshore welded structures like jacket support structure. ‘Jacket’ is constructed from tubular members welded in different geometrical configuration(Y-joint, K-joint or X-joint) (Fig. 3.7). Tubular joints subjected to repeated loadings are exposed to high-level stress concentrations which may initiate fatigue crack [22]. The critical areas where fatigue crack is expected to initiate are called ‘hot spot stress’ areas. Hot spot stress(HSS) is also known as geometrical stress or structural stress.

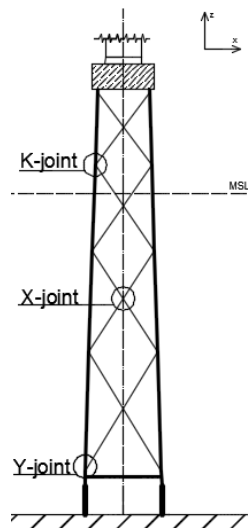


Fig. 3.7. Model of jacket support structure with selected geometrical configurations of joints

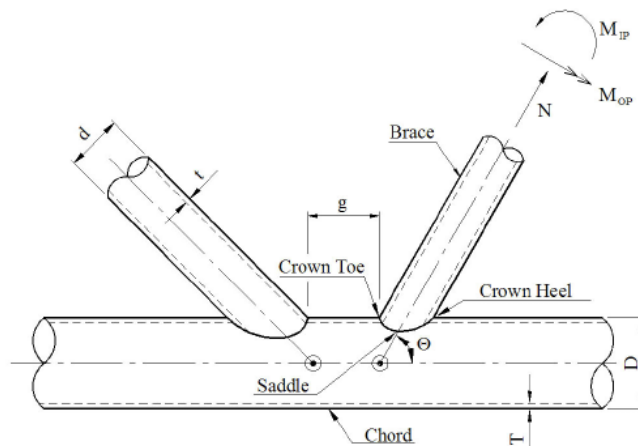


Fig. 3.8. Geometrical definitions for tubular joints [18]

There are two approaches to calculate the hot spot stress: using the Stress Concentration Factor (SCF) model or derived from nominal stresses combined with associated SCF. The SCF factor of the examined joint is a ratio between geometrical stress $\sigma_{hot\ spot}$ to nominal stress $\sigma_{nominal}$ (3.22) and it depends on joint configuration and loading type [18, 22].

$$\sigma_{hot\ spot} = SCF \cdot \sigma_{nominal} \quad (3.22)$$

HSS analysis assumes performing set of eight different equations (3.23-3.30) with appropriate member stresses and SCFs. Technical report *Fatigue Design of Offshore Steel Structures* [18] recommends to use the stress range at the hot spot of tubular joints in combination with T-curve, which symbolizes theoretical probability distribution, similar to the standard normal curve.

$$\sigma_1 = SCF_{AC}\sigma_x + SCF_{MIP}\sigma_{my} \quad (3.23)$$

$$\sigma_2 = \frac{1}{2}(SCF_{AC} + SCF_{AS})\sigma_x + \frac{1}{2}\sqrt{2}SCF_{MIP}\sigma_{my} - \frac{1}{2}\sqrt{2}SCF_{MOP}\sigma_{mz} \quad (3.24)$$

$$\sigma_3 = SCF_{AC}\sigma_x - SCF_{MOP}\sigma_{mz} \quad (3.25)$$

$$\sigma_4 = \frac{1}{2}(SCF_{AC} + SCF_{AS})\sigma_x - \frac{1}{2}\sqrt{2}SCF_{MIP}\sigma_{my} - \frac{1}{2}\sqrt{2}SCF_{MOP}\sigma_{mz} \quad (3.26)$$

$$\sigma_5 = SCF_{AC}\sigma_x - SCF_{MIP}\sigma_{my} \quad (3.27)$$

$$\sigma_6 = \frac{1}{2}(SCF_{AC} + SCF_{AS})\sigma_x - \frac{1}{2}\sqrt{2}SCF_{MIP}\sigma_{my} + \frac{1}{2}\sqrt{2}SCF_{MOP}\sigma_{mz} \quad (3.28)$$

$$\sigma_7 = SCF_{AC}\sigma_x + SCF_{MOP}\sigma_{mz} \quad (3.29)$$

$$\sigma_8 = \frac{1}{2}(SCF_{AC} + SCF_{AS})\sigma_x + \frac{1}{2}\sqrt{2}SCF_{MIP}\sigma_{my} + \frac{1}{2}\sqrt{2}SCF_{MOP}\sigma_{mz} \quad (3.30)$$

where:

σ_x – nominal stress due to axial load [MPa]

σ_y – nominal stress due to in-plane bending [MPa]

σ_z – nominal stress due to out-of-plane bending [MPa]

SCF_{AC} – stress concentration factor at the saddle for axial load [–]

SCF_{AS} – stress concentration factor at the crown for axial load [–]

SCF_{MIP} – stress concentration factor for in-plane moment [–]

SCF_{MOP} – stress concentration factor for out-of-plane moment [–]

Stresses in pipes joints are computed for saddle and crown points (Fig. 3.8). Next, the hot spot stress at the points mentioned above is calculated based on superposition rule in order to achieve a sum of components from axial force, in-plane and out-plane moments. The hot spot stresses for the intermediate points are evaluated by a linear interpolation of the stresses, because higher stress may occur also between saddle and crown points. Proper hot spot stress analysis should include evaluation at 8 spots around the element's intersection circumference [18] (Fig. 3.9).

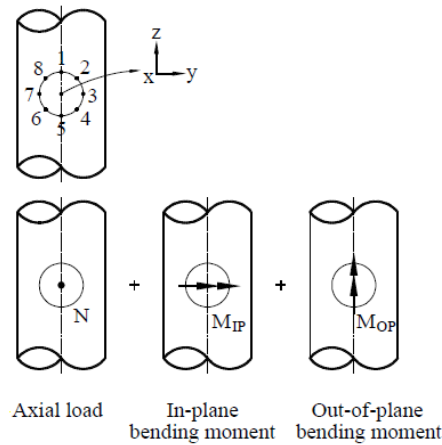


Fig. 3.9. Superposition of stresses [18]

3.3.5. Rainflow counting

The rainflow counting method, first proposed by Endo and Matsuichi, is now the most popular and effective way to predict the fatigue life of a structure subject of a complex loading [15, 16]. This method consist in extraction of equivalent cycles of stress amplitude varying in time (Fig. 3.10.a). The origin of the name comes from association between computation algorithm and mechanism of the drop falling off a Japanese pagoda roof [17].

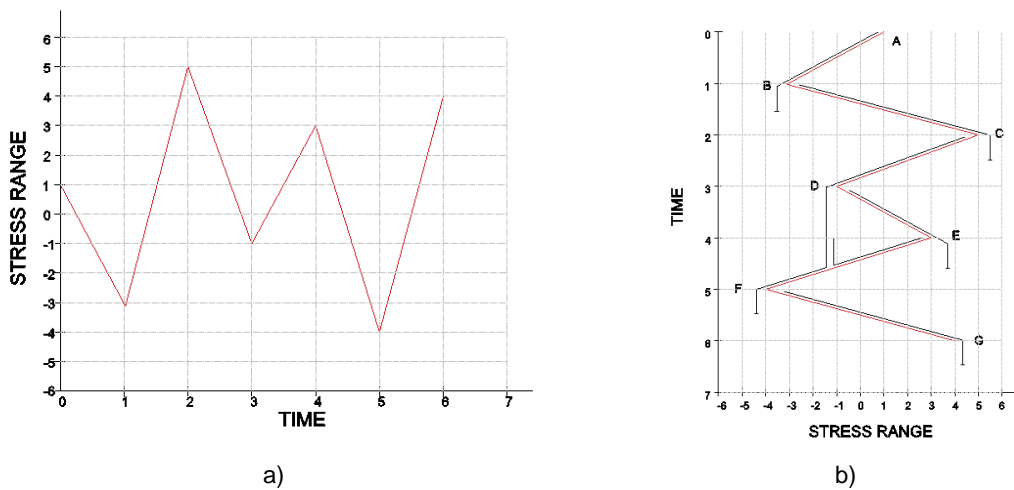


Fig. 3.10. Stress time series

- a) rotated horizontally
- b) rotated clockwise 90°

This method assumes that the stress time series is rotated clockwise 90° and time axis is pointing vertically downwards (Fig. 3.10.b). Peaks (points A, C, E and G) and valleys (points B, D and F) refer to the peaks and valleys of the horizontally rotated time series.

Starting from the peak of the theoretical roof a rain drop is falling down and continues to the next roof if only next roof is lower than previous (point C). If the next roof is higher, then the drop stops (point A). Termination of the flow takes also place, when the drop reaches the flow started at the previous peak (point E). This procedure continues till all peaks are evaluated. Afterwards the same procedure is carried out for the valleys.

The amplitude of each stress starts at respective peak or valley and follow until the raindrop stops. For each amplitude is assigned half-cycle in their respective cycle range. The number of half-cycles is counted into the number of n bins (each amplitude range corresponds to assigned bin). These n bins create a stress range histogram (Fig. 3.12, Scheme 6), which is further used (Palmgren-Miner rule) to assess the fatigue life [11].

3.3.6. Damage Equivalent Load, DEL

Damage equivalent load (DEL) is commonly used factor in fatigue assessment to compare fatigue loading from different simulations when the detailed geometry or material properties are unknown. It may be expressed based on the S-N curve (stress versus number of cycles curve) (Fig. 3.11) assuming linear cumulative damage (Palmgren-Miner rule) [11]. Math expression (3.31) describes that for each stress range $\Delta\sigma_i$, the damage from that range is calculated as a number of cycles for the particular range n_i divided by the total number of cycles to failure at that range N_i . Failure occurs, when total DEL equals 1 [11].

$$DEL = \sum_{i=1}^j \frac{n_i}{N_i} = \frac{1}{\bar{\alpha}} \sum_{i=1}^j n_i \cdot (\Delta\sigma_i)^m \leq 1 \quad (3.31)$$

where:

DEL – damage equivalent load [–]

$\Delta\sigma_i$ – stress range [MPa]

j – total number of stress blocks

$\bar{\alpha}$ – intercept of the design S – N curve with the logN axis

m – negative inverse slope of the S-N curve

n_i – number of stress cycles in stress block *i*

N_i – number of cycles to failure at constant stress range $\Delta\sigma_i$

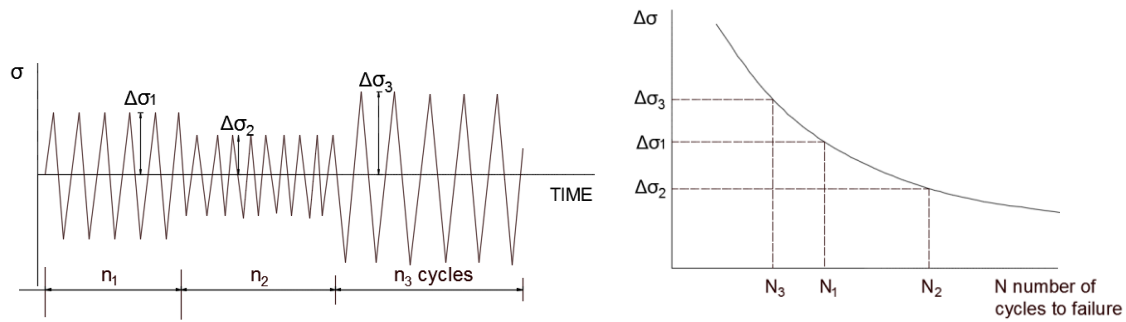


Fig. 3.11. Example of fatigue assessment according to Palmgren-Miner rule

3.3.7. Equivalent Fatigue Load, EFL

Equivalent Fatigue Load (EFL) is also based on Palmgren-Miner's S-N curve and may be determined from DEL definition. EFL can be interpreted as constant stress range which leads to failure within the predefined number of cycles N in turbine lifetime.

$$N = \bar{a} \cdot (\Delta\sigma)^{-m} \quad (3.32)$$

Following equation is another way for expressing damage equivalent load :

$$DEL = \frac{N \cdot (EFL)^m}{\bar{a}} \quad (3.33)$$

The damage caused by N number of cycles with stress range EFL has to equal the damage from equation (3.31).

$$\frac{N \cdot (EFL)^m}{\bar{a}} = \frac{1}{\bar{a}} \sum_{i=1}^j n_i \cdot (\Delta\sigma_i)^m \quad (3.34)$$

Expression transformation results in:

$$EFL = \sqrt[m]{\frac{\sum_{i=1}^j n_i \cdot (\Delta\sigma_i)^m}{N}} \quad (3.35)$$

where:

EFL – equivalent fatigue load [MPa]

m – negative inverse slope of the S-N curve

\bar{a} – intercept of the design S – N curve with the log N axis

n_i – number of stress cycles in stress block *i*

N – predicted number of cycles to failure

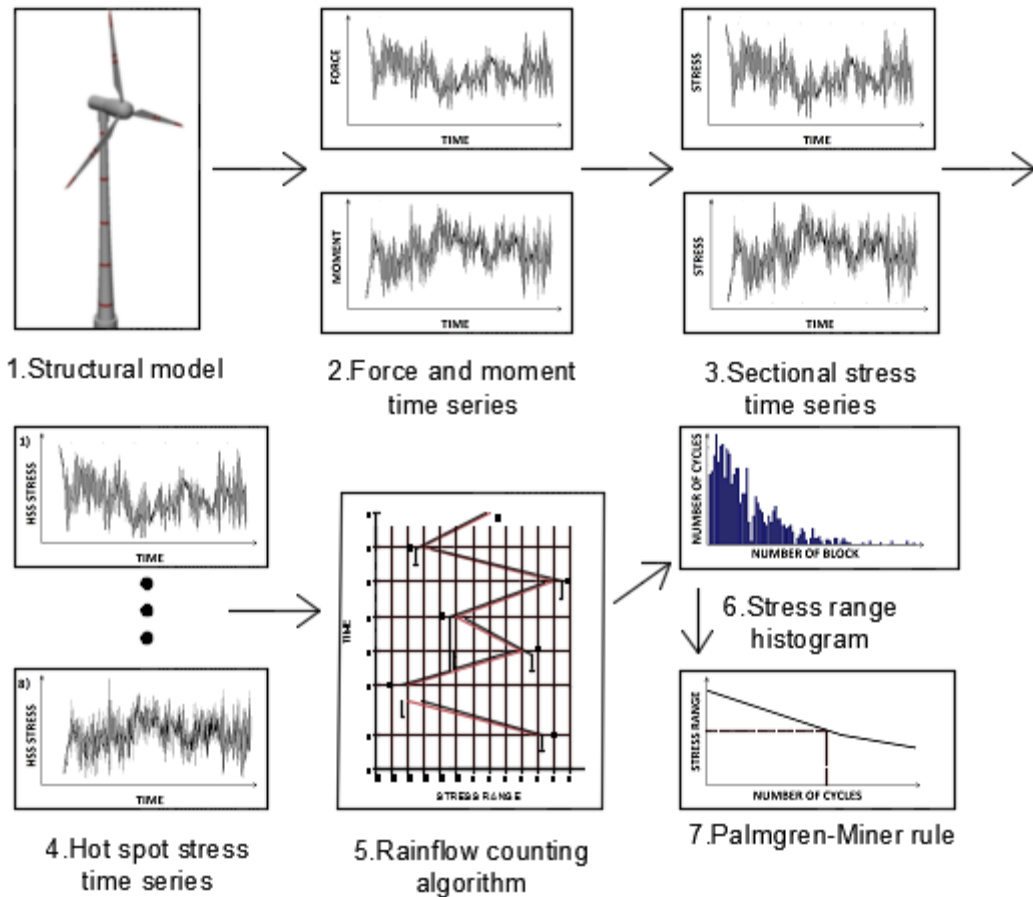


Fig. 3.12. Diagram of fatigue assessment procedure.

3.4. Ultimate strength analysis

3.4.1. General

This chapter presents general procedure of yield check calculations for offshore wind turbine's structural members. The analysis assumes that load measurements, as well as the characteristics of the material binds with the uncertainties. For this reason, the partial safety factors are introduced to prevent against a possibility of occurrence unfavorable deviations from the characteristic values.

The basic requirement for ultimate loading is that the product of the expected 'load function' $S(F_d)$, and a 'consequence of failure' safety factor γ_n , shall not be higher than the 'resistance function', $R(f_d)$

$$\gamma_n \cdot S(F_d) \leq R(f_d) \quad (3.36)$$

In the standard case, the load function takes the maximum value of the anticipated stress, and the resistance function represents highest permissible design value. The condition can be then formed as:

$$\gamma_f \cdot F_k \leq \frac{1}{\gamma_m \gamma_n} f_k \quad (3.37)$$

The design values for the load F_d are determined by multiplying characteristic values of the load F_k by partial safety factor γ_f :

$$F_d = \gamma_f \cdot F_k \quad (3.38)$$

The design values for the materials f_d are found from the characteristic values of the materials, f_k , by applying a global partial safety factor, which is determined by multiplying general factor for materials, γ_m by partial safety factor for consequence of failure γ_n .

$$f_d = \frac{1}{\gamma_m \gamma_n} f_k \quad (3.39)$$

3.5. Modal analysis

Offshore wind turbine elements are mainly designed as partially elastic structures and they tend to vibrate excited by operation of the turbine, wind or waves loads. Vibrations induced at system's resonance frequency are particularly points of interest. Resonant frequency occurrence is undesirable, because in turn, it leads to resonant loads - cyclic loads that may reach high magnitudes. Investigation of wind turbine and its substructure dynamic behavior is essential to prevent turbine components from premature failure due to fatigue [31]. In order to avoid resonance phenomenon, identification of resonant frequencies and corresponding mode shapes is performed using modal analysis.

The basic concept of modal analysis is that any structure may be modeled as superposition of individual contribution of each natural modes.

Modal analysis enables to solve the set of equations concerning the motion of vibrating system in multiple degree of freedom. This method allows coupled equations of motion to be transformed into uncoupled 'modal' equations which then can be easily solved independently. The complete result is obtained by 'superposition' (adding) of partial results of each equation. Solving linear systems with classical damping is the most contributing from this method of analysis.

More details on modal analysis may be found in Fertis (1995) or Chopra (2007).

3.5.1. Free vibrations of discrete multi degrees of freedom system

The dynamic equilibrium equation of multi degrees of freedom (MDOF) system is written as:

$$\mathbf{M}\ddot{\mathbf{u}} + \mathbf{C}\dot{\mathbf{u}} + \mathbf{K}\mathbf{u} = \mathbf{F}(t) \quad (3.40)$$

where:

\mathbf{M} – mass matrix

\mathbf{C} – damping matrix

\mathbf{K} – stiffness matrix

$\mathbf{F}(t)$ – external force vector

$\mathbf{u}(t)$ – displacement vector

$\dot{\mathbf{u}}(t)$ – velocity vector

$\ddot{\mathbf{u}}(t)$ – acceleration vector

Undamped motion will be considered

$$\mathbf{M}\ddot{\mathbf{u}} + \mathbf{K}\mathbf{u} = 0 \quad (3.41)$$

Displacement vector $\mathbf{u}(t)$ is written as:

$$\mathbf{u}(t) = \mathbf{q}_n(t)\boldsymbol{\phi}_n \quad (3.42)$$

where:

$$q_n(t) = A_n \cos \omega_n t + B_n \sin \omega_n t \quad (3.43)$$

$\boldsymbol{\phi}_n$ vector is responsible for mode shape whereas $q_n(t)$ are modal coordinates. After substitution equations (3.43) and (3.44) into (3.42) :

$$(\mathbf{K} - \omega_n^2 \mathbf{M})\boldsymbol{\phi}_n = 0 \quad (3.44)$$

Equation (3.45) has non-trivial solution, if :

$$\det(\mathbf{K} - \omega_n^2 \mathbf{M})\boldsymbol{\phi}_n = 0 \quad (3.45)$$

N roots ω_n^2 of the equation (3.46) determine N system natural angular frequencies ω_n ($n = 1, 2, \dots, N$). Each frequency ω_n corresponds to the natural vector $\boldsymbol{\phi}_n$, calculated to the nearest constant multiplier. Vector given by the relative values of N displacements ϕ_{jn} ($j = 1, 2, \dots, N$) defines a vibration model.

N eigenvalues and eigenvectors (of the vibration model) can be submitted to the matrix. Matrix whose columns are composed of N eigenvectors of the matrix is called a modal:

$$\Phi = [\phi_n] = \begin{pmatrix} \phi_{11} & \phi_{12} & \cdots & \phi_{1N} \\ \phi_{12} & \phi_{22} & \cdots & \phi_{2N} \\ \vdots & \vdots & \ddots & \vdots \\ \phi_{N1} & \phi_{N2} & \cdots & \phi_{NN} \end{pmatrix} \quad (3.46)$$

N eigenvalues ω_n^2 may be combined into diagonal spectral matrix of the equations system:

$$\Omega^2 = \begin{pmatrix} \omega_1^2 & 0 & \cdots & 0 \\ 0 & \omega_2^2 & \cdots & 0 \\ \vdots & \vdots & \ddots & \vdots \\ 0 & 0 & \cdots & \omega_n^2 \end{pmatrix} \quad (3.47)$$

Each eigenvalue ω_n^2 and each eigenvector ϕ_n satisfy the equation:

$$\mathbf{K}\phi_n = \mathbf{M}\phi_n\omega_n^2 \quad (3.48)$$

Use of modal matrix and spectral matrix allows to transform N equations (3.49) to a single matrix equation:

$$\mathbf{K}\Phi = \mathbf{M}\Phi\Omega^2 \quad (3.49)$$

Eigenvectors calculated to the nearest constant multiplier can be normalized so that the largest vector coordinates equals 1.

$$\phi_n = \frac{\tilde{\phi}_n}{\max|\phi_{jn}|} \quad (3.50)$$

If all eigenvalues ω_n^2 are real, then eigenvectors corresponding to different angular frequencies $\omega_n \neq \omega_k$ are orthogonal:

$$\phi_n^T \mathbf{K} \phi_r = 0 \quad (3.51)$$

$$\phi_n^T \mathbf{M} \phi_r = 0 \quad (3.52)$$

Orthogonality of vibration model ensures that the following matrices are diagonal:

$$\bar{\mathbf{K}} = \Phi^T \mathbf{K} \Phi \quad (3.53)$$

$$\bar{\mathbf{M}} = \Phi^T \mathbf{M} \Phi \quad (3.54)$$

Elements on the diagonal:

$$\bar{K}_n = \phi_n^T \mathbf{K} \phi_n \quad (3.55)$$

$$\bar{M}_n = \phi_n^T \mathbf{M} \phi_n \quad (3.56)$$

It is also possible to normalize these eigenvectors:

$$\phi_n = \frac{\tilde{\phi}_n}{\sqrt{\tilde{\phi}_n^T \mathbf{M} \tilde{\phi}_n}} \quad (3.57)$$

so that the modal matrix converts the mass matrix to the unitary one and the stiffness matrix to the spectral one:

$$\boldsymbol{\phi}^T \mathbf{K} \boldsymbol{\phi} = \boldsymbol{\Omega}^2 \quad (3.58)$$

$$\boldsymbol{\phi}^T \mathbf{M} \boldsymbol{\phi} = \mathbf{I} \quad (3.59)$$

Displacement vector may be expressed in modal coordinates:

$$\mathbf{u} = \sum_{r=1}^N \boldsymbol{\phi}_r q_r = \boldsymbol{\phi} \mathbf{q} \quad (3.60)$$

where $\mathbf{q} = [q_1, q_2 \dots q_n]^T$ stands for modal coordinates.

Multiplying (3.61) by $\boldsymbol{\phi}_n^T \mathbf{M}$:

$$\boldsymbol{\phi}_n^T \mathbf{M} \mathbf{u} = \sum_{r=1}^N \boldsymbol{\phi}_n^T \mathbf{M} \boldsymbol{\phi}_r q_r \quad (3.61)$$

Using the orthogonality property:

$$\boldsymbol{\phi}_n^T \mathbf{M} \mathbf{u} = \boldsymbol{\phi}_n^T \mathbf{M} \boldsymbol{\phi}_n q_n \quad (3.62)$$

$$q_n = \frac{\boldsymbol{\phi}_n^T \mathbf{M} \mathbf{u}}{\boldsymbol{\phi}_n^T \mathbf{M} \boldsymbol{\phi}_n} = \frac{\boldsymbol{\phi}_n^T \mathbf{M} \mathbf{u}}{M_n} \quad (3.63)$$

In case of manual calculations often easier is to use compliance matrix \mathbf{F} , where:

$$\mathbf{F} = \mathbf{K}^{-1} \quad (3.64)$$

Multiplying equation (3.42) by matrix \mathbf{K}^{-1} leads to:

$$\mathbf{F} \mathbf{M} \ddot{\mathbf{u}} + \mathbf{u} = \mathbf{0} \quad (3.65)$$

Substituting (3.44) into equation (3.66) results in:

$$(\mathbf{I} - \omega_n^2 \mathbf{F} \mathbf{M}) \boldsymbol{\phi}_n = \mathbf{0} \quad (3.66)$$

Equation (3.67) has non-trivial solution, if:

$$\det(\mathbf{I} - \omega_n^2 \mathbf{F} \mathbf{M}) = 0 \quad (3.67)$$

N roots ω_n^2 of the equation (3.68) are described by N system natural angular frequencies ω_n ($n = 1, 2, \dots, N$). Each frequency ω_n corresponds to the natural vector $\boldsymbol{\phi}_n$.

Harmonic loadings

The rotor speed operational range is usually chosen to avoid only the eigenfrequencies that coincide with 1P (rotor full revolution) and 3P (tower passage of the three blades) frequencies. It results in the offshore wind turbine is endangered by harmonic loadings originated from the

multiples of 1P and 3P frequencies [38]. Moreover, the turbulent wind should be taken into account as harmonic loads amplifier.

3.6. Software implementation

3.6.1. FEDEM Windpower

Fedem Windpower is a sophisticated software developed to simulate and analyse the complete wind turbine system behaviour exposed to dynamic loads. It is intended to be used both for onshore and offshore turbines [9]. This powerful tool is capable to create, solve and elaborate a model in a 3-dimension graphical environment. The structural dynamics are shaped with the finite-element method (FEM) or its multibody representation. Further reduction of the dynamical degrees-of-freedom is carried out with modal analysis [1]. Fig. 3.13. presents a typical offshore wind turbine modeled in Fedem Windpower. Fedem also provides user-friendly postprocessing properties, offering complete stress analysis, eigenmode solutions, study of deformation and fatigue analysis for selected time.

Wind loads are inducted to Fedem software by AeroDyn module, which calculates forces along the turbine blades [10]. Wind loads which are concerned in analysis are derived from either deterministic wind, or a stochastic, turbulent wind, generated by another modul - TurbSim [1]. Hydrodynamic loads from drags, currents and buoyancy are possible to simulate setting regular or irregular waves in Fedem Sea Environment dialog [10].

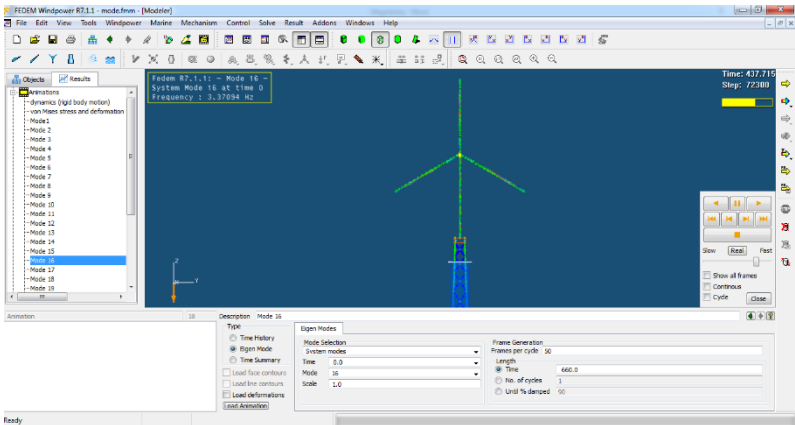


Fig. 3.13. Fedem’s main window with an offshore wind turbine model in workspace area

3.6.2. AeroDyn

AeroDyn is a software developed for wind and water power research with the support of the U.S. Department of Energy and the National Renewable Energy Laboratory (NREL) National Wind Technology Center (NWTC). AeroDyn computes the aerodynamic loads on wind turbine blade elements considering velocities and positions provided by dynamics analysis routines and simulated wind inputs[12]. AeroDyn offers two models for evaluation of the wind turbine impact effects:

- the blade element momentum theory - classical standard methodology used by most wind turbine design enterprises
- the generalized theory of dynamic stimulation - recently developed model for analysing skewed and unsteady impact dynamics [13].

3.6.3. TurbSim

TurbSim is a randomly determined, full-field, turbulent-wind simulator. It bases on a statistical wind model to numerically generate time series of 3-D windspeed vector at points being a part of a 2-D vertical grid that is fastened in space. TurbSim produces data used as input into AeroDyn[14].

4. FATIGUE, ULTIMATE STRENGTH AND DYNAMIC ANALYSIS

4.1. Introduction

This chapter presents a fatigue, ultimate strength and dynamic computational procedure of jacket support structure OC4. The fatigue analysis goal is to apply damage to chosen structural member and afterwards, conduct an inspection of damage distribution among remaining elements. The ultimate strength analysis is carried out in order to check the strength utilization in structural members and resistivity to possible exceedance. The natural frequency analysis concerns verification of allowable frequency range and difference of jacket substructure behavior in eigenmode between undamaged and damaged structure.

The simulations were conducted in Fedem Windpower (ver. R7.1.1., Fedem Technology AS, Norway). All the post-processing calculations were performed using custom code in Matlab (ver. R2013a, The Mathworks, Inc., Natick, MA, USA).

The complete investigation of fatigue limit state (FLS) and ultimate limit state (ULS) considering different load and state cases results in enormous number of time-consuming simulations. Due to limited time and computer capacity, number of design load cases were reduced. The analysis embraces only 3 design load cases, nevertheless, they were selected cautiously and lead to interesting conclusions.

4.2. Design Load Cases

The Design Load Cases (DLC) were adapted from guideline *IEC 61400-3* [3]. It should be noted that some simplification were introduced. The analysis is performed considering the following assumptions:

- no wind and wave misalignment
- wind and waves uni-directional, co-directional
- no currents

Co-directionality assumes that waves are always coming from the same direction as wind whereas uni-directionality means that wind and waves loads act from a single direction. This aforementioned assumptions excludes wind and wave misalignment.

Currents influence on substructure is insignificant and hence, negligible.

Design situation	DLC	Wind conditions	Waves conditions	Wind and waves directionality	Water level	Type of analysis
Power production	1.2	NTM $V_{in} < V_{hub} < V_{cut}$ $V_{hub} = 4\text{m/s}, 6\text{m/s} \dots 24\text{m/s}$	NSS $H_s = E[H_s V_{hub}]$	COD, UNI	MSL	FATIGUE
	1.3	ETM $V_{in} < V_{hub} < V_{cut}$ $V_{hub} = 4\text{m/s}, 6\text{m/s} \dots 24\text{m/s}$	NSS $H_s = E[H_s V_{hub}]$	COD, UNI	MSL	ULTIMATE STRENGTH
Parked (standing still or idling)	6.1a	EWM $V_{hub} = 42.73\text{m/s}$	ESS $H_s = 9.4\text{m}$	COD, UNI	HSWL	ULTIMATE STRENGTH

Legend

V_{in} -cut in wind speed [m/s] NTM- normal turbulence model NSS- normal sea state COD- co-directional MSL- mean sea level
 V_{out} -cut out wind speed [m/s] ETM- extreme turbulence model ESS- extreme sea state UNI- uni-directional HSLWL- highest still water level
 V_{hub} -wind speed at hub height [m/s] EWM- extreme wind speed model
 H_s -significant wave height [m]

Table 4.1. Overview of design load cases

In DLC 1.2 a fatigue analysis is performed when offshore wind turbine is running and connected to electrical load. The DLC 1.2 assumes that OWT is subjected to environmental loads i.e. atmospheric normal turbulence (NTM) and normal stochastic sea state (NSS) during normal operation of OWT throughout designed lifetime.

In DLC 1.3 an ultimate strength analysis is carried out during normal power production. DLC 1.3 is similar to DLC 1.2 except that an extreme turbulence (ETM) conditions are prescribed.

In DLC 6.1a an ultimate strength analysis is performed. However, a combination of extreme wind and waves conditions is assumed when an offshore wind turbine is standing still or idling.

In DLC 6.1a extreme wind speed is used and a water level is increased to highest still water level (3.29 m).

4.3. Model preparation

4.3.1. Wind and wave input

DLC 1.2 and DLC 1.3 are calculated based on Table 4.2. Wind and waves loads listed in that table are adapted from lumped load cases table (*UpWind Design Basis* [8]), where wind speeds are sorted in 2m/s bins.

V[m/s]	TI[%]		Hs [m]	Tp [s]	Peakness[-]		f [%]	Occ./year [hrs]	Scaled f [%]	Scaled Occ./year [hrs]
	normal	extreme			Fatigue	Extreme				
4	20,4	53,1	1,1	5,88	1	3,3	0,08911	780,6	0,09621	842,8
6	17,5	37,1	1,18	5,76	1	3,3	0,14	1230,6	0,15115	1324,0
8	16	30	1,31	5,67	1	3,3	0,13923	1219,7	0,15032	1316,8
10	15,2	25,4	1,48	5,74	1	3,3	0,1444	1264,9	0,15590	1365,7
12	14,6	22,3	1,7	5,88	1	3,3	0,12806	1121,8	0,13826	1211,1
14	14,2	20,1	1,91	6,07	1	3,3	0,10061	881,3	0,10862	951,5
16	13,9	18,5	2,19	6,37	1	3,3	0,07554	661,7	0,08155	714,4
18	13,6	17,2	2,47	6,71	1	3,3	0,04878	427,3	0,05266	461,3
20	13,4	16,1	2,76	6,99	1	3,3	0,03151	276,1	0,03402	298,0
22	13,3	15,3	3,09	7,4	1	3,3	0,01924	168,6	0,02077	182,0
24	13,1	14,6	3,42	7,8	1	3,3	0,00977	85,6	0,01055	92,4

Table 4.2. Lumped environmental loads of the offshore wind turbine site

Turbulence intensities (TI) are dependent on offshore wind turbine class. In this study, class IC are established according to guideline IEC-61400[3]. Listed values of TI are used to create normal or extreme turbulence model. Detailed weather conditions (NTM, ETM) are simulated respectively by the TurbSim unit for the purpose of this thesis.

Significant height (Hs), peak period (Ts) and peakness factor are used in Pierson-Moskowitz spectrum to describe sea state. For the DLC 1.2 a Pierson-Moskowitz spectrum has a peakness factor of 1.0. whereas for the DLC 1.3 a peakness factor of 3.3 is applied [8].

Table consist of columns with probability of occurrence and occurrence per year in hours for wind speed and corresponding waves. However, values for probability and occurrence per year are inaccurate in the Table 4.2 as it shows only loads used in computations and therefore they have to be scaled. Total number of damage registered over a period of time will depend on the damage resulting from particular wind conditions and the fraction of time that those various conditions take place. Therefore, the wind speed distribution is an important factor which has to be considered. Wind distribution with Weibull distribution curve is presented in Fig. 4.1. Scaled values are used later in fatigue assessment.

DLC 6.1a is based on Table 4.3 adapted from extreme wave conditions table [8]. The table consists of wind speed and wave height with 50 years recurrence period and its peak period.

Parameter	Value	Unit
V_{50}	42.73	m/s
$H_{s,50}$	9.40	m
$T(H_{s,50})$	13.7	s

Table 4.3. Extreme conditions

4.3.2. Wind speed distributions

Initial and scaled wind speed distribution are based on probability of occurrence from the Table 4.2. Weibull distribution was created according to Weibull distribution parameters from the Table 4.4.

Wind speed distribution	Scale parameter a	Shape parameter b
Baseline wind speed distribution	0.02699	2.04
Scaled wind speed distribution	0.01626	2.312

Table 4.4. Weibull distribution parameters obtained from Matlab Curve Fitting Tool

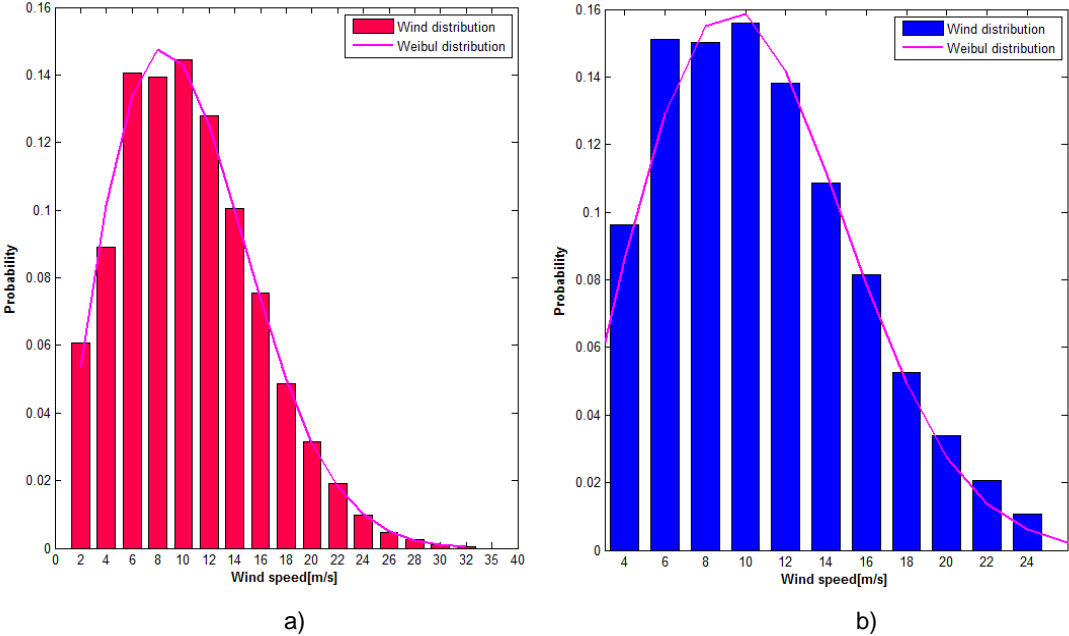


Fig. 4.1. Wind speed distribution for the measurement location

- a) Baseline wind speed distribution
- b) Scaled wind speed distribution

4.3.3. State structure cases

The analysis assumes performing simulations for intact (undamaged) state structure and two damaged state structure cases according to design load cases (Table 4.1). It results in 253 one hour simulations.

Design situation	DLC	Structure state cases	Wind conditions	Type of analysis	Total number of simulations
Power production	1.2	Intact (1)	Different wind speeds (11) $V_{hub} = 4\text{ m/s}, 6\text{ m/s}, 8\text{ m/s}, 10\text{ m/s}, 12\text{ m/s}, 14\text{ m/s}, 16\text{ m/s}, 18\text{ m/s}, 20\text{ m/s}, 22\text{ m/s}, 24\text{ m/s}$	FATIGUE	121
		Damaged X-brace 86 (5) $E = [0.1, 0.3, 0.5, 0.7]E_0$ Free-joint mechanism			
		Damaged X-brace 45 (5) $E = [0.1, 0.3, 0.5, 0.7]E_0$ Free-joint mechanism			
	1.3	Intact (1)	Different wind speeds (11) $V_{hub} = 4\text{ m/s}, 6\text{ m/s}, 8\text{ m/s}, 10\text{ m/s}, 12\text{ m/s}, 14\text{ m/s}, 16\text{ m/s}, 18\text{ m/s}, 20\text{ m/s}, 22\text{ m/s}, 24\text{ m/s}$	ULTIMATE STRENGTH	121
		Damaged X-brace 86 (5) $E = [0.1, 0.3, 0.5, 0.7]E_0$ Free-joint mechanism			
		Damaged X-brace 45 (5) $E = [0.1, 0.3, 0.5, 0.7]E_0$ Free-joint mechanism			
Parke d (standing still or idling)	6.1a	Intact (1)	Extreme wind speed (1) $V_{hub} = 42.73\text{ m/s}$	ULTIMATE STRENGTH	11
		Damaged X-brace 86 (5) $E = [0.1, 0.3, 0.5, 0.7]E_0$ Free-joint mechanism			
		Damaged X-brace 45 (5) $E = [0.1, 0.3, 0.5, 0.7]E_0$ Free-joint mechanism			

Table 4.5. Overview of performed simulations

Damage is applied by stiffness reduction and applying free-joint mechanism to X-brace number 86 at the water level and X-brace number 45 at the lowest level of jacket substructure (Fig. 4.2). Damage of first element can imitate the result of a collision with ship whereas second one is suspected to experience high vibrations, due to harmonic frequencies governed by rotor blades. Harmonic frequencies may be coupled with local vibration of X-brace, because selected brace is one of the longest and therefore, have the lowest natural frequency [38].

A wind turbine NREL 5MW and jacket substructure OC4 were implemented in FEDEM software. The turbine blades, tower, jacket substructure, and pile members were modeled as flexible linear beam elements, while the transition piece was represented as a rigid body [37].

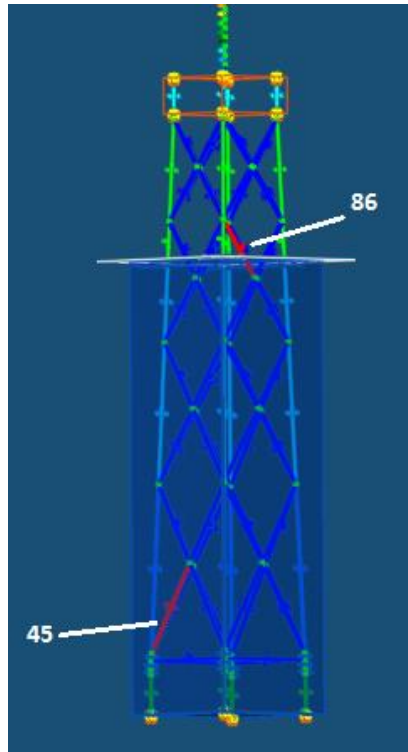


Fig. 4.2. Jacket support structure model with marked damaged members

According to *Fedem User's Guide*[1] flexible linear beam is represented by two-noded finite element beam. Its stiffness matrix is based on Euler-Bernoulli beam theory and therefore, scaling dynamic properties of each individual beam is possible. This option allows to apply damage in a selected structural members by reducing stiffness scale. The intensity of the structural member damage was varied by changing the Young's modulus (elastic modulus) in steps 0.2 over the range of 0.1-0.7 of the full value. The effect remains for the entire simulation. The free-joint mechanism is inserted in the middle of chosen brace and it has six degrees of freedom. It means that beam in this point may rotate and displace in any direction without constraints. From technical point of view, the beam is splitted into two elements and the mechanism is attached to ends of newly created beams (Fig. 4.3). In other words, free-joint mechanism reflects a crack along the whole cross-section. The effect of free-joint mechanism insertion remains for the entire simulation.

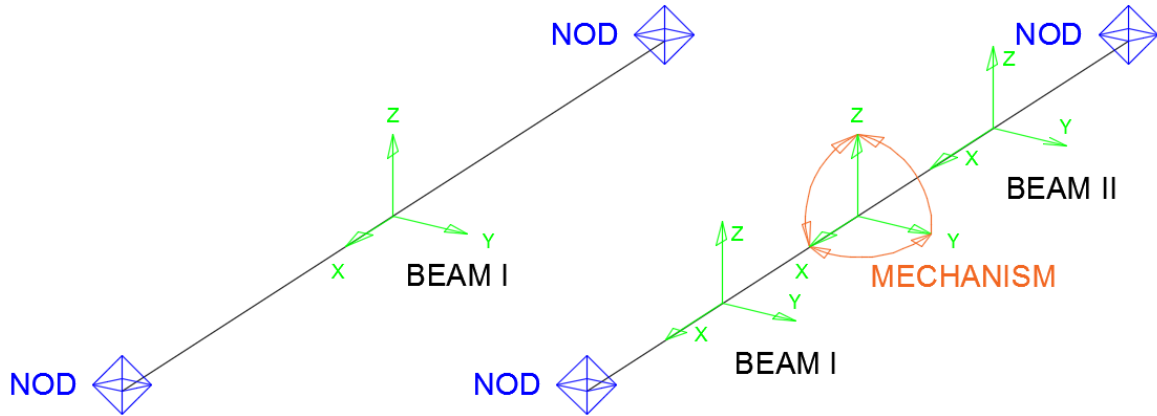


Fig. 4.3. Scheme of free-joint mechanism

In order to provide simpler orientation through presented results, calculated damage cases are numbered and listed in the Table 4.6.

Case	Design load case	Type of analysis	Damaged element	Type of damage
0	DLC 1.2	Fatigue	-	-
1			X-brace 45	$E=0.7E_0$
2			X-brace 45	$E=0.5E_0$
3			X-brace 45	$E=0.3E_0$
4			X-brace 45	$E=0.1E_0$
5			X-brace 45	Free-joint
6			X-brace 86	$E=0.7E_0$
7			X-brace 86	$E=0.5E_0$
8			X-brace 86	$E=0.3E_0$
9			X-brace 86	$E=0.1E_0$
10	X-brace 86	Free-joint		

Table 4.6. Denotation of structural damage cases

4.4. Fatigue analysis

This section consists of fatigue assessment conducted for jacket support structure, with the designed lifetime of 20 years. However, fatigue analysis approach presented hereinafter slightly differs from the one presented in section 3.3. The analysis assumes a comparison between various structural states therefore some part of recommended procedure may be dropped.

Fatigue analysis was conducted in accordance with DLC 1.2. Wind and wave data was extracted from Table 4.2 and inserted as an input to model. Jacket support structure model consists of 116 structural members, 29 members per side (excluding piles).

Analysis consists of 121 simulations considering 11 different wind speeds and 11 different state structures. A comparison method is based on so called, 'Equivalent Fatigue Load' ratio.

4.4.1. Loading time series

Loads time series were extracted from the response of the structure simulated in Fedem Windpower Software, as stated in section 3.3.2. In order to exclude transient loads from response time history, response analysis were performed for 3800 seconds and first 200 seconds were cut off. Eventually, it resulted in loads time series lasting for 3600 seconds and comprising axial force, in- and out - bending moment. Local coordinate system is presented in the Fig. 4.3. Simulations accuracy was set to 0.025 time increment, which means 40 time steps per 1 second of simulation.

For simplicity, in-plane bending moment M_y and out-bending moment M_z were combined into equivalent bending moment according to the formula :

$$M = \sqrt{M_y^2 + M_z^2} \quad (4.1)$$

4.4.2. Sectional stress time series and HSS time series

The main concept of this fatigue analysis concerns a comparison between undamaged and damaged state structure using EFL ratio. In general, EFL ratio is a factor used to equate an equivalent load occurring in structural member with and without damage during examined time. EFL ratio is further discussed in section 4.4.4.

Although structural damage is modeled by stiffness reduction or free-joint mechanism, the geometry of the entire system remains conserved. This implies that stress concentration factors (SCFs) listed in equations (3.23-3.30) are the same for both states of structure. According to section 3.3.7 EFL is expressed in stress units, but it is quite acceptable to use load (force or moment) instead of stress, because stress is proportional to load [7]. Due to conserved geometry and EFL's unit, analysis requires neither sectional stresses nor hot spot stresses calculations. According to Fig. 3.12 steps 3 and 4 may be skipped and the procedure goes directly to step 5.

4.4.3. Rainflow counting method

The next fatigue assessment step predicts an extraction of cycles and corresponding load cycles amplitudes from force and equivalent bending moment time series using rainflow counting

algorithm. Computations were carried out with rainflow counting code in Matlab. The script with rainflow counting algorithm may be found in Appendix D. The algorithm was prepared in such a way that upper boundary of subsequent load amplitude range constitutes multiplicity of one hundredth maximal load amplitude. Setting 0.5% of maximal load amplitude as first lower boundary, the algorithm acts as a filter and removes small cycles in a load process. It leads to 100 load amplitude ranges.

The number of half-cycles is counted into 100 bins assigned to respective amplitude range. In consequence, these bins create a load range histogram (Fig. 4.4).

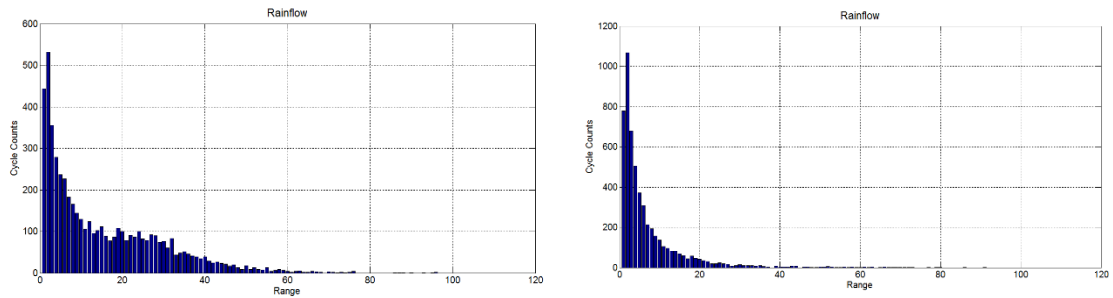


Fig. 4.4. Load range histogram

a) Force range histogram

b) Equivalent moment range histogram

Set of histograms like presented above were elaborated for jacket structural members.

More explanation on using the rainflow counting method may be found in section 3.3.5.

4.4.4. Equivalent fatigue load, EFL

EFL is expressed in force or equivalent bending moment units (kN or kNm) as mentioned in section 4.4.2. This implies that EFL definition (3.35) has slightly changed and EFL may be written as:

$$EFL = \sqrt[m]{\frac{\sum_{i=1}^j n_i \cdot (\Delta L_i)^m}{N}} \quad (4.2)$$

where:

EFL – equivalent fatigue load [kN, kNm]

ΔL_i – load range [kN, kNm]

m – negative inverse slope of the S-N curve

n_i – number of stress cycles in load block *i*

N – predicted number of cycles to failure for load range

Due to wind and wave loads, number of stress cycles in welded tubular joints can exceed annually 7×10^7 cycles [40]. According to table with S-N curve for tubular joints in seawater

with cathodic protection from DNV-RP-C203 [18], negative inverse slope for number of stress cycles more than 10^7 cycles equals $m=5$.

EFL diagrams expressed in force and moment units is shown below.

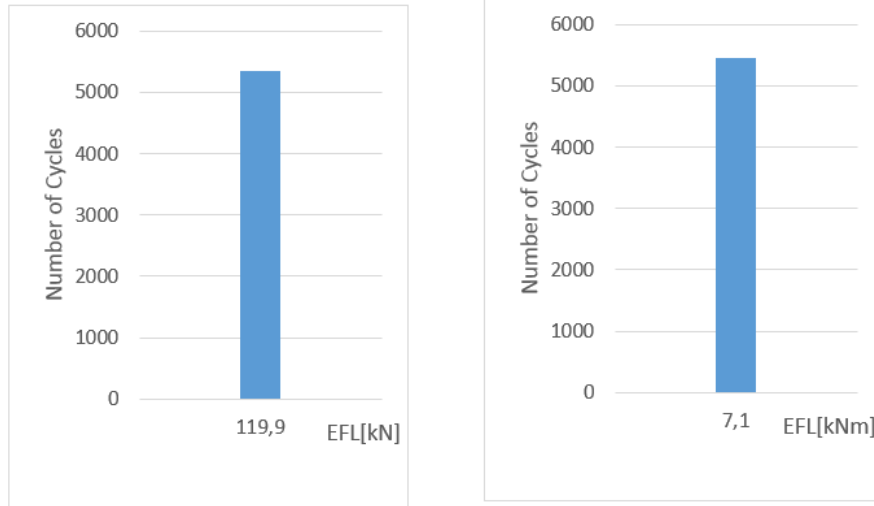


Fig. 4.5. EFL diagrams in force and moment units

Load amplitude ranges and corresponding rainflow cycles were extracted from a load range histogram for each structural member. EFL computations were combined with rainflow counting algorithm into one Matlab code which is included in Appendix D.

EFL ratio is dimensionless factor which denotes relation between equivalent load occurring in damaged structural member referred to undamaged one. EFL ratio equals 2 denotes that equivalent loads applied to joint in damaged state increased twice compared to joint in intact (undamaged) state.

EFL ratio is defined by the following equation:

$$EFL_{ratio} = \frac{EFL_D}{EFL_I} \quad (4.3)$$

where:

EFL_D – EFL in damaged structural member [kN,kNm]

EFL_I – EFL in intact(undamaged) structural member [kN,kNm]

As mentioned in section 3.3.1, wind speed distribution is crucial for fatigue assessment. EFL ratio as representative of fatigue loads, is multiplied by scaled probability of occurrence for respective wind speed bin basing on Table 4.2. Total EFL ratio may be calculated basing on the equation 4.5:

$$EFL_{TOT} = EFL_{ratio,1} \cdot f_{s,1} + EFL_{ratio,2} \cdot f_{s,2} + \dots + EFL_{ratio,n} \cdot f_{s,n} \quad (4.4)$$

where:

EFL_{TOT} – total equivalent fatigue ratio

$EFL_{ratio,1}$ – equivalent fatigue ratio at respective wind speed

$f_{s,n}$ – scaled probability of occurrence at respective wind speed

4.5. Ultimate strength analysis.

4.5.1. General

The ultimate strength analysis was conducted in accordance with DLC 1.3 and DLC 6.1a. For the DLC 1.3 wind and wave data was extracted from Table 4.2 whereas DLC 6.1 assumes extreme conditions from Table 4.3. Computations were conducted for two representative elements, which are subjected to extreme loads. The computations procedure complies with the guideline NORSOK N-004.

4.5.2. Load time series

First step of the ultimate strength analysis overlaps with the fatigue analysis step. As in fatigue assessment, loads are extracted from the response of the structure in time domain for each structural damaged case. Afterwards, highest values occurring in structural members are selected. The sample of sectional force and moment time series are presented in Fig. 4.6.

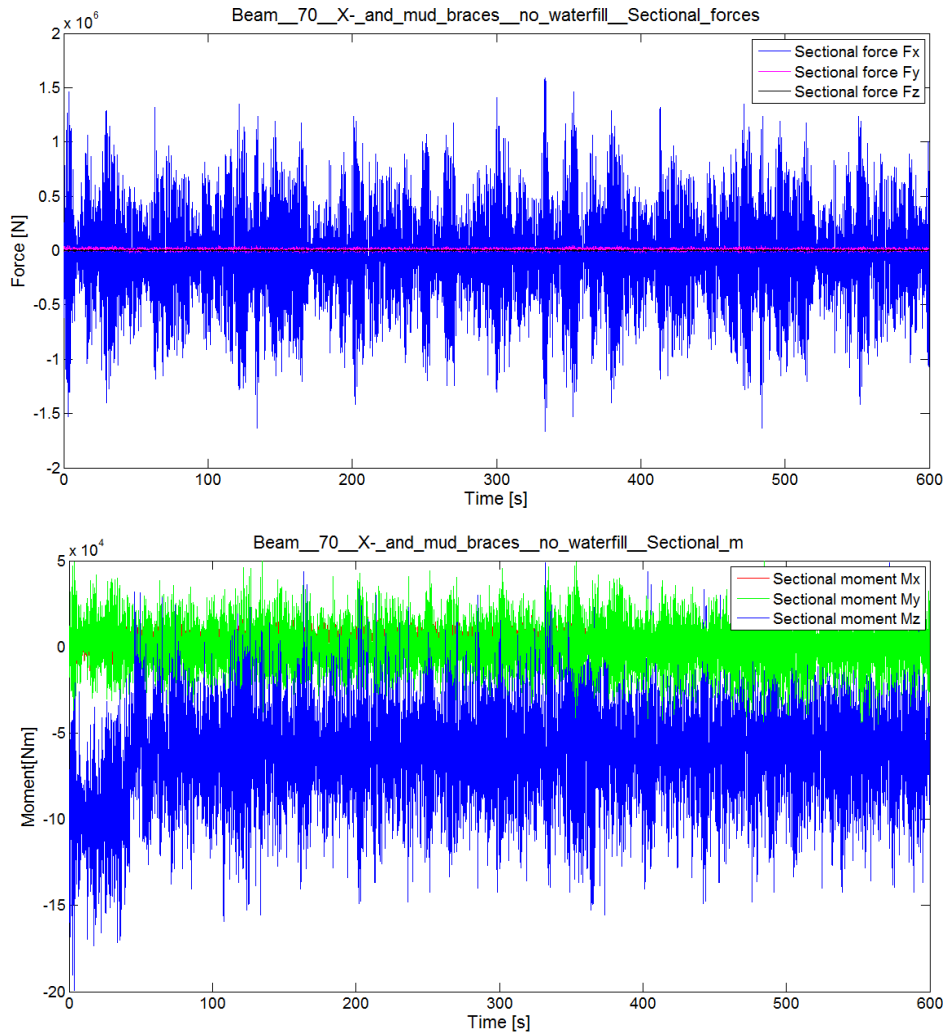


Fig. 4.6. Sample of sectional loads at the jacket cross-brace

The local coordinate system is shown in Fig.4.3.

4.5.3. Yield check

According to NORSOK N00-4[44], the strength analysis is relevant for structural members, which diameter-to-thickness ratio is no less than 120 and thickness of tubular section is no less than 6 mm.

Property set	Component	Outer diameter [m]	Thickness[mm]	Diameter to thickness ratio
1	x-and mud braces	0,80	20	40,00
2	leg at the lowest level	1,20	50	24,00
3	leg 2 to 4 level	1,20	35	34,29

Table 4.7. Tubular member properties

Basing on the Table 4.7 jacket members satisfy this criterions

Loads acting on offshore wind turbine modeled in Fedem Software has already included hydrostatic pressure. This means that there is no necessity to calculate tubular member strength with additional hydrostatic pressure.

Basic geometrical characteristic of tubular members are listed in Table 4.5.2.

Property set	D[mm]	t [mm]	A [cm ²]	G [kg/m]	I _y =I _z [cm ⁴]	W [cm ³]	i [cm]
1	800,000	20,000	490,088	384,719	372 957,313	9 323,933	27,586
2	1 200,000	50,000	1 806,416	1 418,036	2 991 876,129	49 864,602	40,697
3	1 200,000	35,000	1 280,984	1 144,294	2 175 191,580	36 253,193	41,208
4	1 200,000	40,000	1 457,699	1 005,579	2 454 765,101	40 912,752	41,037

Table 4.8. Geometrical characteristics of sections

The highest values extracted from all load cases were collected and multiplied by partial safety factor $\gamma_f=1.35$. From the guideline IEC 61400-3 recommended general safety factor for material is equal $\gamma_m=1.2$. Characteristic yield strength equals 240 MPa.

4.5.3.1. Design load case 1.3- Power production

Set 1 Case 5	Loads					
	F _x [kN]	F _y [kN]	F _z [kN]	M _x [kNm]	M _y [kNm]	M _z [kNm]
max	1 094,925	0,044	0,016	14,964	374,471	299,282
min	-1 121,538	-56,077	-56,077	-12,707	0,018	-254,147

Table 4.9. Design load – DLC 1.3, Set 1

4.5.3.1.1. Axial tension

$$N_{sd} = 1121,54 \text{ kN}$$

$$N_{t,rd} = \frac{A \cdot f_y}{\gamma_M} = \frac{490,088 \cdot 240}{1,2} = 9801,77 \text{ kN}$$

$$\frac{N_{sd}}{N_{t,Rd}} = \frac{1151,54}{9801,77} = 0,114 \leq 1,0$$

where:

N_{sd} - design axial force (tension positive) [kN]

f_y - characteristic yield strength [kN/cm²]

A - cross sectional area [cm²]

4.5.3.1.2. Axial compression

$$N_{sd} = 1094,93 \text{ kN}$$

$$N_{c,Rd} = \frac{A \cdot f_c}{\gamma_M} = \frac{490,088 \cdot 24}{1,2} = 9801,77 \text{ kN}$$

$$\frac{N_{Sd}}{N_{c,Rd}} = \frac{1094,93}{9801,77} = 0,112 \leq 1,0$$

4.5.3.1.3. Bending

$$M_{Sd,y} = 374,471 \text{ kNm}$$

$$M_{Rd} = \frac{f_m \cdot W}{\gamma_M} = \frac{24 \cdot 9323,933}{1,2} = 1864,787 \text{ kNm}$$

$$\frac{M_{Sd,y}}{M_{Rd}} = \frac{374,471}{1864,787} = 0,201 \leq 1,0$$

$$M_{Sd,z} = 299,282 \text{ kNm}$$

$$M_{Rd} = \frac{f_m \cdot W}{\gamma_M} = \frac{24 \cdot 9323,933}{1,2} = 1864,787 \text{ kNm}$$

$$\frac{M_{Sd,z}}{M_{Rd}} = \frac{299,282}{1864,787} = 0,160 \leq 1,0$$

where:

M_{Sd} - design bending moment [kNm]

f_m - characteristic bending strength [kN/cm²]

W - elastic section modulus [cm³]

4.5.3.1.4. Shear

$$V_{Sd,y} = 0,044 \text{ kN}$$

$$V_{Rd} = \frac{A \cdot f_y}{2\sqrt{3} \cdot \gamma_M} = \frac{490,088 \cdot 24}{2\sqrt{3} \cdot 1,2} = 2829,527 \text{ kN}$$

$$\frac{V_{Sd,y}}{V_{Rd}} = \frac{0,044}{2829,527} \cong 0,000 \leq 1,0$$

$$V_{Sd,z} = 0,016 \text{ kN}$$

$$V_{Rd} = \frac{A \cdot f_y}{2\sqrt{3} \cdot \gamma_M} = \frac{490,088 \cdot 24}{2\sqrt{3} \cdot 1,2} = 2829,527 \text{ kN}$$

$$\frac{V_{Sd,z}}{V_{Rd}} = \frac{0,016}{2829,527} \cong 0,000 \leq 1,0$$

where:

V_{Sd} - design shear force [kN]

f_y - characteristic yield strength [kN/cm²]

A - cross sectional area [cm²]

4.5.3.1.5. Axial tension and bending

$$\left(\frac{N_{Sd}}{N_{t,Rd}}\right)^{1,75} + \frac{\sqrt{M_{y,Sd}^2 + M_{z,Sd}^2}}{M_{Rd}} = \left(\frac{1121,538}{9801,769}\right)^{1,75} + \frac{\sqrt{374,471^2 + 299,282^2}}{1864,787} = 0,280$$

where:

$M_{y,Sd}$ - design bending moment about member y-axis (in-plane)

$M_{z,Sd}$ - design bending moment about member z-axis (out-of-plane)

N_{Sd} - design axial tensile force

4.5.3.1.6. Axial compression and bending

$$\frac{N_{Sd}}{N_{c,Rd}} + \frac{1}{M_{Rd}} \left\{ \left[\frac{C_{my} \cdot M_{y,Sd}}{1 - \frac{N_{Sd}}{N_{Ey}}} \right]^2 + \left[\frac{C_{mz} \cdot M_{z,Sd}}{1 - \frac{N_{Sd}}{N_{Ez}}} \right]^2 \right\}^{0,5}$$

$$= \frac{1121,538}{9801,769} + \frac{1}{1864,787} \left\{ \left[\frac{0,7 \cdot 374,471}{1 - \frac{1094,925}{120871,808}} \right]^2 + \left[\frac{0,7 \cdot 299,282}{1 - \frac{1094,925}{120871,808}} \right]^2 \right\}^{0,5} = 0,296$$

and

$$\frac{N_{Sd}}{N_{cl,Rd}} + \frac{\sqrt{M_{y,Sd}^2 + M_{z,Sd}^2}}{M_{Rd}} = \frac{1121,538}{9801,77} + \frac{\sqrt{374,471^2 + 299,282^2}}{1864,787} = 0,371$$

where:

N_{Sd} - design axial compression force

C_{my}, C_{mz} - reduction factors corresponding to the member y and z axes, respectively

N_{Ey}, N_{Ez} - Euler buckling strengths corresponding to the member y and z axes, respectively

$N_{cl,Rd} = \frac{f_{cl} \cdot A}{\gamma_M}$ - design axial local buckling resistance

$$N_{cl,Rd} = \frac{f_{cl} \cdot A}{\gamma_M} = \frac{490,088 \cdot 24}{1,2} = 9801,77 \text{ kN}$$

$$N_{Ey} = \frac{\pi^2 \cdot E \cdot A}{\left[\frac{k \cdot l}{i}\right]_y^2} = \frac{\pi^2 \cdot 21000 \cdot 490,088}{\left[\frac{0,7 \cdot 1142,4}{27,586}\right]_y^2} = 120871,808 \text{ kN}$$

$$N_{Ez} = \frac{\pi^2 \cdot E \cdot A}{\left[\frac{k \cdot l}{i}\right]_z^2} = \frac{\pi^2 \cdot 21000 \cdot 490,088}{\left[\frac{0,7 \cdot 1142,4}{27,586}\right]_z^2} = 120871,808 \text{ kN}$$

Interaction shear and bending moment

$$\frac{M_{Sd,y}}{M_{Rd}} = \frac{374,471}{1864,787} = 0,201 \leq 1,0 \quad \text{for} \quad \frac{V_{Sd,y}}{V_{Rd}} = \frac{0,044}{2829,527} \cong 0,000 \leq 0,4$$

$$\frac{M_{Sd,z}}{M_{Rd}} = \frac{299,282}{1864,787} = 0,160 \leq 1,0 \quad \text{for} \quad \frac{V_{Sd,z}}{V_{Rd}} = \frac{0,016}{2829,527} \cong 0,000 \leq 0,4$$

Set 3	Loads					
Case 10	Fx [kN]	Fy [kN]	Fz [kN]	Mx [kNm]	My [kNm]	Mz [kNm]
max	12 473,758	0,754	0,202	34,501	775,864	690,012
min	-12 459,483	-622,974	-622,974	-33,590	0,000	-671,793

Table 4.10. Design load – DLC 1.3, Set 3

4.5.3.1.7. Axial tension

$$N_{Sd} = 12\,459,483 \text{ kN}$$

$$N_{t,Rd} = \frac{A \cdot f_y}{\gamma_M} = \frac{1280,984 \cdot 24}{1,2} = 25619,688 \text{ kN}$$

$$\frac{N_{Sd}}{N_{t,Rd}} = \frac{12\,459,483}{25619,688} = 0,486 \leq 1,0$$

where:

N_{Sd} - design axial force (tension positive) [kN]

f_y - characteristic yield strength [kN/cm²]

A - cross sectional area [cm²]

4.5.3.1.8. Axial compression

$$N_{Sd} = 12473,758 \text{ kN}$$

$$N_{c,Rd} = \frac{A \cdot f_c}{\gamma_M} = \frac{1280,984 \cdot 24}{1,2} = 25619,688 \text{ kN}$$

$$\frac{N_{Sd}}{N_{c,Rd}} = \frac{12473,758}{25619,688} = 0,487 \leq 1,0$$

4.5.3.1.9. Bending

$$M_{Sd,y} = 775,864 \text{ kNm}$$

$$M_{Rd} = \frac{f_m \cdot W}{\gamma_M} = \frac{24 \cdot 36253,193}{1,2} = 7250,639 \text{ kNm}$$

$$\frac{M_{Sd,y}}{M_{Rd}} = \frac{775,864}{7250,639} = 0,107 \leq 1,0$$

$$M_{Sd,z} = 690,012 \text{ kNm}$$

$$M_{Rd} = \frac{f_m \cdot W}{\gamma_M} = \frac{24 \cdot 36253,193}{1,2} = 7250,639 \text{ kNm}$$

$$\frac{M_{Sd,z}}{M_{Rd}} = \frac{690,012}{7250,639} = 0,095 \leq 1,0$$

where:

M_{Sd} - design bending moment [kNm]

f_m - characteristic bending strength [kN/cm²]

W - elastic section modulus [cm³]

4.5.3.1.10. Shear

$$V_{Sd,y} = 0,754 \text{ kN}$$

$$V_{Rd} = \frac{A \cdot f_y}{2\sqrt{3} \cdot \gamma_M} = \frac{1280,984 \cdot 24}{2\sqrt{3} \cdot 1,2} = 7395,767 \text{ kN}$$

$$\frac{V_{Sd,y}}{V_{Rd}} = \frac{0,754}{7395,767} \cong 0,000 \leq 1,0$$

$$V_{Sd,z} = 0,202 \text{ kN}$$

$$V_{Rd} = \frac{A \cdot f_y}{2\sqrt{3} \cdot \gamma_M} = \frac{1280,984 \cdot 24}{2\sqrt{3} \cdot 1,2} = 7395,767 \text{ kN}$$

$$\frac{V_{Sd,z}}{V_{Rd}} = \frac{0,202}{7395,767} \cong 0,000 \leq 1,0$$

where:

V_{Sd} - design shear force [kN]

f_y - characteristic yield strength [kN/cm²]

A - cross sectional area [cm²]

4.5.3.1.11. Axial tension and bending

$$\left(\frac{N_{Sd}}{N_{t,Rd}}\right)^{1,75} + \frac{\sqrt{M_{y,Sd}^2 + M_{z,Sd}^2}}{M_{Rd}} = \left(\frac{12\,459,483}{25619,688}\right)^{1,75} + \frac{\sqrt{775,864^2 + 690,012^2}}{7250,639} = 0,426$$

where:

$M_{y,Sd}$ - design bending moment about member y-axis (in-plane)

$M_{z,Sd}$ - design bending moment about member z-axis (out-of-plane)

N_{Sd} - design axial tensile force

4.5.3.1.12. Axial compression and bending

$$\frac{N_{Sd}}{N_{c,Rd}} + \frac{1}{M_{Rd}} \left\{ \left[\frac{C_{my} \cdot M_{y,Sd}}{1 - \frac{N_{Sd}}{N_{Ey}}} \right]^2 + \left[\frac{C_{mz} \cdot M_{z,Sd}}{1 - \frac{N_{Sd}}{N_{Ez}}} \right]^2 \right\}^{0,5}$$

$$= \frac{12473,758}{25619,688} + \frac{1}{7250,639} \left\{ \left[\frac{0,7 \cdot 775,864}{1 - \frac{12473,758}{131260,627}} \right]^2 + \left[\frac{0,7 \cdot 690,012}{1 - \frac{12473,758}{131260,627}} \right]^2 \right\}^{0,5} = 0,600$$

and

$$\frac{N_{Sd}}{N_{cl,Rd}} + \frac{\sqrt{M_{y,Sd}^2 + M_{z,Sd}^2}}{M_{Rd}} = \frac{12473,758}{25619,688} + \frac{\sqrt{775,864^2 + 690,012^2}}{7250,639} = 0,630$$

where:

N_{Sd} - design axial compression force

C_{my}, C_{mz} - reduction factors corresponding to the member y and z axes, respectively

N_{Ey}, N_{Ez} - Euler buckling strengths corresponding to the member y and z axes, respectively

$N_{cl,Rd} = \frac{f_{cl} \cdot A}{\gamma_M}$ - design axial local buckling resistance

$$N_{cl,Rd} = \frac{f_{cl} \cdot A}{\gamma_M} = \frac{1280,984 \cdot 24}{1,2} = 25619,688 \text{ kN}$$

$$N_{Ey} = \frac{\pi^2 \cdot E \cdot A}{\left[\frac{k \cdot l}{i} \right]_y^2} = \frac{\pi^2 \cdot 21000 \cdot 1280,984}{\left[\frac{1,0 \cdot 1853,28}{41,208} \right]_y^2} = 131260,627 \text{ kN}$$

$$N_{Ez} = \frac{\pi^2 \cdot E \cdot A}{\left[\frac{k \cdot l}{i} \right]_z^2} = \frac{\pi^2 \cdot 21000 \cdot 1280,984}{\left[\frac{1,0 \cdot 1853,28}{41,208} \right]_y^2} = 131260,627 \text{ kN}$$

4.5.3.1.13. Interaction shear and bending moment

$$\frac{M_{Sd,y}}{M_{Rd}} = \frac{775,864}{7250,639} = 0,107 \leq 1,0 \quad \text{for} \quad \frac{V_{Sd,y}}{V_{Rd}} = \frac{0,754}{7395,767} \cong 0,000 \leq 0,4$$

$$\frac{M_{Sd,z}}{M_{Rd}} = \frac{690,012}{7250,639} = 0,095 \leq 1,0 \quad \text{for} \quad \frac{0,202}{7395,767} \cong 0,000 \leq 0,4$$

4.5.3.2. Design load case 6.1a - Parked(standing still or idling)

Set 1	Loads					
Case 10	F _x [kN]	F _y [kN]	F _z [kN]	M _x [kNm]	M _y [kNm]	M _z [kNm]
max	1 799,864	0,092	0,033	14,121	324,359	282,420
min	-1 826,853	-91,343	-91,343	-14,091	0,000	-281,818

Table 4.11. Design load – DLC 6.1a, Set 1

4.5.3.2.1. Axial tension

$$N_{Sd} = 1826,853 \text{ kN}$$

$$N_{t,Rd} = \frac{A \cdot f_y}{\gamma_M} = \frac{490,088 \cdot 24}{1,2} = 9801,77 \text{ kN}$$

$$\frac{N_{Sd}}{N_{t,Rd}} = \frac{1826,853}{9801,77} = 0,186 \leq 1,0$$

where:

N_{Sd} - design axial force (tension positive) [kN]

f_y - characteristic yield strength [kN/cm²]

A - cross sectional area [cm²]

4.5.3.2.2. Axial compression

$$N_{Sd} = 1799,864 \text{ kN}$$

$$N_{c,Rd} = \frac{A \cdot f_c}{\gamma_M} = \frac{490,088 \cdot 24}{1,2} = 9801,77 \text{ kN}$$

$$\frac{N_{Sd}}{N_{c,Rd}} = \frac{1799,864}{9801,77} = 0,184 \leq 1,0$$

4.5.3.2.3. Bending

$$M_{Sd,y} = 324,359 \text{ kNm}$$

$$M_{Rd} = \frac{f_m \cdot W}{\gamma_M} = \frac{24 \cdot 9323,933}{1,2} = 1864,787 \text{ kNm}$$

$$\frac{M_{Sd,y}}{M_{Rd}} = \frac{324,359}{1864,787} = 0,174 \leq 1,0$$

$$M_{Sd,z} = 282,420 \text{ kNm}$$

$$M_{Rd} = \frac{f_m \cdot W}{\gamma_M} = \frac{24 \cdot 9323,933}{1,2} = 1864,787 \text{ kNm}$$

$$\frac{M_{Sd,z}}{M_{Rd}} = \frac{282,420}{1864,787} = 0,151 \leq 1,0$$

where:

M_{Sd} - design bending moment [kNm]

f_m - characteristic bending strength [kN/cm²]

W - elastic section modulus [cm³]

4.5.3.2.4. Shear

$$V_{Sd,y} = 0,092 \text{ kN}$$

$$V_{Rd} = \frac{A \cdot f_y}{2\sqrt{3} \cdot \gamma_M} = \frac{490,088 \cdot 24}{2\sqrt{3} \cdot 1,2} = 2829,527 \text{ kN}$$

$$\frac{V_{Sd,y}}{V_{Rd}} = \frac{0,092}{2829,527} \cong 0,000 \leq 1,0$$

$$V_{Sd,z} = 0,033 \text{ kN}$$

$$V_{Rd} = \frac{A \cdot f_y}{2\sqrt{3} \cdot \gamma_M} = \frac{490,088 \cdot 24}{2\sqrt{3} \cdot 1,2} = 2829,527 \text{ kN}$$

$$\frac{V_{Sd,z}}{V_{Rd}} = \frac{0,033}{2829,527} \cong 0,000 \leq 1,0$$

where:

V_{Sd} - design shear force [kN]

f_y - characteristic yield strength [kN/cm²]

A - cross sectional area [cm²]

4.5.3.2.5. Axial tension and bending

$$\left(\frac{N_{Sd}}{N_{t,Rd}} \right)^{1,75} + \frac{\sqrt{M_{y,Sd}^2 + M_{z,Sd}^2}}{M_{Rd}} = \left(\frac{1826,853}{9801,769} \right)^{1,75} + \frac{\sqrt{324,359^2 + 282,420^2}}{1864,787} = 0,284$$

where:

$M_{y,Sd}$ - design bending moment about member y-axis (in-plane)

$M_{z,Sd}$ - design bending moment about member z-axis (out-of-plane)

N_{Sd} - design axial tensile force

4.5.3.2.6. Axial compression and bending

$$\frac{N_{Sd}}{N_{c,Rd}} + \frac{1}{M_{Rd}} \left\{ \left[\frac{C_{my} \cdot M_{y,Sd}}{1 - \frac{N_{Sd}}{N_{Ey}}} \right]^2 + \left[\frac{C_{mz} \cdot M_{z,Sd}}{1 - \frac{N_{Sd}}{N_{Ez}}} \right]^2 \right\}^{0,5}$$

$$= \frac{1826,853}{9801,769} + \frac{1}{1864,787} \left\{ \left[\frac{0,7 \cdot 324,359}{1 - \frac{1826,853}{120871,808}} \right]^2 + \left[\frac{0,7 \cdot 282,420}{1 - \frac{1826,853}{120871,808}} \right]^2 \right\}^{0,5} = 0,350$$

and

$$\frac{N_{Sd}}{N_{cl,Rd}} + \frac{\sqrt{M_{y,Sd}^2 + M_{z,Sd}^2}}{M_{Rd}} = \frac{1826,853}{9801,769} + \frac{\sqrt{324,359^2 + 282,420^2}}{1864,787} = 0,417$$

where:

N_{Sd} - design axial compression force

C_{my}, C_{mz} - reduction factors corresponding to the member y and z axes, respectively

N_{Ey}, N_{Ez} - Euler buckling strengths corresponding to the member y and z axes, respectively

$N_{cl,Rd} = \frac{f_{cl} \cdot A}{\gamma_M}$ - design axial local buckling resistance

$$N_{cl,Rd} = \frac{f_{cl} \cdot A}{\gamma_M} = \frac{490,088 \cdot 24}{1,2} = 9801,77 \text{ kN}$$

$$N_{Ey} = \frac{\pi^2 \cdot E \cdot A}{\left[\frac{k \cdot l}{i} \right]_y^2} = \frac{\pi^2 \cdot 21000 \cdot 490,088}{\left[\frac{0,7 \cdot 1142,4}{27,586} \right]_y^2} = 120871,808 \text{ kN}$$

$$N_{Ez} = \frac{\pi^2 \cdot E \cdot A}{\left[\frac{k \cdot l}{i} \right]_z^2} = \frac{\pi^2 \cdot 21000 \cdot 490,088}{\left[\frac{0,7 \cdot 1142,4}{27,586} \right]_z^2} = 120871,808 \text{ kN}$$

4.5.3.2.7. Interaction shear and bending moment

$$\frac{M_{Sd,y}}{M_{Rd}} = \frac{324,359}{1864,787} = 0,174 \leq 1,0 \quad \text{for} \quad \frac{V_{Sd,y}}{V_{Rd}} = \frac{0,092}{2829,527} \cong 0,000 \leq 0,4$$

$$\frac{M_{Sd,z}}{M_{Rd}} = \frac{282,420}{1864,787} = 0,151 \leq 1,0 \quad \text{for} \quad \frac{V_{Sd,z}}{V_{Rd}} = \frac{0,033}{2829,527} \cong 0,000 \leq 0,4$$

Set 3 Case 10	Loads					
	Fx [kN]	Fy [kN]	Fz [kN]	Mx [kNm]	My [kNm]	Mz [kNm]
max	12 288,825	0,743	0,199	50,032	1 154,284	1 000,649
min	-12 274,551	-613,728	-613,728	-53,920	0,000	-1 078,406

Table 4.12. Design load – DLC 6.1a, Set 3

4.5.3.2.8. Axial tension

$$N_{sd} = 12\,274,551 \text{ kN}$$

$$N_{t,Rd} = \frac{A \cdot f_y}{\gamma_M} = \frac{1280,984 \cdot 24}{1,2} = 25619,688 \text{ kN}$$
$$\frac{N_{sd}}{N_{t,Rd}} = \frac{12\,274,551}{25619,688} = 0,479 \leq 1,0$$

where:

N_{sd} - design axial force (tension positive) [kN]

f_y - characteristic yield strength [kN/cm²]

A - cross sectional area [cm²]

4.5.3.2.9. Axial compression

$$N_{sd} = 12288,825 \text{ kN}$$

$$N_{c,Rd} = \frac{A \cdot f_c}{\gamma_M} = \frac{1280,984 \cdot 24}{1,2} = 25619,688 \text{ kN}$$
$$\frac{N_{sd}}{N_{c,Rd}} = \frac{12288,825}{25619,688} = 0,480 \leq 1,0$$

4.5.3.2.10. Bending

$$M_{sd,y} = 1154,284 \text{ kNm}$$

$$M_{Rd} = \frac{f_m \cdot W}{\gamma_M} = \frac{24 \cdot 36253,193}{1,2} = 7250,639 \text{ kNm}$$

$$\frac{M_{sd,y}}{M_{Rd}} = \frac{1154,284}{7250,639} = 0,159 \leq 1,0$$

$$M_{sd,z} = 1000,649 \text{ kNm}$$

$$M_{Rd} = \frac{f_m \cdot W}{\gamma_M} = \frac{24 \cdot 36253,193}{1,2} = 7250,639 \text{ kNm}$$

$$\frac{M_{sd,z}}{M_{Rd}} = \frac{1000,649}{7250,639} = 0,138 \leq 1,0$$

where:

M_{sd} - design bending moment [kNm]

f_m - characteristic bending strength [kN/cm²]

W - elastic section modulus [cm³]

4.5.3.2.11. Shear

$$V_{Sd,y} = 0,743 \text{ kN}$$

$$V_{Rd} = \frac{A \cdot f_y}{2\sqrt{3} \cdot \gamma_M} = \frac{1280,984 \cdot 24}{2\sqrt{3} \cdot 1,2} = 7395,767 \text{ kN}$$

$$\frac{V_{Sd,y}}{V_{Rd}} = \frac{0,743}{7395,767} \cong 0,000 \leq 1,0$$

$$V_{Sd,z} = 0,199 \text{ kN}$$

$$V_{Rd} = \frac{A \cdot f_y}{2\sqrt{3} \cdot \gamma_M} = \frac{1280,984 \cdot 24}{2\sqrt{3} \cdot 1,2} = 7395,767 \text{ kN}$$

$$\frac{V_{Sd,z}}{V_{Rd}} = \frac{0,199}{7395,767} \cong 0,000 \leq 1,0$$

where:

V_{Sd} - design shear force [kN]

f_y - characteristic yield strength [kN/cm²]

A - cross sectional area [cm²]

4.5.3.2.12. Axial tension and bending

$$\left(\frac{N_{Sd}}{N_{t,Rd}} \right)^{1,75} + \frac{\sqrt{M_{y,Sd}^2 + M_{z,Sd}^2}}{M_{Rd}} = \left(\frac{12\,274,551}{25619,688} \right)^{1,75} + \frac{\sqrt{1154,284^2 + 1000,649^2}}{7250,639} = 0,487$$

where:

$M_{y,Sd}$ - design bending moment about member y-axis (in-plane)

$M_{z,Sd}$ - design bending moment about member z-axis (out-of-plane)

N_{Sd} - design axial tensile force

4.5.3.2.13. Axial compression and bending

$$\frac{N_{Sd}}{N_{c,Rd}} + \frac{1}{M_{Rd}} \left\{ \left[\frac{C_{my} \cdot M_{y,Sd}}{1 - \frac{N_{Sd}}{N_{Ey}}} \right]^2 + \left[\frac{C_{mz} \cdot M_{z,Sd}}{1 - \frac{N_{Sd}}{N_{Ez}}} \right]^2 \right\}^{0,5}$$

$$= \frac{12\,274,551}{25619,688} + \frac{1}{7250,639} \left\{ \left[\frac{0,7 \cdot 1154,284}{1 - \frac{12\,274,551}{131260,627}} \right]^2 + \left[\frac{0,7 \cdot 1000,649}{1 - \frac{12\,274,551}{131260,627}} \right]^2 \right\}^{0,5} = 0,642$$

and

$$\frac{N_{Sd}}{N_{cl,Rd}} + \frac{\sqrt{M_{y,Sd}^2 + M_{z,Sd}^2}}{M_{Rd}} = \frac{12\,274,551}{25619,688} + \frac{\sqrt{1154,284^2 + 1000,649^2}}{7250,639} = 0,690$$

where:

N_{Sd} - design axial compression force

C_{my}, C_{mz} - reduction factors corresponding to the member y and z axes, respectively

N_{Ey}, N_{Ez} - Euler buckling strengths corresponding to the member y and z axes, respectively

$N_{cl,Rd} = \frac{f_{cl} \cdot A}{\gamma_M}$ - design axial local buckling resistance

$$N_{cl,Rd} = \frac{f_{cl} \cdot A}{\gamma_M} = \frac{1280,984 \cdot 24}{1,2} = 25619,688 \text{ kN}$$

$$N_{Ey} = \frac{\pi^2 \cdot E \cdot A}{\left[\frac{k \cdot l}{i}\right]_y^2} = \frac{\pi^2 \cdot 21000 \cdot 1280,984}{\left[\frac{1,0 \cdot 1853,28}{41,208}\right]_y^2} = 131260,627 \text{ kN}$$

$$N_{Ez} = \frac{\pi^2 \cdot E \cdot A}{\left[\frac{k \cdot l}{i}\right]_z^2} = \frac{\pi^2 \cdot 21000 \cdot 1280,984}{\left[\frac{1,0 \cdot 1853,28}{41,208}\right]_y^2} = 131260,627 \text{ kN}$$

4.5.3.2.14. Interaction shear and bending moment

$$\frac{M_{Sd,y}}{M_{Rd}} = \frac{1154,284}{7250,639} = 0,159 \leq 1,0 \quad \text{for} \quad \frac{V_{Sd,y}}{V_{Rd}} = \frac{0,743}{7395,767} \cong 0,000 \leq 0,4$$

$$\frac{M_{Sd,z}}{M_{Rd}} = \frac{1000,649}{7250,639} = 0,138 \leq 1,0 \quad \text{for} \quad \frac{0,199}{7395,767} \cong 0,000 \leq 0,4$$

4.6. Modal analysis

4.6.1. Allowable rotor frequency range

Offshore Wind Turbines current dynamic design recommendation consists in establishing rotor operation between 1P frequency and 3P frequency for three-bladed rotor. According to *Upwind Design basis* [8] examined support structure may be excited by rotor rotation frequency (1P) in frequency range between 0.115 Hz and 0.202 Hz. Offshore Wind Turbine allowable operation range lies between frequency 0.222 Hz and 0.31 Hz, because rotor frequency range includes additional 10% safety margin.

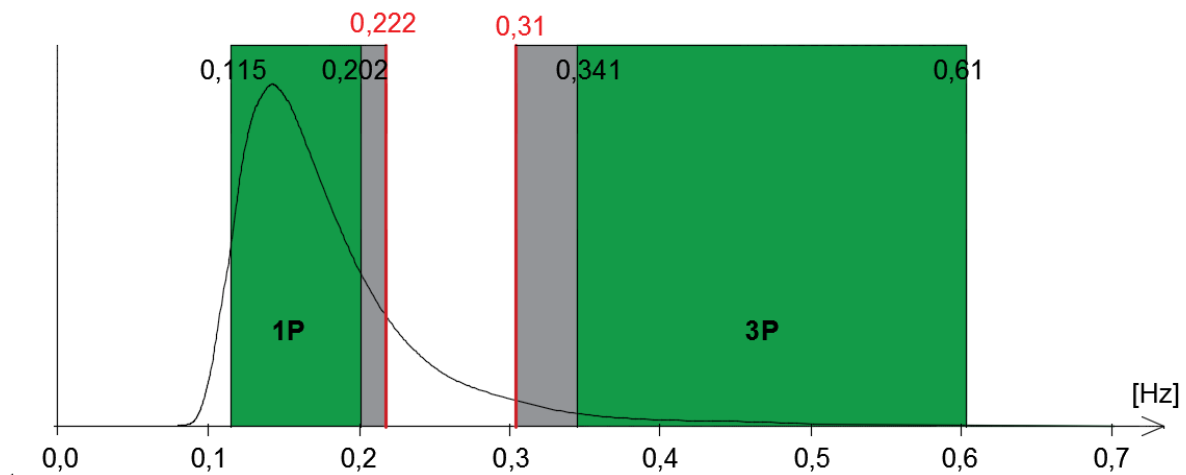


Fig. 4.7. Allowable rotor frequency range [8]

4.6.2. Campbell diagram and Modal analysis

A relation between natural frequencies of the construction and stimulation from the rotor may be analysed by means of a Campbell diagram. This chart consists of the most important natural frequencies of the turbine drawn horizontally as independent of a rotor speed. Lines corresponding to excitation frequency are applied above it as a function of a rotor speed. Intersection points determine operating speeds that should be avoided to prevent resonance. The example Campbell diagram for a three-bladed turbine is presented in Fig. 4.8. [31]

Eigenfrequencies are printed simply horizontally, however in reality they slightly change with the rotational speed of the rotor due to the centrifugal stiffening effect. The angled lines represent multiples of the frequencies 1P (generated by the rotor full revolution) and 3P (arising from the tower shadowing by the blades). [38]

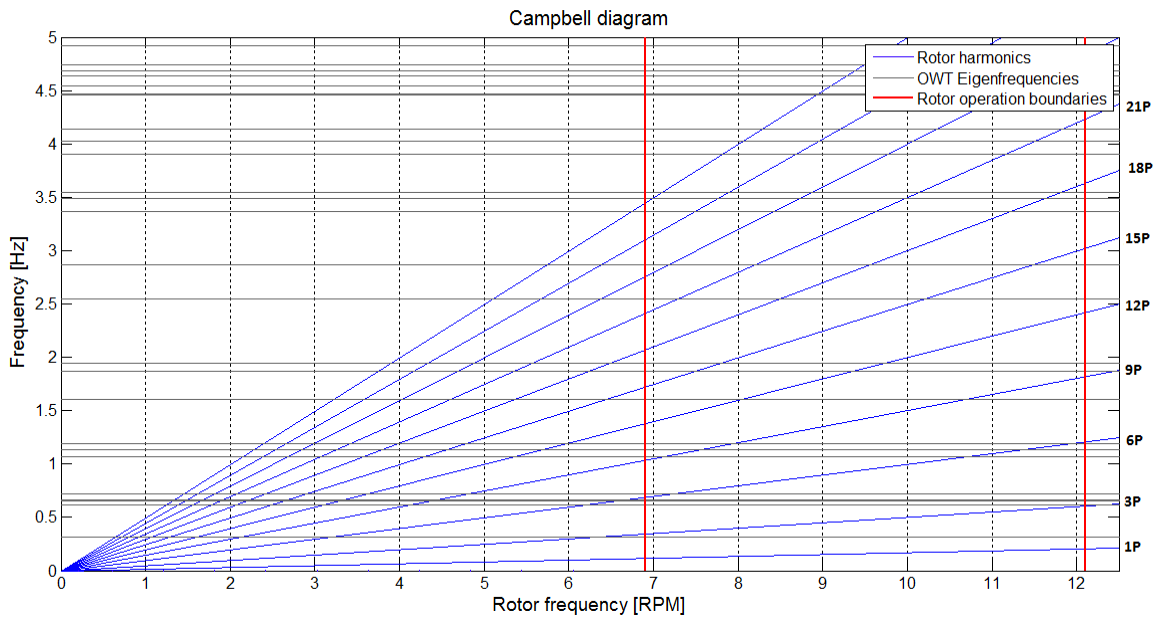
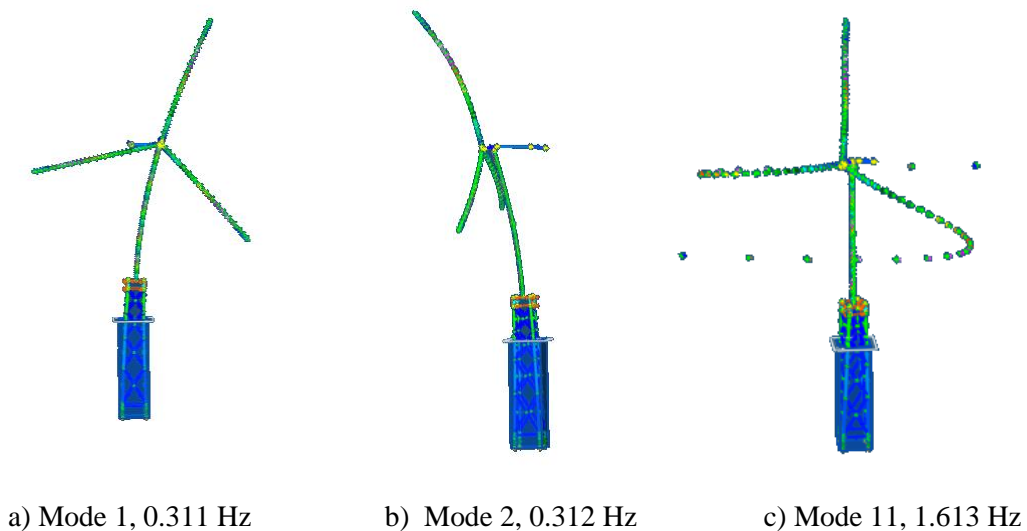
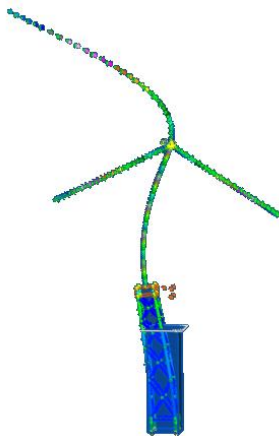
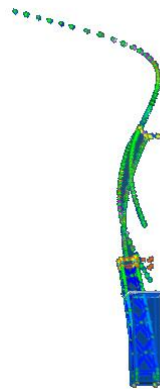
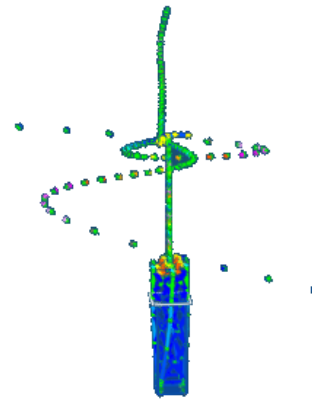


Fig. 4.8. Campbell diagram of the OWT model [38]

Red lines in the Fig. 4.8 present rotor operation range. It can be seen that rotor harmonics in this range does not intersect the first two eigenfrequencies (1P and 3P).

As it was stated in section 3.4, investigation of system vibration and natural frequencies is performed in order to protect OWT against premature failure. Detecting eigenfrequencies is crucial, because they may excite the system natural vibration modes, so called eigenmodes. Thus, the first step of modal analysis assumes eigenfrequencies extraction from FEDEM Windpower. First 50 eigenfrequencies in undamaged state structure as well as damaged are listed in Appendix F. Next important step of OWT natural frequency analysis includes natural bending and torsion modes of the tower. The side view of the mode shapes are presented in the Fig. 4.9.



1st Tower Side-to-Side1st Tower Fore-Aft1st Tower Torsiond) Mode 10, 1.18867 Hz
2nd Tower Side-to-Sidee) Mode 9, 1.15669 Hz
2nd Tower Fore-Aftf) Mode 14, 2.59462 Hz
2nd Tower Torsion**Fig. 4.9. 1st and 2nd Tower Eigenmodes**

Comparing to tower large displacements, jacket substructure deforms only for the first two eigenmodes [7]. Looking at the Fig. 4.9 it can be questionable, but quite easily to explain. In order to show OWT behavior in eigenmode, the mode shapes are presented in scale 1:10000.

Another method, which enables to check jacket structure behavior in a given frequency is a power spectral density (PSD). Power spectral density reveals strength of the energy as a function of frequency. The integral of the PSD over a given frequency range results in the average power within this frequency range. Particularly useful in structure analysis is displacement power spectral density (DPSD), which allows to calculate at which frequencies displacement is large and at which frequencies displacement is small. Exemplary DPSD plot is shown in Fig. 4.10.

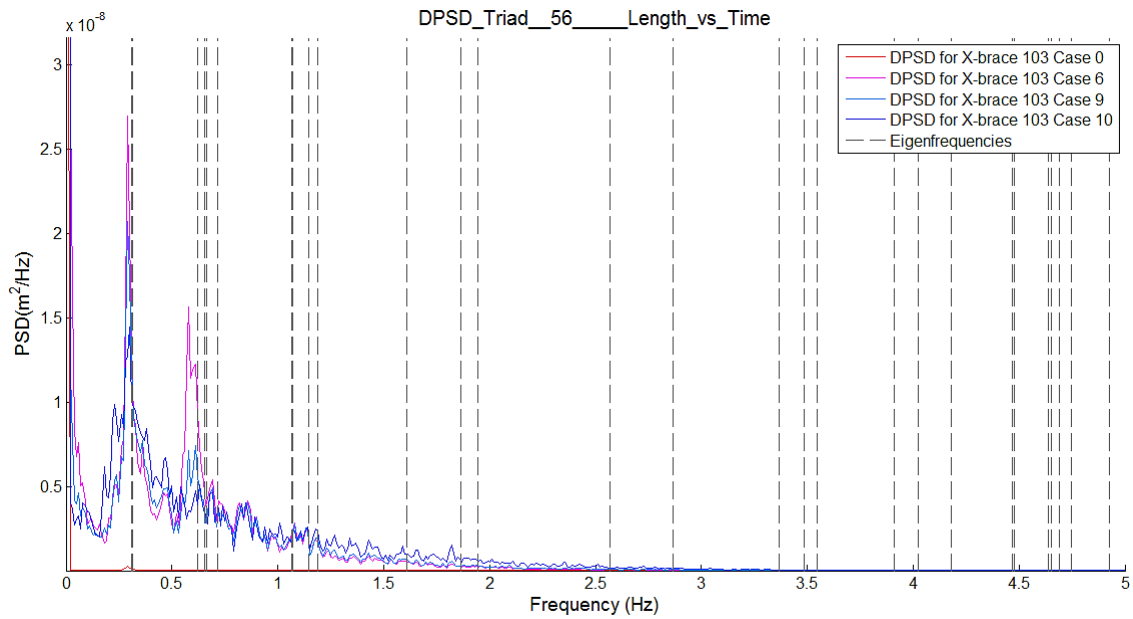


Fig. 4.10. Displacement power spectral density for X-brace 103
(deterministic wind speed $V=12\text{m/s}$, different structure states)

DPSD in Fig. 4.10 agrees with the statement that jacket substructure deforms significantly for first few eigenfrequencies only. The DPSD's peak may be found at eigenfrequency 0.3 Hz and between $0.6\div 0.7$ Hz. Red curve denotes DPSD for X-brace 103 in undamaged state and it shifts to much lower range than the others. This implies that the more damaged structure is, the more displacement in braces occur, however it should be further investigated.

From the Fig. 4.10 one can notice a gradual displacement decrease with increased frequency. It would be worth to change rotor operation range so as to omit first few eigenfrequencies.

In general, eigenfrequencies depend on structure shape and a material the structure is built of. According to vibration theory, stiffness reduction leads to natural frequency reduction and eigenmodes modification.

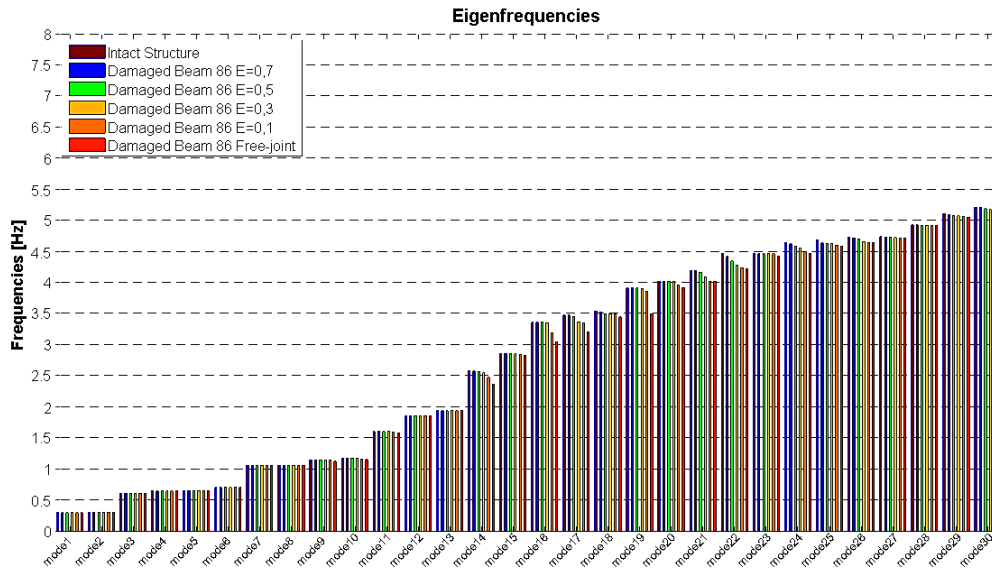


Fig. 4.11. Summary of eigenfrequencies in different structure states – beam 86

Analyzing 30 modes the maximal difference in eigenfrequencies is 2.16% (Mode 24) whereas for 50 modes the maximal difference in eigenfrequencies exceeds 8.01% (Mode 39).

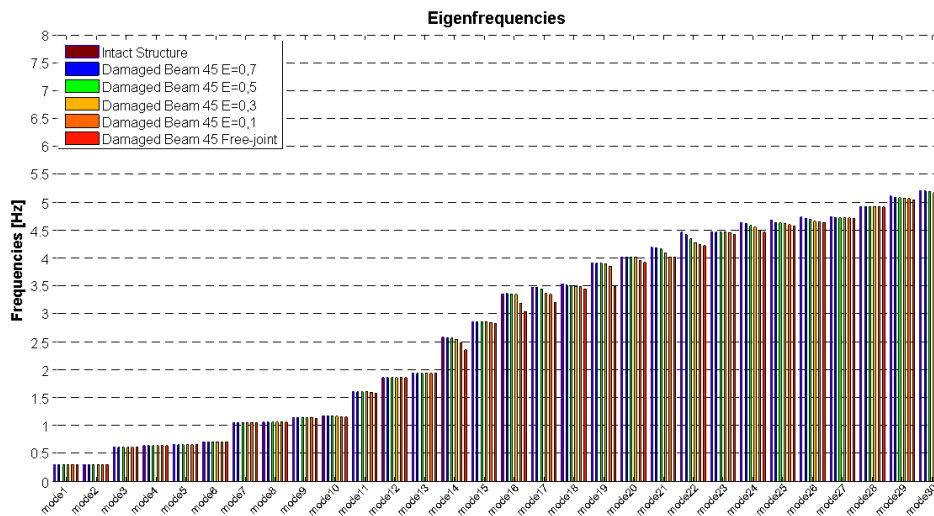


Fig. 4.12. Summary of eigenfrequencies in different structure states – beam 45

In the scope of 30 as well as 50 modes the maximum difference in eigenfrequencies is 11,9% (mode 19). Although the differences are relatively small, they should be taken into account in detailed analysis.

5. RESULTS

5.1. Fatigue analysis results

5.1.1. General

Fatigue analysis were conducted for both ends each structural member of jacket support structure, 232 positions in total. Equivalent fatigue loads were calculated by using Matlab code *abaqus4side.m* attached in Appendix D. Results were condensed and presented in the graphical form. The drawings depict fatigue damage distribution in tubular joints from 4 sides of jacket substructure. Illustrated EFL ratios are the average of coefficient EFL which occur in both beam ends. The figures with description may be found in Appendix B. Drawings with fatigue damage distribution in tubular joints and all tables submitted in this chapter were generated with Matlab code *tpabaqus4side.m* attached in Appendix E.

Following designations are introduced in this chapter:

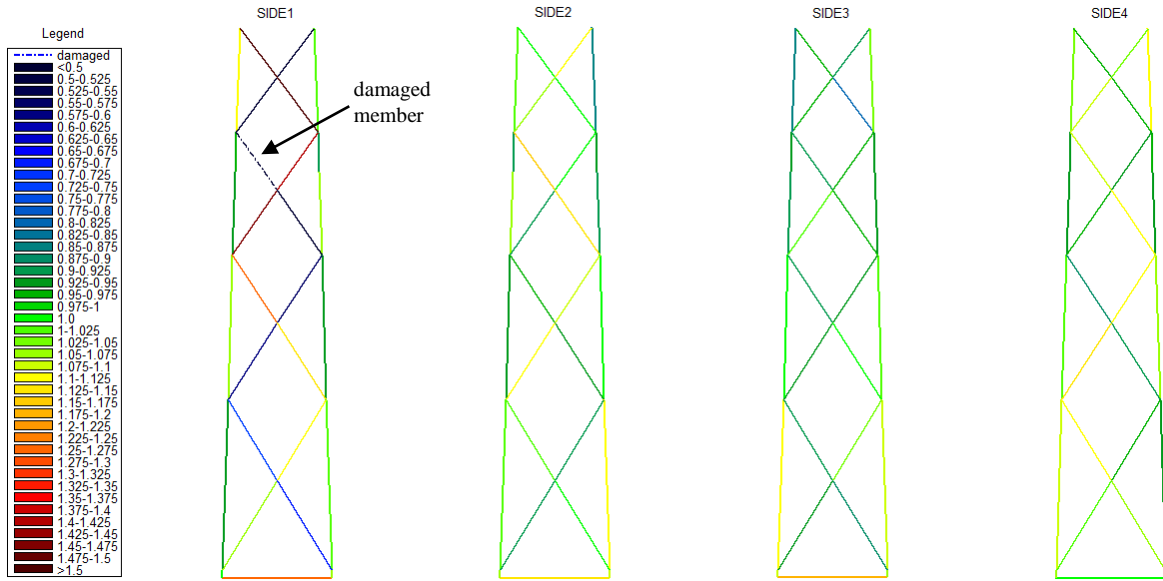
EFL_M – EFL ratio resulted from equivalent bending moment [-]

EFL_F – EFL ratio derived from axial force [-]

DEL_M – EFL ratio resulted from equivalent bending moment [-]

DEL_F – EFL ratio derived from axial force [-]

Representative view of fatigue damage distribution (Case 10) is shown below in figure 4.1



Design situation	DLC	Wind condition	Waves	Wind and wave directionality	Water level	Type of analysis	Type of EFL	Damaged element	Type of damage
Power Production	1.2	NTM 3<Vhub<25 4:2:24 m/s	NSS Hs=E[Hs Vhub]	COD, UNI	MSL	FATIGUE	FORCE	X-Brace 86 Level III-IV	Free-joint

Fig. 5.1. Representative view of fatigue damage distribution

On first sight, one can notice alternating fatigue in cross-braces, especially in side where damage in structural member was applied. Distribution of fatigue damage keep a certain scheme, the lowest amount of fatigue damage accumulates in flawed brace and the braces located diagonally. On the other hand, the highest amount of fatigue damage appears on the opposite side.

It can be interpreted in such way that damaged element is capable to transmit loadings partially or hardly any. This implies that the braces welded diagonally in relation to damaged element are less loaded and therefore, the values of stress amplitudes are lower. On the contrary, the cross-braces situated on the opposite side are overloaded and subjected to excessive fatigue loads. The conclusions are consistent with the Table 5.1.

This alternating fatigue damage pattern may be also seen in adjacent sides of jacket substructure, however this observation occurs only for damages raised from axial forces. The fatigue damage differences are lower comparing to jacket side with damaged element. Fig.5.3 shows values of EFL_F and EFL_M at III-IV level of jacket substructure.

Case 10	max/ min	EFL _{ratio}				DEL _{ratio}			
		Mem.,Node	EFL _F	Mem.,Node	EFL _M	Mem.,Node	DEL _F	Mem.,Node	DEL _M
Horizontal brace level I	max	'39,18'	1,318	'40,3'	1,139	'39,18'	9,753	'40,3'	2,695
	min	'38,8'	0,968	'39,18'	0,849	'38,8'	1,139	'39,18'	0,587
X-mud braces level I-II	max	'56,20'	1,123	'54,15'	1,508	'48,42'	2,548	'54,15'	12,711
	min	'53,44'	0,668	'50,10'	0,853	'53,44'	0,192	'50,10'	0,717
Legs at the lowest level	max	'4,5'	1,141	'12,15'	1,870	'4,5'	3,632	'12,15'	61,354
	min	'12,15'	0,930	'8,9'	0,779	'12,15'	0,845	'8,9'	0,566
X-mud braces level II-III	max	'70,48'	1,250	'72,33'	2,503	'70,48'	3,782	'72,33'	236,030
	min	'72,33'	0,562	'61,46'	0,865	'72,33'	0,073	'59,20'	0,729
Legs level II-III	max	'25,29'	1,102	'25,15'	1,548	'25,29'	2,976	'29,20'	16,347
	min	'29,33'	0,907	'17,5'	0,896	'29,33'	0,811	'25,29'	1,145
X-mud braces level III-IV	max	'88,34'	1,460	'87,29'	2,953	'88,34'	9,029	'87,29'	833,107
	min	'86,52'	0,000	'86,52'	0,001	'86,52'	0,000	'86,52'	0,000
Legs level III-IV	max	'30,33'	1,067	'30,33'	1,726	'30,33'	2,767	'30,33'	28,657
	min	'3000,34'	0,895	'1800,22'	0,888	'3000,34'	0,901	'1800,22'	0,849
X-mud braces level IV-V	max	'102,31'	1,836	'103,30'	2,315	'102,31'	31,791	'103,30'	114,518
	min	'104,35'	0,461	'89,22'	0,817	'104,35'	0,040	'89,22'	0,744
Legs level IV-V	max	'27,31'	1,139	'31,34'	1,230	'31,34'	3,983	'31,34'	5,647
	min	'19,23'	0,841	'19,23'	0,851	'19,23'	0,867	'31,35'	0,842

Table 5.1. Overview of extreme EFL and DEL ratio values

From the Table 5.1 one can observe an alternating pattern in each level of jacket support. It is worth to mention about DEL ratio. The values are extremely high, especially DEL_M which reached beyond 100 for X-brace 87. Based on the table 5.2 it can be deduced which element is affected the most.

Case	Member	Node	Max EFL _F [-]	Min EFL _F [-]	Member	Node	Max EFL _M [-]	Min EFL _M [-]
1	Chord 4	5	1.123	-	Chord 7	8	1.053	-
	Chord 1800	22	-	0.8294	X-brace 45	9	-	0.616
2	Chord 4	4	1.126	-	X-brace 38	13	1.13	-
	Chord 2200	26	-	0.8242	X-brace 45	9	-	0.442
3	X-brace 61	46	1.180	-	Chord 12	15	1.315	-
	X-brace 46	15	-	0.743	X-brace 45	9	-	0.298
4	X-brace 61	46	1.324	-	Chord 12	15	1.901	-
	X-brace 45	9	-	0.402	X-brace 45	9	-	0.12
5	X-brace 48	42	1.708	-	Chord 12	15	2.824	-
	X-brace 45	9	-	0.00003	X-brace 45	42	-	0.0018
6	X-brace 39	18	1.129	-	X-brace 79	50	1.098	-
	Chord 2200	2500	-	0.818	X-brace 86	52	-	0.702
7	X-brace 40	3	1.148	-	X-brace 87	29	1.175	-
	Chord 22	2500	-	0.85	X-brace 86	30	-	0.507
8	X-brace 40	3	1.184	-	X-brace 87	29	1.388	-
	X-brace 86	52	-	0.796	X-brace 86	30	-	0.380
9	X-brace 102	31	1.3171	-	X-brace 87	29	2.197	-
	X-brace 86	30	-	0.53	X-brace 86	30	-	0.151
10	X-brace 102	31	1.8359	-	X-brace 87	29	2.953	-
	X-brace 86	52	-	0.0004	X-brace 86	30	-	0.0009

Table. 5.2 Overview of extreme EFL ratio values

There is no doubt, the most significant damages occur with the use of free-joint mechanism. In the Table 4.2 one can notice extreme EFL ratio governed by force and equivalent moment in Case 5 and 10.

It is hard to conclude one versatile pattern for extreme fatigue damages but some cases have a lot of common.

The maximum ratio of fatigue damage governed by equivalent moment appears in the joint near damaged element, where the brace and chord meet. It shows the more damaged element the higher EFL ratio occurs but extreme fatigue damage remains in the same joint.

The maximal EFL_F is received in the joints of braces situated diagonally. The highest fatigue damage ratios occur usually in joints connecting brace and chord, but cases 3 & 4 shows it may also appear in cross-braces joints.

A large incidence of damage occurs also in the joints of mudline braces. In case 9, EFL_M it raises even up to 2.03 for the beam 38.

In most cases the minimum EFL ratio occurs in joints of damaged element where the chord and brace are welded.

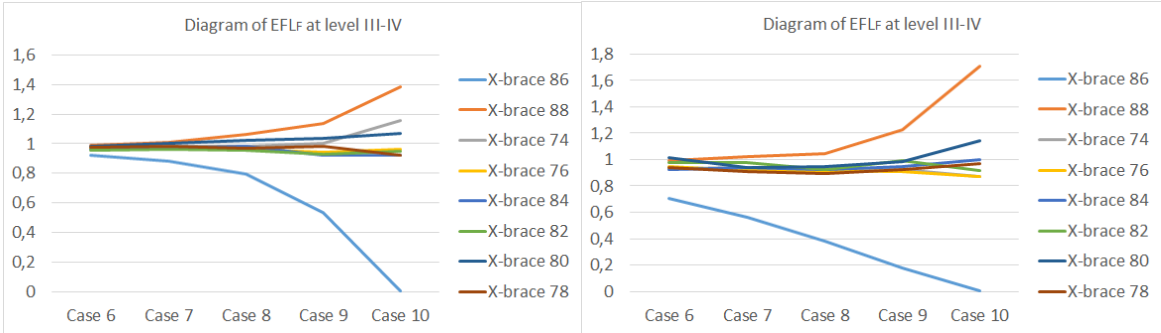


Fig. 5.2. Diagrams presenting EFL ratio in cross-braces considering different cases

The Fig. 5.2 presents how the fatigue damage is distributed at the level, where damage was applied. It may be seen that EFL_F and EFL_M in structural members close to flawed element do not exceed value of 1.2 From the Fig. 5.2 can be concluded that the more serious damage of the element occurs the higher change in EFL increase. It may be noticed that EFL_M change is even steeper than the change of EFL_F . In case 10 the EFL_M value is minimal, close to zero.

5.1.2. More detailed analysis

In order to better present the fatigue damage distribution, results are printed at one side of jacket substructure with damaged element. This section considers case 8 which assumes damage in element 86 implemented as 90% Young’s modulus reduction.

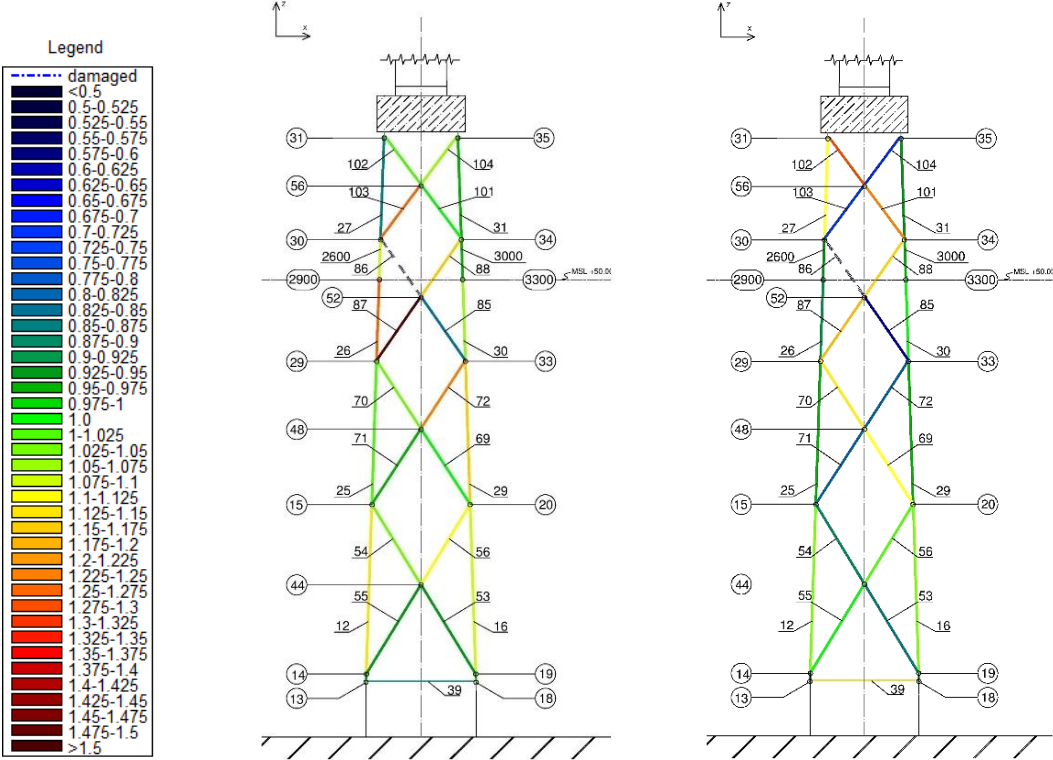


Fig. 5.3. Fatigue damage distribution showed in one side of jacket support structure by:
 a) EFL referred to equivalent moment b) EFL referred to axial force

Alternating pattern for EFL_F agrees in all cases whereas for EFL_M is not clear. This discrepancy may result from the assumption of the equivalent moment in the calculation. Another possibility of discrepancy is accepted calculation method which assumes the average from both ends of beam.

The additional loads resulting from the damaged element are distributed to other members. In consequence, not only cross-braces, but even legs may fail like for instance element 26 in the Figure 5.3a. The table 5.3 presents extreme EFL and DEL ratios at one side of jacket structure.

Case 10	max/ min	EFL _{ratio}				DEL _{ratio}			
		Mem.,Node	EFL _F	Mem.,Node	EFL _M	Mem.,Node	DEL _F	Mem.,Node	DEL _M
Horizontal brace level I	max	'39,18'	1,318	'40,3'	1,139	'39,18'	9,753	'40,3'	2,695
	min	'38,8'	0,968	'39,18'	0,849	'38,8'	1,139	'39,18'	0,587
X-mud braces level I-II	max	'56,20'	1,123	'54,15'	1,508	'48,42'	2,548	'54,15'	12,711
	min	'53,44'	0,668	'50,10'	0,853	'53,44'	0,192	'50,10'	0,717
Legs at the lowest level	max	'4,5'	1,141	'12,15'	1,870	'4,5'	3,632	'12,15'	61,354
	min	'12,15'	0,930	'8,9'	0,779	'12,15'	0,845	'8,9'	0,566
X-mud braces level II-III	max	'70,48'	1,250	'72,33'	2,503	'70,48'	3,782	'72,33'	236,030
	min	'72,33'	0,562	'61,46'	0,865	'72,33'	0,073	'59,20'	0,729
Legs level II-III	max	'25,29'	1,102	'25,15'	1,548	'25,29'	2,976	'29,20'	16,347
	min	'29,33'	0,907	'17,5'	0,896	'29,33'	0,811	'25,29'	1,145
X-mud braces level III-IV	max	'88,34'	1,460	'87,29'	2,953	'88,34'	9,029	'87,29'	833,107
	min	'86,52'	0,000	'86,52'	0,001	'86,52'	0,000	'86,52'	0,000
Legs level III-IV	max	'30,33'	1,067	'30,33'	1,726	'30,33'	2,767	'30,33'	28,657
	min	'3000,34'	0,895	'1800,22'	0,888	'3000,34'	0,901	'1800,22'	0,849
X-mud braces level IV-V	max	'102,31'	1,836	'103,30'	2,315	'102,31'	31,791	'103,30'	114,518
	min	'104,35'	0,461	'89,22'	0,817	'104,35'	0,040	'89,22'	0,744
Legs level IV-V	max	'27,31'	1,139	'31,34'	1,230	'31,34'	3,983	'31,34'	5,647
	min	'19,23'	0,841	'19,23'	0,851	'19,23'	0,867	'31,35'	0,842

Table 5.3 EFL ratio and DEL ratio at one side of jacket structure

Normalized summary of EFL_F and EFL_M from 1 side of jacket substructure is presented in Fig. 5.4:

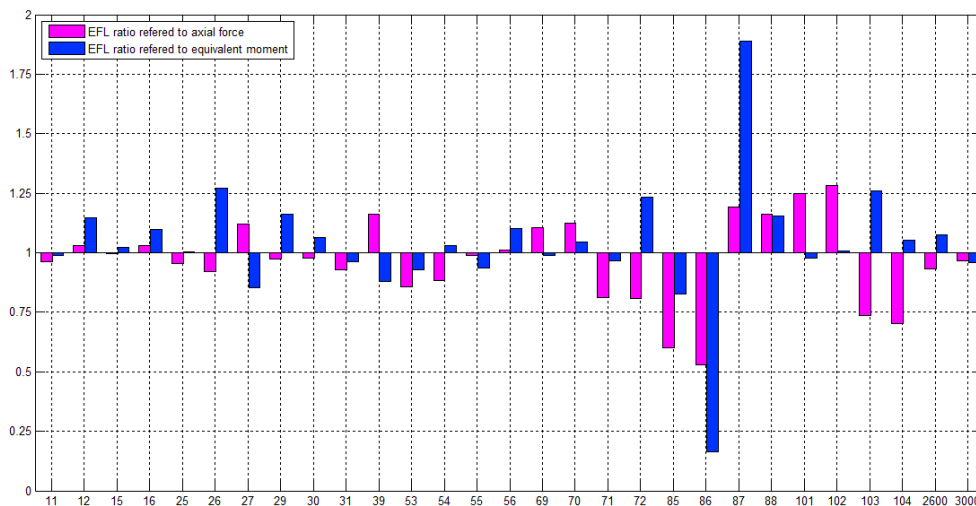


Fig. 5.4. Normalized summary of force and equivalent moment EFL ratio change

On the first sight, one can notice high value of EFL ratio for member 87 and 103. On the other hand the lowest values occur in elements 86 and 85. It confirms the theory that fatigue damage distribution depends on the position of the damaged element. The highest differences in EFL ratio occur locally and with the larger distance gradually decrease.

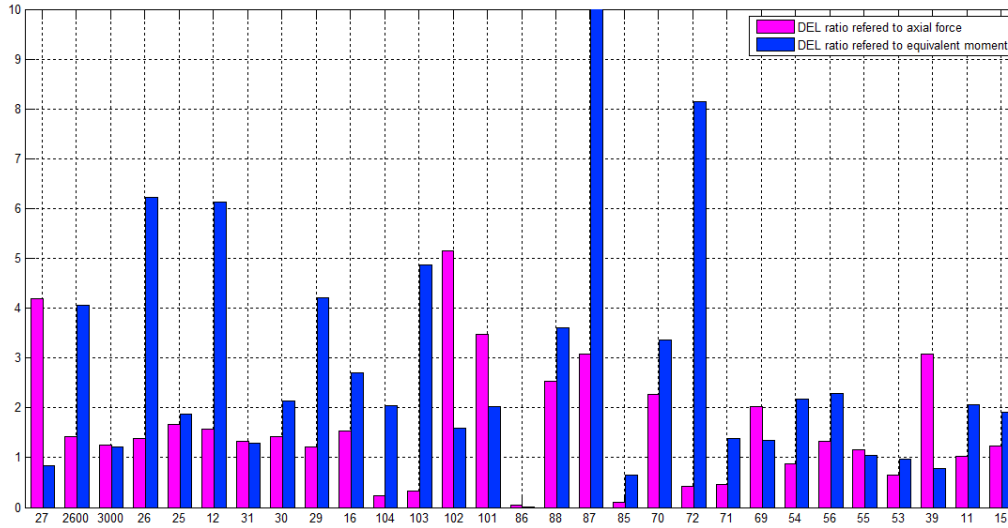


Fig. 5.5. Summary of Force and equivalent moment DEL ratios

Basing on Fig. 5.4 and Fig. 5.5 one may deduce, that small increase of EFL ratio results in much higher increment of DEL ratio. It's easily seen that enormous DEL ratio is assigned to element 87, which goes beyond the scale. Assuming DEL ratio equals 10 (at undamaged structure lifetime of 20 years) leads to the conclusion that the element withstand the loadings for 2 years only after the construction gets damaged. For element 72 in turn, DEL ratio is equal to 0.425 what tells that the element may survive theoretically even 47 years.

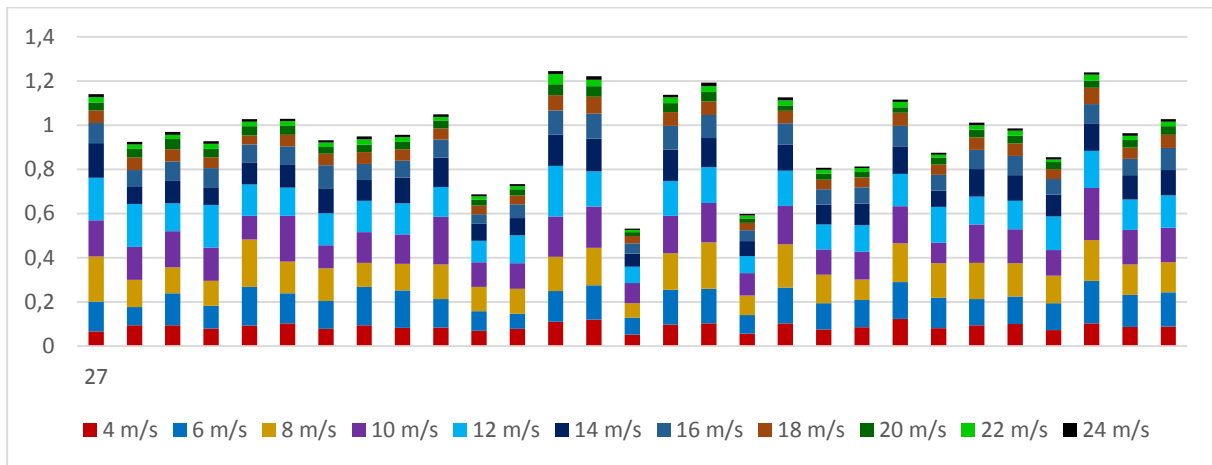


Fig. 5.6. EFL_F stacked column chart consists of wind speed distribution

Based on Fig. 5.6 the fatigue loads caused by wind speeds between 6-16 m/s constitute the 76-82,7 % contribution of total fatigue damage. This dependence results mainly from wind speed probability of occurrence. The sum of scaled probability of occurrence listed in Table 4.2 for aforementioned wind speeds equals 78,6% of total wind speeds occurrence. It can be concluded that fatigue damage is highly dependant on wind speed distribution.

6. ADJUSTING THE CONTROLLER CONSTANTS AND INVESTIGATION OF FATIGUE LOADS

6.1. Introduction

Fatigue results obtained from first part of this thesis showed that damaged structural element has a significant influence on remaining members' lifetime. It can be seen that even small defect in structural member cause drastic vitality reduction in a long term. Under full operational loads from the turbine, some structural members reached fatigue limit. Such structure state is unacceptable and current regulations clearly demand to shut-down the wind turbine until the damaged element is repaired. However, it would be worth to verify whether it is not enough just to down-regulate the turbine.

The second part of this thesis proposes the fatigue loads mitigation by turbine down-regulation. This involves changing the operating range of the turbine, which can be done by modifying the control system. Additionally, new rated wind speed was selected so that corresponding rotor frequency has not imposed the harmonic frequencies.

This chapter includes a brief description of how the controller system is designed, a steady-state response of the OWT and computational steps how the rated wind speed was determined.

6.2. Control system

As it was mentioned in chapter 2.1.1, wind turbine NREL 5 MW has a variable speed system. This means that turbine can operate at different speeds and alter tip speed ratio. Moreover, turbine has an active pitch-regulation system, which enables to change blade pitch angle and in turn it results in decrease the rotational speed. This control strategy is usually used at high wind speeds in order to prevent turbine equipment from excessive aerodynamic torques. The power production for wind turbines of this type rely mainly on two basic controller systems: blade-pitch controller and generator torque controller.

Blade-pitch controller is designed in order to regulate generator speed above the rated wind speed. As the wind speed rises, blade-pitch controller keeps a constant power output by adjusting the pitch angle until a cut-out wind speed is reached. This phenomenon consists in that pitch regulation causes less lift and more drag force due to increasing flow separation along the blade length and it results in turbine slowdown [].

Generator torque controller is mainly responsible for extraction maximum energy from the wind below the rated operation point. Above the rated operation point, the generator torque is inversely proportional to filtered generator speed to keep the power output at a constant level [4].

6.3. Steady-state response of the offshore wind turbine

According to Technical Report [4] wind turbine operation range is divided into 5 control zones:

- Region 1 – part of operation range before turbine start-up when the wind is lower than cut-in wind speed, there is no generator torque and no power is extracted from the wind; all aerodynamic force is used to accelerate the rotor up before start-up
- Region $1\frac{1}{2}$ – start-up region, linear passage connecting Regions 1 and 2, used to limit wind turbine's operational speed range
- Region 2 – control region optimized for power capture; a constant (optimal) tip-speed ratio is maintained and the generator torque is proportional to the square of the filtered generator speed
- Region $2\frac{1}{2}$ – linear passage connecting Regions 2 and 3 with a torque slope corresponding to the gradient of an induction machine. Region $2\frac{1}{2}$ is typically used to limit tip speed and noise emission at nominal power
- Region 3 – in this area the rated power is held constantly by pitching so the generator torque and the filtered generator speed are inversely proportional

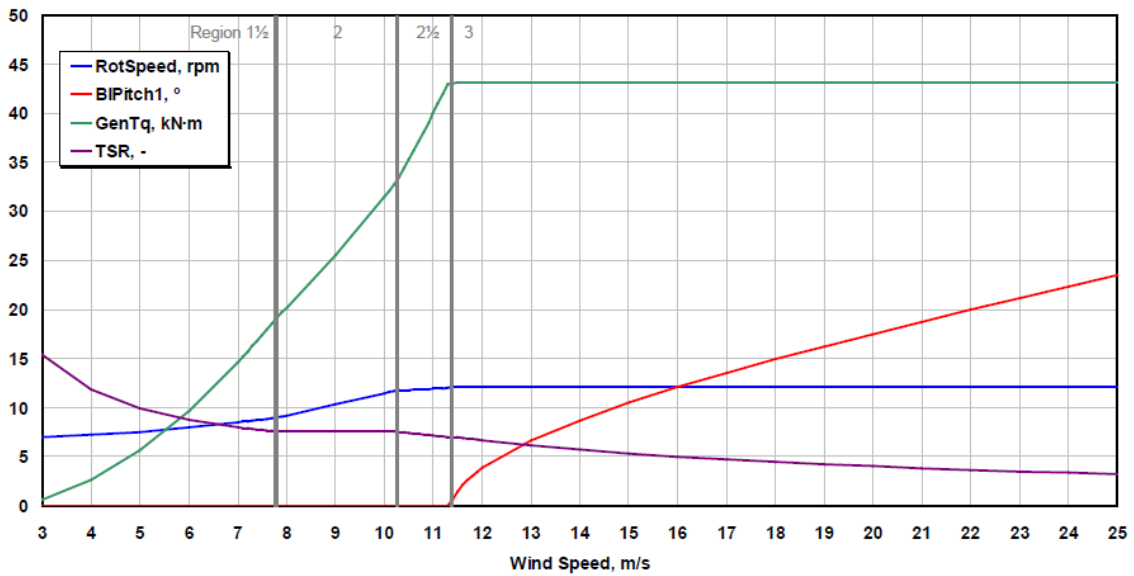
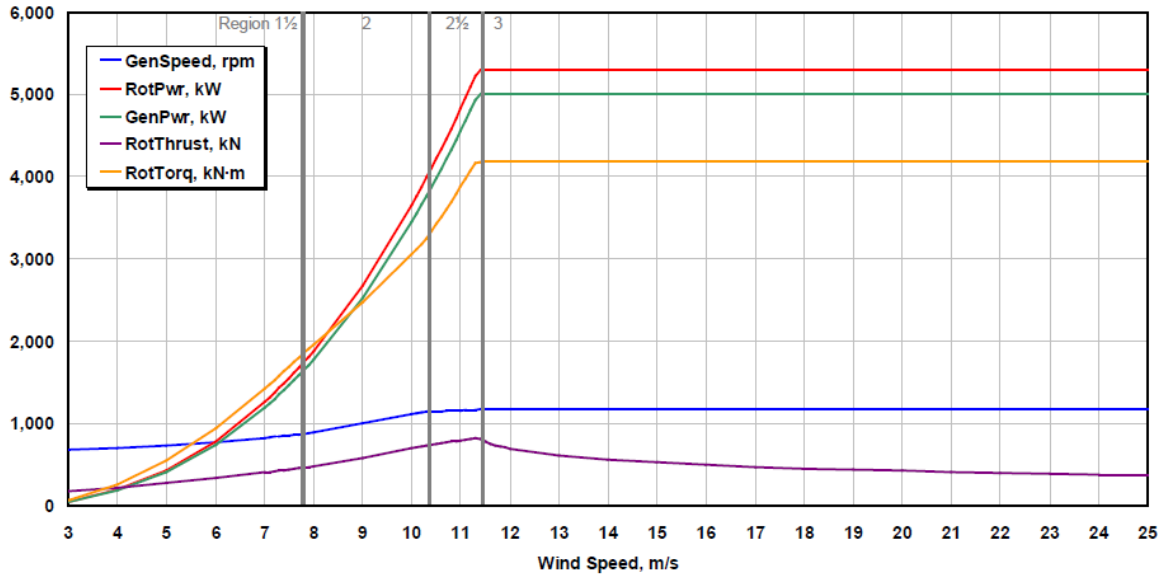


Fig. 6.1. Steady-state responses as a function of wind speed [4]

where:

GenSpeed – rotational speed of the generator (high-speed shaft) [rpm]

RotPwr – mechanical power within the rotor [kW]

GenPwr – electrical output of the generator [kW]

RotThrust- rotor thrust [kN]

RotTorq- mechanical torque in the low-speed shaft [kNm]

RotSpeed-rotational speed of the rotor(low-speed shaft) [rpm]

BIPitch-pitch angle of Blade 1[°]

GenTrq-electrical torque of the generator [kNm]

TSR- tip-speed ratio [-]

The numerical values and more detailed description about each region may be found in *Definition of a 5-MW Reference Wind Turbine for Offshore System Development* [4].

6.4. Controller modification

Fatigue damage accumulates in the offshore wind turbine structural members due to varying stress levels. The main sources that cause periodic stresses are loads originating from wind and waves and resonance-induced loads from rotor rotation. The contribution of individual loads in fatigue damage is a challenging task due to complexity of loads acting in the same time on the structure.

The wind produces mainly thrust (force in wind direction) and torque (moment). However unstable behavior of wind causes forces and moments in every other direction. Since the loads are not static, they induce cyclic stresses.

Waves acting on the support structure produces mainly force in wave direction, which causes a bending moments at mudline. However, the wave forces has a minor significance for jacket structure, since the diameter of the structure elements is usually small.

The imposition of rotor frequency and one of system natural frequency results in cyclic loads which may reach high amplitudes.

It is not possible to say that only one force or moment causes the fatigue damage. However, the thrust and torque dominate it. Thus, thrust and torque mitigation seems to be right way for fatigue damage reduction. Choice of the rotor frequency range is also of a great importance.

6.4.1. Rotor frequency analysis

The analysis intention is to identify these rotor frequencies, which intersect set of eigenfrequencies lines. Basing on the Fig. 4.8 analysis assumes to avoid first 13 eigenfrequencies($< 2\text{Hz}$), because these natural frequencies are suspected to excite system the most. Rotor frequency investigation considers eigenfrequencies from all structure states. Basing on the Campbell diagram (Fig. 4.8), natural frequencies were found and denoted on Fig. 6.2 and 6.3 with 1% margin. I should be noted that this analysis is very sensitive to applied accuracy and small margin extension significantly reduce rotor operation range.

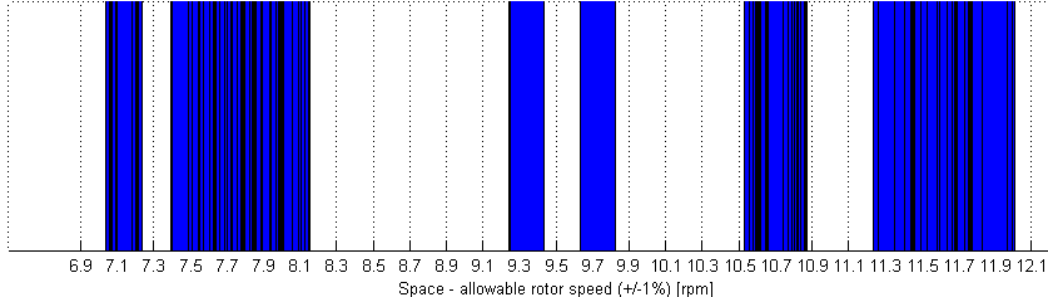


Fig. 6.2. Allowable ranges of rotor frequencies

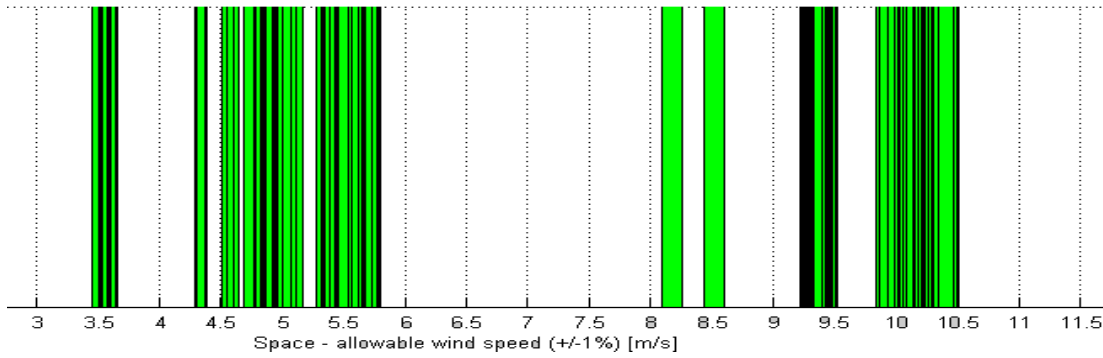


Fig. 6.3. Allowable ranges of wind speed

Basing on the diagrams above, rated rotor speed 11[rpm] and rated wind speed 9.61[m/s] have been chosen as safe working point for higher wind speeds.

6.4.2. Rated wind speed

New rated wind speed binds with updated wind turbine specification. Excluding region 2.5 Rated power was determined basing on the Betz law. Tip speed ratio and peak power coefficient were extracted from Technical Report [4] and they equal 7.55 and 0.482 respectively. Rotor diameter is listed in Table 2.1.

Basing on the equation 3.12 rated power is defined as:

$$P_{rotor} = \frac{1}{2} \rho v_1^3 A C_p = \frac{1}{2} \cdot 1.25 \cdot 9.61^3 \pi \cdot \frac{126^2}{4} \cdot 0.482 = 3\,267\,039 \text{ [W]} \quad (6.1)$$

With the generator efficiency 94,4% rated electric power is:

$$P_{electric} = 0.94 * P_{rotor} = 3084084 \text{ [W]} \quad (6.2)$$

With the gearbox ratio $N_g = 97$ and rated rotor speed $R_s = 11$ [rpm] generator angular velocity(speed) is calculated as:

$$\omega = N_g * \frac{R_s}{60} * 2\pi = 111.736 \text{ [rad/s]} \quad (6.3)$$

And the corresponding rated generator torque may be computed using equation 3.16:

$$T = \frac{P}{\omega} = \frac{3267039}{111.736} = 29244.9 \text{ [Nm]} \quad (6.4)$$

Rated generator torque in baseline controller was equal $T_0 = 43093.55 \text{ Nm}$. Thus, generator torque change is calculated as:

$$\Delta T = 1 - \frac{T}{T_0} = 1 - \frac{29244.9}{43093.5} = 0.3214 (32,14\%) \quad (6.5)$$

New wind turbine specification is shown in Fig. 6.4

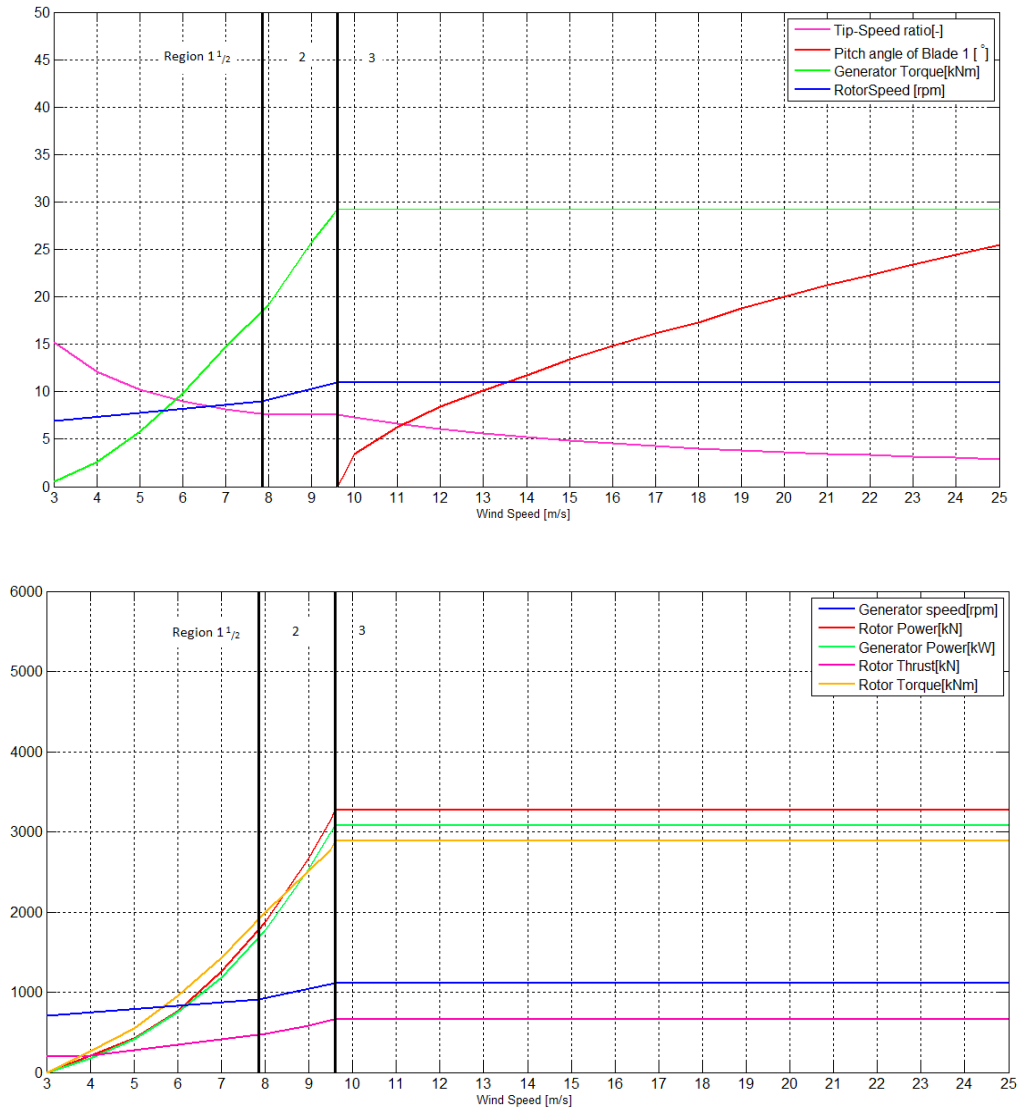


Fig. 6.4. Modified steady-state responses as a function of wind speed

7. RESULTS SUMMARY

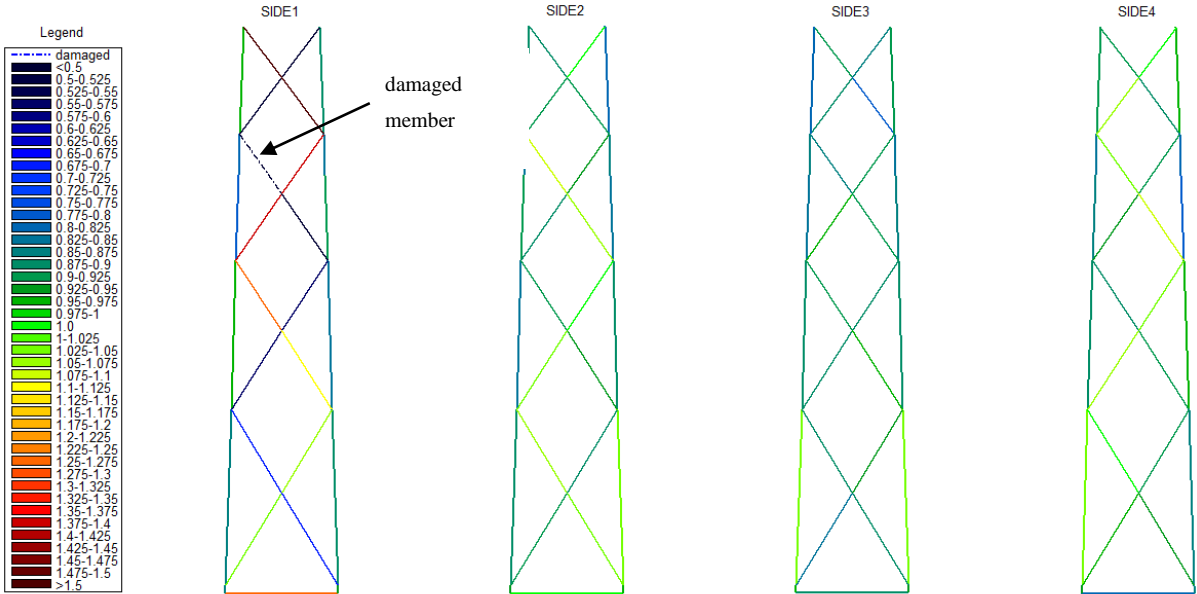
7.1. Fatigue analysis

In this chapter fatigue damage distribution of all jacket members and general behavior of structure with damaged element is discussed. Computational procedure was analogous to one shown in section 4.4, resulting in total number of 121 simulations. Condensed results may be found in Appendix F. The chapter contains also a results summary from model with unmodified and modified controller.

7.1.1. Results from model with modified controller

The comparison method using EFL ratio was performed between results from damaged model with modified controller and undamaged model with baseline controller. This assumption simulates the situation, in which damage in structural member had been detected and turbine down-regulation was applied in order to protect remaining elements. The Fig.7.1 presents representative side view of damaged jacket support structure (Case 10).

Based on the Fig. 7.1 it can be seen that red lines denoting fatigue damage in the structural member are still there. This implies that controller modification does not completely meet the assumptions and still operation of damaged OWT poses a real threat.



Design situation	DLC	Wind condition	Waves	Wind and wave directionality	Water level	Type of analysis	Type of EFL	Damaged element	Type of damage
Power Production	1.2	NTM 3<Vhub<25 4:2:24 m/s	NSS Hs=E[Hs Vhub]	COD,UNI	MSL	FATIGUE	FORCE	X-Brace 86 Level III-IV	FREE-JOINT

Fig. 7.1 Representative view of fatigue damage distribution

As in the Fig. 5.1 one may see an alternating pattern of fatigue damage distribution. This means that fatigue distribution keeps the certain scheme which is independent of rotor frequency.

Case 10	max/ min	EFL _{ratio}				DEL _{ratio}			
		Mem.,Node	EFL _F	Mem.,Node	EFL _M	Mem.,Node	DEL _F	Mem.,Node	DEL _M
Horizontal brace level I	max	'39,18'	1,332	'40,3'	1,036	'39,18'	14,448	'40,3'	1,831
	min	'38,13'	0,806	'39,13'	0,849	'38,8'	0,495	'39,18'	0,618
X-mud braces level I-II	max	'56,20'	1,086	'54,15'	1,479	'42,20'	2,116	'54,15'	12,984
	min	'53,19'	0,672	'49,43'	0,754	'53,19'	0,192	'47,42'	0,442
Legs at the lowest level	max	'4,5'	1,050	'12,15'	1,556	'4,4'	3,411	'12,15'	51,177
	min	'12,15'	0,835	'8,10'	0,708	'12,15'	0,598	'8,10'	0,664
X-mud braces level II-III	max	'70,48'	1,258	'72,33'	2,440	'70,29'	7,394	'72,33'	161,727
	min	'72,48'	0,559	'68,47'	0,746	'72,33'	0,074	'68,47'	0,385
Legs level II-III	max	'25,29'	1,012	'29,20'	1,395	'25,29'	2,779	'29,20'	19,979
	min	'29,33'	0,844	'17,5'	0,645	'29,20'	0,599	'17,5'	0,301
X-mud braces level III-IV	max	'88,34'	1,432	'87,29'	2,931	'88,34'	9,464	'87,29'	649,000
	min	'86,52'	0,000	'86,52'	0,001	'86,52'	0,000	'86,52'	0,000
Legs level III-IV	max	'30,33'	0,917	'26,29'	1,674	'30,33'	1,307	'26,2900'	17,453
	min	'2600,30'	0,782	'1800,22'	0,816	'2600,30'	0,501	'1800,22'	0,619
X-mud braces level IV-V	max	'102,31'	1,716	'103,30'	2,129	'102,31'	22,359	'103,30'	79,021
	min	'104,35'	0,423	'96,27'	0,633	'104,35'	0,030	'102,56'	0,444
Legs level IV-V	max	'27,31'	0,973	'27,31'	1,130	'27,31'	3,523	'23,27'	6,584
	min	'19,22'	0,796	'19,22'	0,779	'19,23'	0,645	'19,22'	0,585

Table 7.7.1. Overview of extreme EFL and DEL ratio values

Although model with modified controller does not protect structural members from excessive fatigue damages, comparing Table 5.1 and Table 7.1 it can be observed that fatigue damages were slightly reduced. For instance, the maximal EFL_M in X-brace 102 is equal 2.315 whereas with modified controller EFL_M is 2.129. Small difference in EFL ratio leads to large difference in DEL ratio. DEL_M was reduced from 114.518 to 79.021.

Similar change occurs in EFL_F. For X-brace 102 EFL_F is equal 1,716 whereas with modified control system is 1,836. And for the same brace corresponding DEL_F is equal 22,359 instead of 31,791.

The figures 7.2-7.4 show how the fatigue damage was reduced due to new rated wind speed. The diagram considers one side of jacket support, where damage occurs. Torque and thrust mitigation together with frequency which does not coincide with natural frequency caused noticeable reduction of fatigue loads.

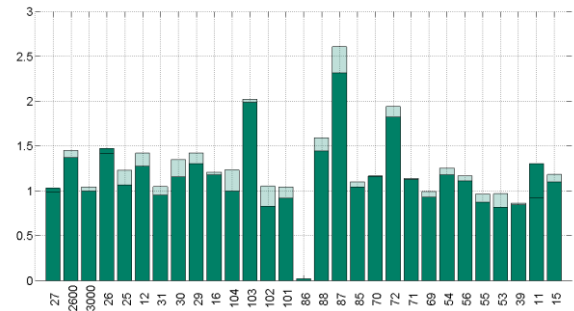
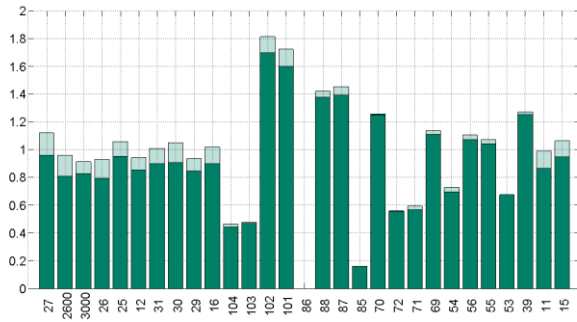


Fig. 7.2 Diagrams presenting EFL_F and EFL_M

from 1 side of jacket structure - CASE 10

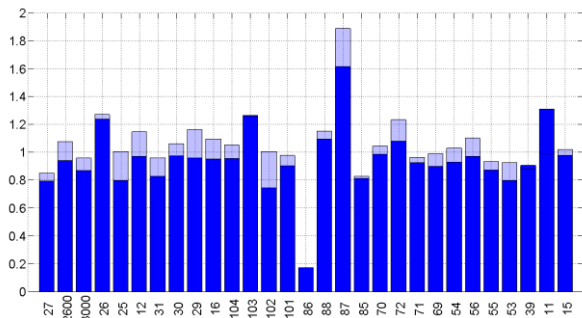
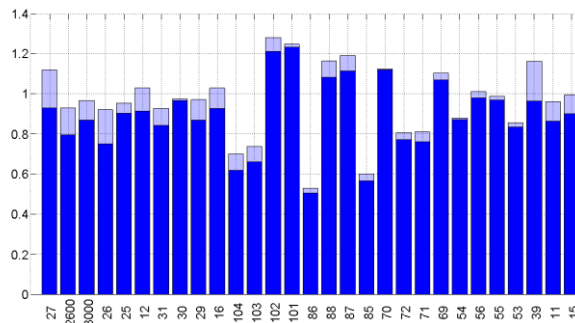


Fig. 7.3 Diagrams presenting EFL_F and EFL_M

from 1 side of jacket structure - CASE 8

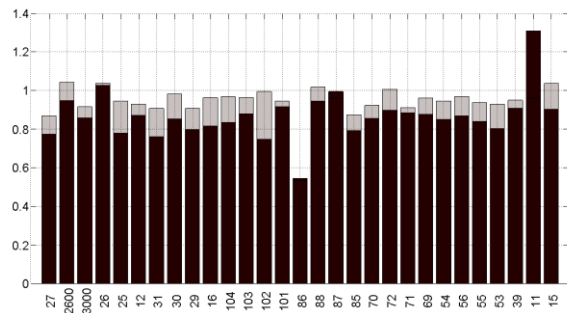
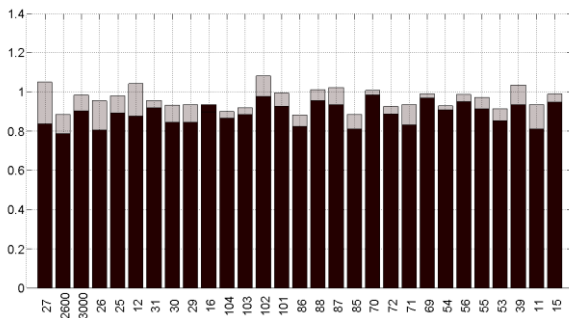


Fig. 7.4 Diagrams presenting EFL_F and EFL_M

from 1 side of jacket structure - CASE 6

As it was mentioned previously, the most susceptible to fatigue damage are structural members close to damaged element. The load transfer path is longer, the fatigue loads caused by damage element are less. Thus, it seems logical to check the modified controller ‘efficiency’ in terms of fatigue reduction not from all members, but only members from one side.

EFL _F	Case 1	Case 2	Case 3	Case 4	Case 5	Case 6	Case 7	Case 8	Case 9	Case 10
Mean value from basin controller	0,965	0,966	0,967	0,966	0,966	0,977	0,964	0,960	0,965	0,963
Mean value from modified controller	0,894	0,888	0,893	0,898	0,888	0,880	0,891	0,886	0,893	0,895
Change [-]	0,079	0,088	0,083	0,075	0,087	0,111	0,082	0,083	0,081	0,076
Efficiency' [%]	7,905	8,833	8,276	7,512	8,707	11,079	8,157	8,274	8,138	7,574

Table 7.2 Mean values of EFL_F and modified controller ‘efficiency’

EFL _M	Case 1	Case 2	Case 3	Case 4	Case 5	Case 6	Case 7	Case 8	Case 9	Case 10
Mean value from basin controller	0,946	0,950	0,955	0,993	1,141	0,930	0,942	0,949	1,036	1,237
Mean value from modified controller	0,874	0,878	0,876	0,897	0,951	0,860	0,868	0,874	0,951	1,162
Change [-]	0,083	0,082	0,089	0,107	0,200	0,081	0,085	0,085	0,090	0,064
Efficiency' [%]	8,254	8,229	8,914	10,691	19,987	8,114	8,542	8,526	8,961	6,446

Table 7.3 Mean values of EFL_M and modified controller ‘efficiency’

8. CONCLUSIONS

Fatigue analysis and ultimate analysis were performed for intact and damaged offshore wind turbine's foundation – jacket substructure OC4. Both analysis are carried out in accordance with guideline IEC 61400-3. The jacket structure damage is modeled by stiffness reduction or free-joint mechanism application into structural member. The analysis' goal is to examine what happens in remaining structural members.

The conclusion is that fatigue damage distribution follows a certain pattern that can be described. In general, the element with defect is partially or not at all capable to carry loads and this causes the elements located diagonally carry less loads too. On the other hand, structural members located oppositely are overloaded and more exposed to fatigue damage accumulation. It leads to the conclusion that the stiffer element is, the higher load magnitude attracts and the alternating path remains in the diagonal direction. On the contrary, stiffness reduction or crack imitation along the whole cross-section leads to loads relaxation. Moreover, it can be noticed that highest fatigue damage occurs locally and decreases gradually.

However not only cross-braces are affected, but also leg welded to the damaged element transfers part of the loads. In addition, alternating pattern is visible in adjacent sides of jacket, but fatigue loads are lower comparing to jacket side with damaged element.

Fatigue estimation assumes a comparison between various structural states using equivalent fatigue load ratio. Based on this factor one can conclude how the loads acting on the specific element have changed due to damage occurrence. If the expected lifetime of the one structural member is exceeded, it is worth to know which remaining elements are exposed to more loads.

This information may be particularly valuable for the structural designers to know which elements should be designed more carefully. The knowledge which structural elements are more loaded enables to provide a suitable dimensioning of structural members or designed in the such a way that the failure element is expected, but the structure's lifetime will not be significantly reduced.

Fatigue damage reduction may be applied by modifying controller settings. The thrust force and torque mitigation caused by change rated rotor speed, results in global fatigue loads reduction. Additionally, the choice of new rated rotor frequency was dictated by the frequency which does not impose with first 13 eigenfrequencies. The average EFLF reduction ranges from 7.5 to 11.1, whereas the average EFLM varies from 6.4 to almost 20.

9. DISCUSSION

Although this thesis has considered some damage state cases, the subject can be developed much more in terms of the fatigue assessment of jacket substructure. The following points reflect the author's suggestions on what can be further done and what other aspects of fatigue should be investigated.

- Fatigue analysis procedure of a complicated system like an offshore wind turbine requires a proper approach. The response of the structure is performed in the time-domain in order to capture all the non-linearities, however, this procedure is very time-consuming. Moreover, each change of system properties requires a new set of results. It could be worth introducing a simplified method, which limits the number of the necessary simulations.
- Insightful investigation considering rated rotor speed reduction should be performed. Controller modification applied in this thesis considers 32% of torque and thrust reduction. Though current standards do not accept operation when a structural element is damaged, the controller modification reached the goal, the fatigue damage in remaining elements was reduced. However, there is still a certain potential for preventing jacket elements against fatigue by turbine down-regulation.
- The topic of this thesis assumes damage or failure only in one structural member. However, it could be worth checking how the fatigue loads distribute when the number of elements with defect increases. Consideration of various damaged elements configurations could lead to a certain scheme describing the path of fatigue damage distribution. This method could facilitate the work of quality control inspectors during failure.
- The current design approach of offshore wind turbines assumes exclusion of these system natural frequencies that coincide with frequencies caused by rotor full revolution and tower passage of the three blades. It could be worth changing the rotor operation range in order to omit other eigenfrequencies that excite and lead to high vibrations.
- Fatigue assessment is a complicated issue and a full understanding of this problem requires lots of data. It is obvious, however, that fatigue distribution is highly dependent on the structural shape and it could be worth investigating different jacket structure configurations and geometrical properties.

10. BIBLIOGRAPHY

1. *Fedem User's Guide, release 7.1.* Fedem Technology, Trondheim, 2014.
2. *Fedem Theory Guide, release 7.1.* Fedem Technology, Trondheim, 2014.
3. International Electrotechnical Commission. *Wind turbines - Part 3: Design requirements for offshore wind turbines.* Tech. Rep. IEC:2009 61400-3, Geneva, 2009.
4. J. M Jonkman and National Renewable Energy Laboratory (US). *Definition of a 5-MW reference wind turbine for offshore system development.* National Energy Laboratory Golden, CO, 2009.
5. K.H. Chew, Michael Muskulus, Daniel Zwick, E.Y.K. Ng, K. Tai. *Offshore Wind Turbine Jacket Substructure-A Comparison Study between Four-Legged and Three-Legged Designs.* Journal of Ocean and Wind Energy, ISOPE, Vol 1, No 2 (2014), pp. 74-81.
6. Fabian Vorpahl, Wojciech Popko, Daniel Kaufer. *Description of a basic model of the 'UpWind reference jacket' for code comparison in the OC4 project under IEA Wind Annex 30.* Technical Report, July 2013.
7. Naveen Kumar Vemula. *UpWind D4.2.5 Design solution. Upwind reference offshore support structure.* Deliverable Report, October 2010.
8. T. Fischer, W. de Vries, B. Schmidt. *Upwind Design_Basis.* Endowed Chair of Wind Energy (SWE) at the Institute of Aircraft Design Universität Stuttgart, October 2010.
9. FEDEM Windpower.
<http://www.fedem.com/services/software/fedem-windpower>
(date of access 28.04.2015).
10. FEDEM Windpower - Simulation Software.
<http://www.feapro.com/upload/file/1294983935.pdf>
(date of access 28.04.2015).
11. G. Freebury, W. Musial, *Determining Equivalent Damage Loading for Full-Scale Wind Turbine Blade Fatigue Tests.* NREL, 19th American Society of Mechanical Engineers (ASME) Wind Energy Symposium Reno, Nevada, January, 2000
12. David J. Laino, A. Craig Hansen. *AeroDyn User's Guide, Version 12.50.* Windward Engineering, LC, Salt Lake City, December 2002.
13. Patrick J. Moriarty and National Renewable Energy Laboratory. *AeroDyn Theory Manual.* National Renewable Energy Laboratory Golden, CO, December 2004.
14. B.J. Jonkman. *TurbSim User's Guide: Version 1.50.* National Renewable Energy Laboratory. Technical Report, September 2009.
15. I. Rychlik. *A new definition of the rainflow cycle counting method.* Int Fatigue9 No 2,1987, pp. 119-121.
16. C. Amzallag, *Standardization of the rainflow counting method for fatigue analysis,* International Journal of Fatigue, June 1994

17. Rainflow Counting Technical Background.
<https://www.efatigue.com/variable/background/rainflow.html>
 (date of access 02.05.2015).
18. Det Norske Veritas. *Fatigue Design of Offshore Steel Structures*. Recommended practice DNV-RP-C203, October 2011.
19. Rainflow counting tutorial.
<https://vibrationdata.wordpress.com/2012/10/31/rainflow-fatigue-cycle-counting/>
 (date of access 02.05.2015).
20. Stress range histories and Rain Flow counting.
<http://homes.civil.aau.dk/lda/Advanced%20Structural%20Engineering/Stress%20range%20histories%20and%20Rain%20Flowcounting.pdf>,
 (date of access 02.05.2015).
21. Offshore wind turbine location.
<https://www.google.com/maps/place/53%C2%B013'04.0%22N+3%C2%B013'13.0%22E/@53.0616395,3.3352028,6z/data=!4m2!3m1!1s0x0:0x0>
 (date of access 04.05.2015).
22. Parametric Study of Hot Spot Stresses around Tubular Joints with Doubler Plates.
<http://ascelibrary.org/doi/abs/10.1061/%28ASCE%291084-0680%282007%2912%3A1%2838%29>
 (date of access 04.05.2015).
23. Jae-Myung Lee, Jung-Kwan Seo. *Comparison of hot spot stress evaluation methods for welded structures*. International Journal of Naval Architecture and Ocean Engineering. Volume 2, Issue 4, Pages 200–210, ISSN (Online) 2092-6782, February 2014
24. Stress Concentrations in Offshore Welded Tubular Joints Subjected to Combined Loadings.
<http://www.jmst.org/fileup/PDF/20s35.pdf>,
 (date of access 07.05.2015).
25. Wind Power(Technology and Economic).
http://www.mpoweruk.com/wind_power.htm,
 (date of access 10.05.2015).
26. Gary L. Johnson, *Wind Energy Systems*, Kansas State University 2006
27. European Wind Energy Association, *The European offshore wind industry - key trends and statistics 2014*, Report, January 2015.
28. Offshore wind energy.
<http://www.boem.gov/renewable-energy-program/renewable-energy-guide/offshore-wind-energy.aspx>
 (date of access 13.05.2015).
29. <http://www.offshorewind.biz/2012/01/03/keppel-acquires-stake-in-offshore-wind-turbine-foundation-specialist-norway/keppel-acquires-stake-in-offshore-wind-turbine-foundation-specialist-norway/>
30. <http://www.qatarmark.com/companies/information/gulf-agency-qatar-co.html>
31. J.F Manwell, J.G. McGowan, A.L. Rogers, *Wind Energy Explained. Theory, Design and Application*, University of Massachusetts. Amherst. USA

32. Understanding Coefficient of Power (Cp) and Betz Limit,
http://learn.kidwind.org/sites/default/files/betz_limit_0.pdf
 (date of access 22.05.2015)
33. Tip speed ratio,
http://en.wikipedia.org/wiki/Tip-speed_ratio
 (date of access 22.05.2015)
34. Optimal tip speed ratio.
<http://mragheb.com/NPRE%20475%20Wind%20Power%20Systems/Optimal%20Rotor%20Tip%20Speed%20Ratio.pdf>
 (date of access 22.05.2015)
35. Søren Gundtoft, *Wind turbines*, Department of Mechanical Engineering at the University College of Århus, June 2009
36. Betz limit,
<http://www.reuk.co.uk/Betz-Limit.htm>
37. Daniel Zwick, Michael Muskulus, *Simplified fatigue load assessment in offshore wind turbine structural analysis*, Research article, Norwegian University of Science and Technology, Trondheim, 2015. Wind Energy DOI: 10.1002/we.1831
38. Wojciech Popko, Panagiotis Antonakas, Fabian Vorpahl, *Investigation of Local Vibration Phenomena of a Jacket Sub-structure Caused by Coupling with Other Components of an Offshore Wind Turbine*, Fraunhofer Institute for Wind Energy and Energy System Technology IWES
39. Wind turbine power output variation with steady wind speed,
http://www.wind-power-program.com/turbine_characteristics.htm
 (date of access 26.05.2015)
40. B.Yeter,Y.Garbatov,C.Guedes Soares, *Spectral fatigue assessment of an offshore wind turbine structure under wave and wind loading*, Technical University of Lisbon, Lisbon, 2014.
41. Selection, Design and Construction of Offshore Wind Turbine Foundations.
<http://cdn.intechopen.com/pdfs-wm/14804.pdf>
 (date of access 27.05.2015)
42. Peter Dalhoff, Kimon Argyriadis, Marcus Klose, *Integrated Load and Strength Analysis for Offshore Wind Turbines with Jacket Structures*, Germanischer Lloyd Industrial Services GmbH, Business Segment Wind Energy, Hamburg, Germany
43. Pitch-regulated and Stall regulated Wind turbines,
<http://www.bindichen.co.uk/post/Fundamentals/Pitch-regulated-and-Stall-regulated-Wind-Turbine.html>
44. *Design of steel structures*, NORSOK STANDARD N-004:2013, Rev. 3, Feb. 2013

11. APPENDICES

APPENDIX A

Nodal coordinates, members and their properties were extracted from Technical report 'UpWind reference jacket' [6]. The nodes numeration starts from the lowest level in the mathematically positive direction around the z-axis (Fig.A.1).The member properties are listed in Table A.2 with designation in Fig. A.1. Table A.3. presents more detailed description of particular member properties.

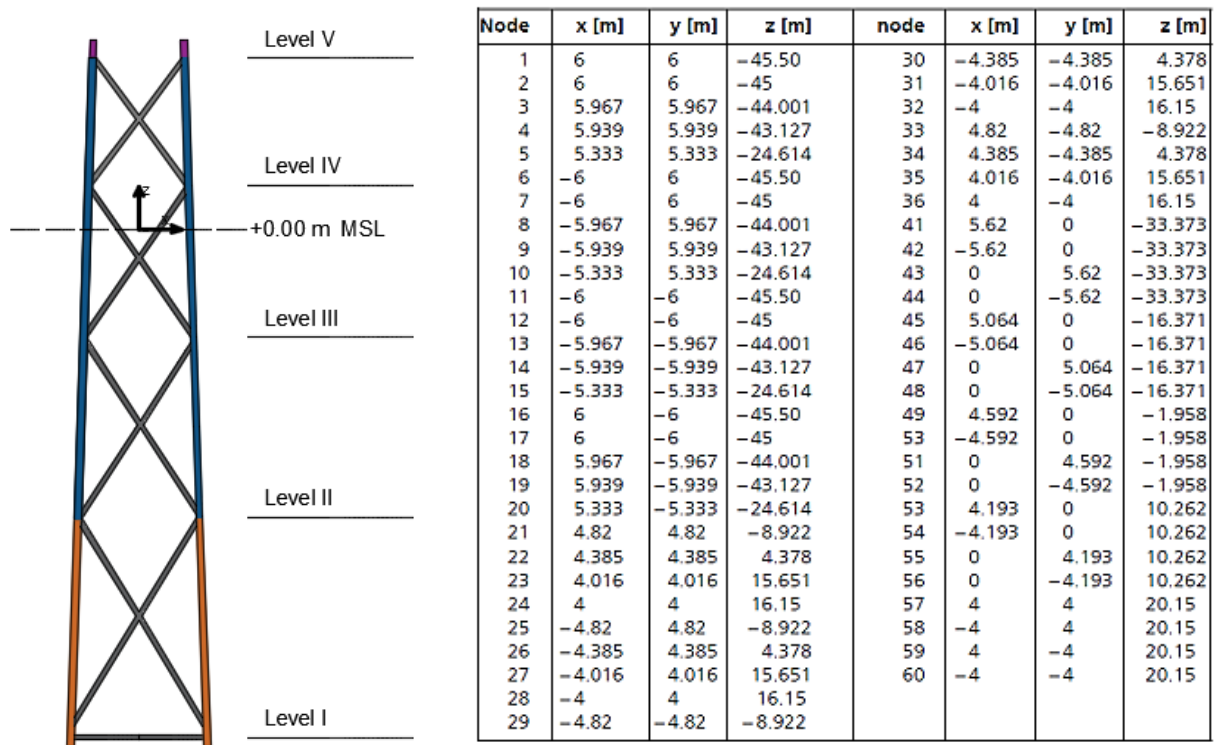


Table A. 1. Nodal coordinates

Fig. A.1. Member properties

Property set	Component	Outer diameter [m]	Thickness [mm]	Color in Figure
1	x- and mud braces	0.8	20	grey
2	leg at lowest level	1.2	50	orange
3	leg 2 to 4 level	1.2	35	Blue
4	leg crossing TP	1.2	40	purple
5	pile	2.082	60	not shown

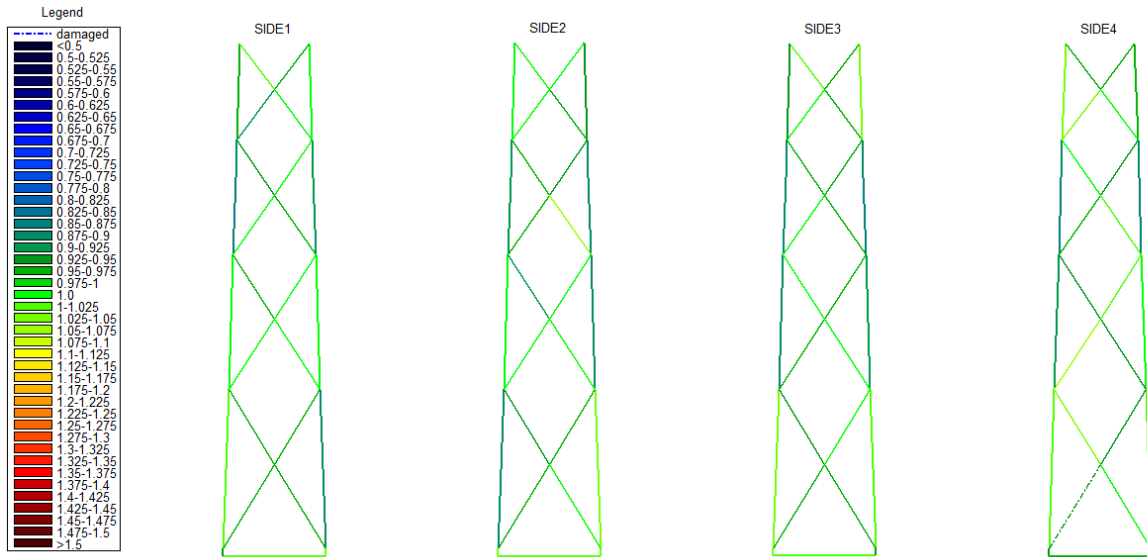
Table A.2. Property sets for jacket members

Member	Node 1	Node 2	Property set	Member	Node 1	Node 2	Property set
1	1	2	2	57	5	45	1
2	2	3	2	58	45	33	1
3	3	4	2	59	20	45	1
4	4	5	2	60	45	21	1
5	6	7	2	61	10	46	1
6	7	8	2	62	46	29	1
7	8	9	2	63	15	46	1
8	9	10	2	64	46	25	1
9	11	12	2	65	5	47	1
10	12	13	2	66	47	25	1
11	13	14	2	67	10	47	1
12	14	15	2	68	47	21	1
13	16	17	2	69	20	48	1
14	17	18	2	70	48	29	1
15	18	19	2	71	15	48	1
16	19	20	2	72	48	33	1
17	5	21	3	73	21	49	1
18	21	22	3	74	49	34	1
19	22	23	3	75	33	49	1
20	23	24	3	76	49	22	1
21	10	25	3	77	25	50	1
22	25	26	3	78	50	30	1
23	26	27	3	79	29	50	1
24	27	28	3	80	50	26	1
25	15	29	3	81	21	51	1
26	29	30	3	82	51	26	1
27	30	31	3	83	25	51	1
28	31	32	3	84	51	22	1
29	20	33	3	85	33	52	1
30	33	34	3	86	52	30	1
31	34	35	3	87	29	52	1
32	35	36	3	88	52	34	1
37	3	8	1	89	22	53	1
38	8	13	1	90	53	35	1
39	13	18	1	91	34	53	1
40	18	3	1	92	53	23	1
41	4	41	1	93	26	54	1
42	41	20	1	94	54	31	1
43	19	41	1	95	30	54	1
44	41	5	1	96	54	27	1
45	9	42	1	97	22	55	1
46	42	15	1	98	55	27	1
47	14	42	1	99	26	55	1
48	42	10	1	100	55	23	1
49	4	43	1	101	34	56	1
50	43	10	1	102	56	31	1
51	9	43	1	103	30	56	1
52	43	5	1	104	56	35	1
53	19	44	1	105	24	57	4
54	44	15	1	106	28	58	4
55	14	44	1	107	32	60	4
56	44	20	1	108	36	59	4

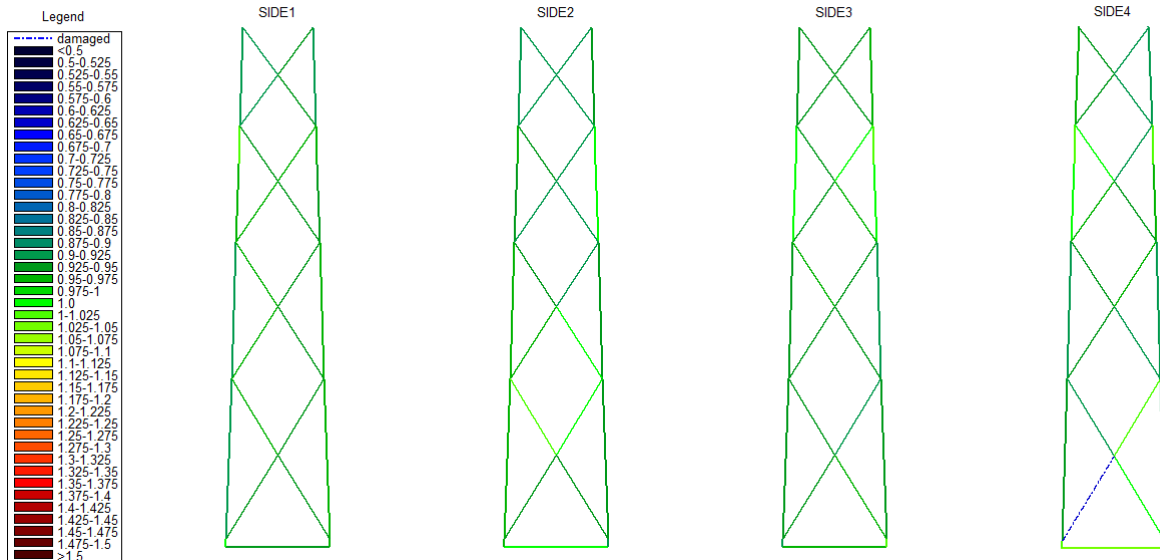
Table A.3. Members

APPENDIX B

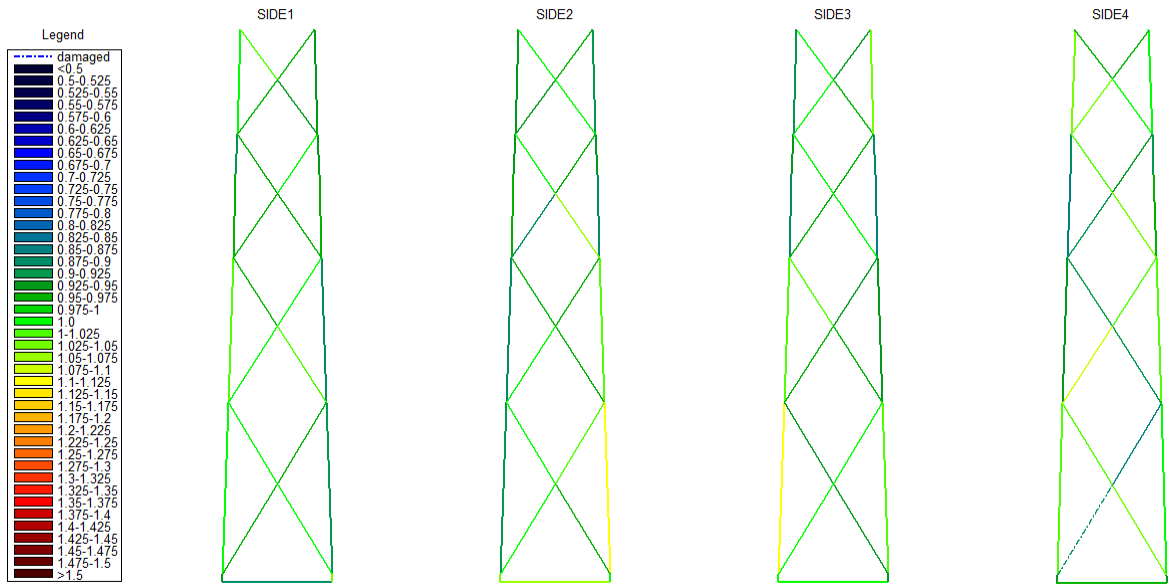
Results of fatigue analysis. Turbine operating with standard controller.



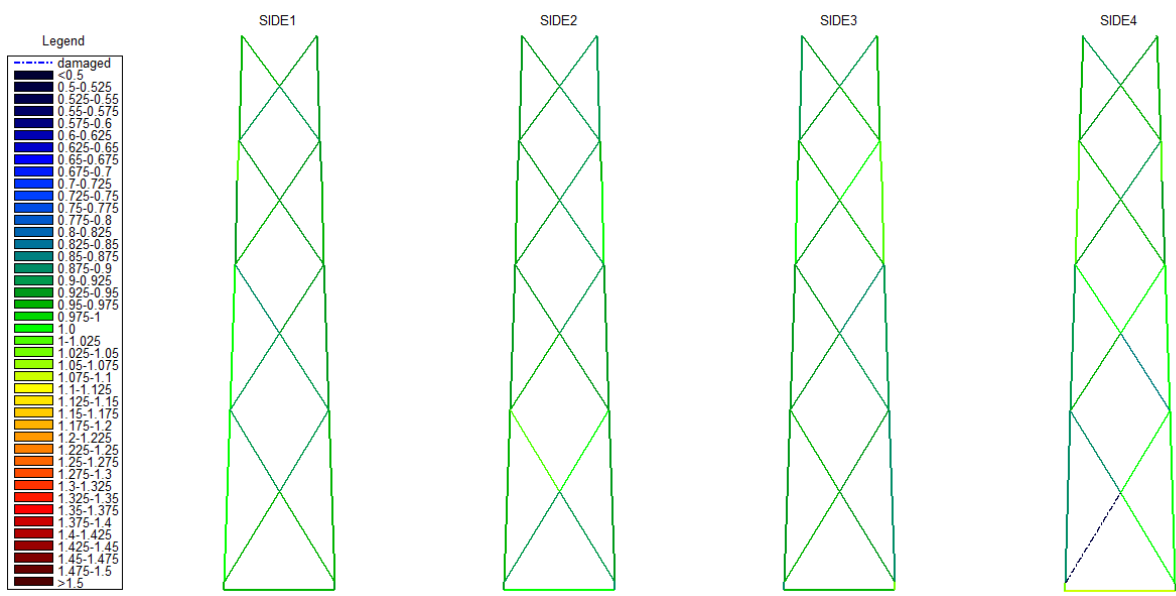
Design situation	DLC	Wind condition	Waves	Wind and wave directionality	Water level	Type of analysis	Type of EFL	Damaged element	Type of damage
Power Production	1.2	NTM 3<Vhub<25 4:2:24 m/s	NSS Hs=E[Hs Vhub]	COD,UNI	MSL	FATIGUE	FORCE	X-Brace 45 Level I-II	E=0.7E0



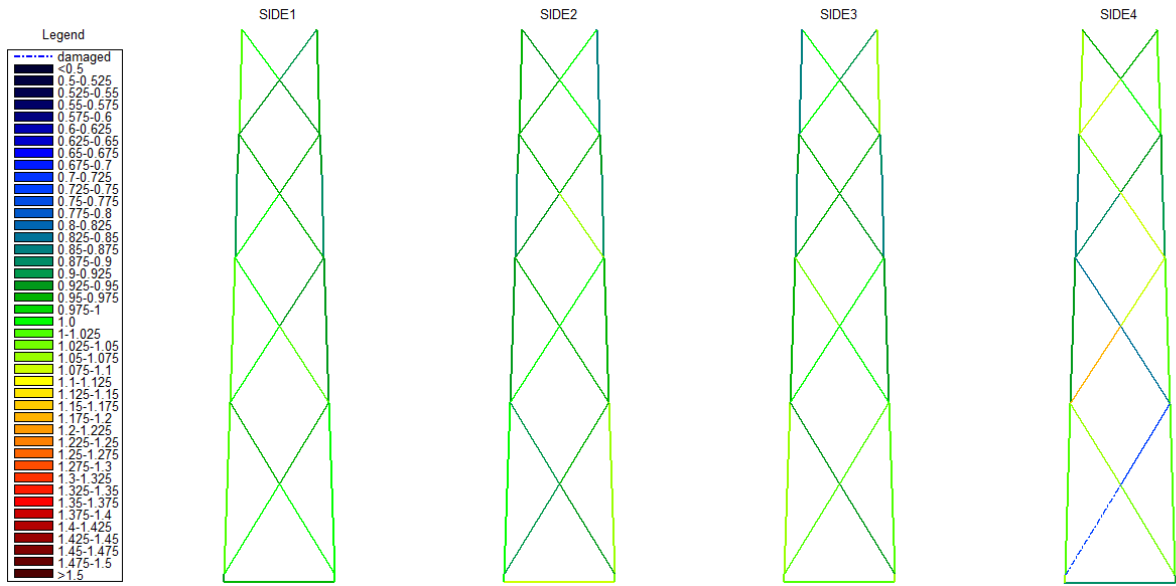
Design situation	DLC	Wind condition	Waves	Wind and wave directionality	Water level	Type of analysis	Type of EFL	Damaged element	Type of damage
Power Production	1.2	NTM 3<Vhub<25 4:2:24 m/s	NSS Hs=E[Hs Vhub]	COD,UNI	MSL	FATIGUE	MOMENT	X-Brace 45 Level I-II	E=0.7E0



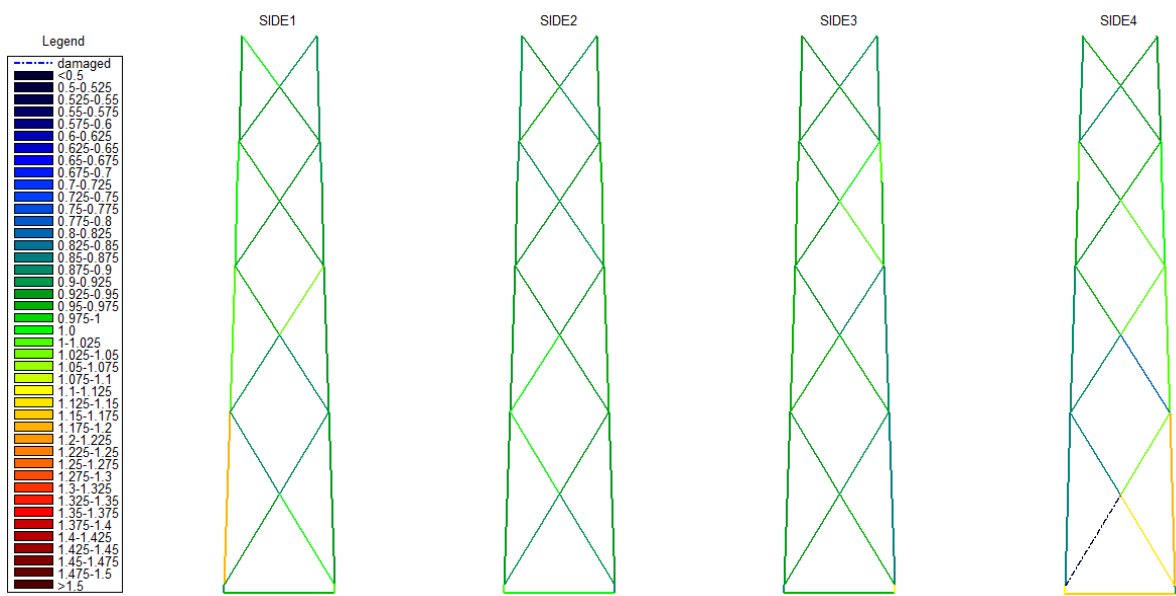
Design situation	DLC	Wind condition	Waves	Wind and wave directionality	Water level	Type of analysis	Type of EFL	Damaged element	Type of damage
Power Production	1.2	NTM 3<Vhub<25 4:2:24 m/s	NSS Hs=E[Hs Vhub]	COD,UNI	MSL	FATIGUE	FORCE	X-Brace 45 Level I-II	E=0.5E0



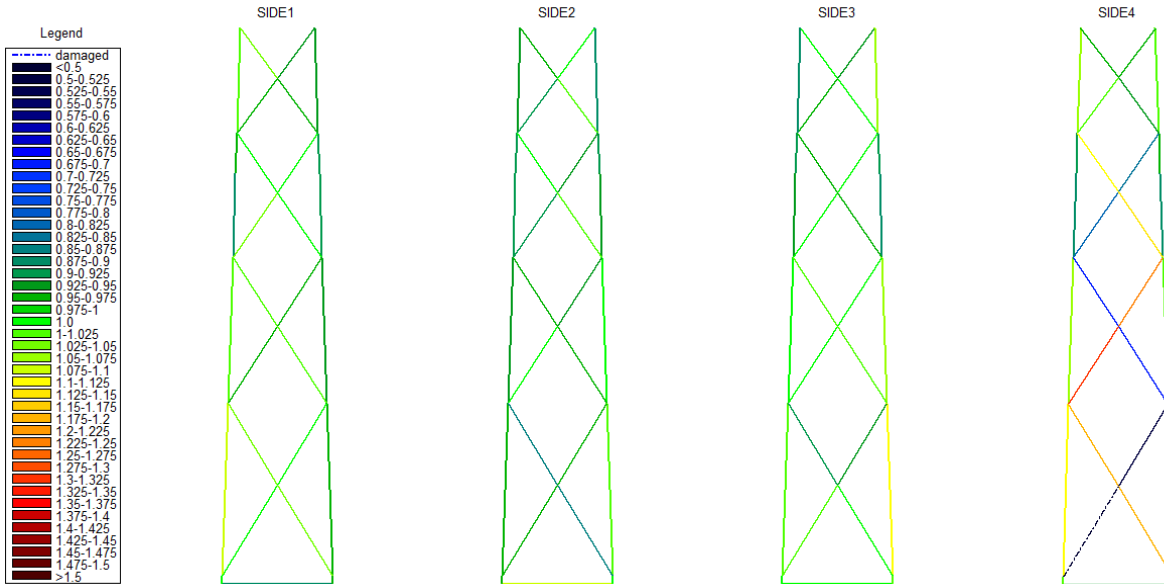
Design situation	DLC	Wind condition	Waves	Wind and wave directionality	Water level	Type of analysis	Type of EFL	Damaged element	Type of damage
Power Production	1.2	NTM 3<Vhub<25 4:2:24 m/s	NSS Hs=E[Hs Vhub]	COD,UNI	MSL	FATIGUE	MOMENT	X-Brace 45 Level I-II	E=0.5E0



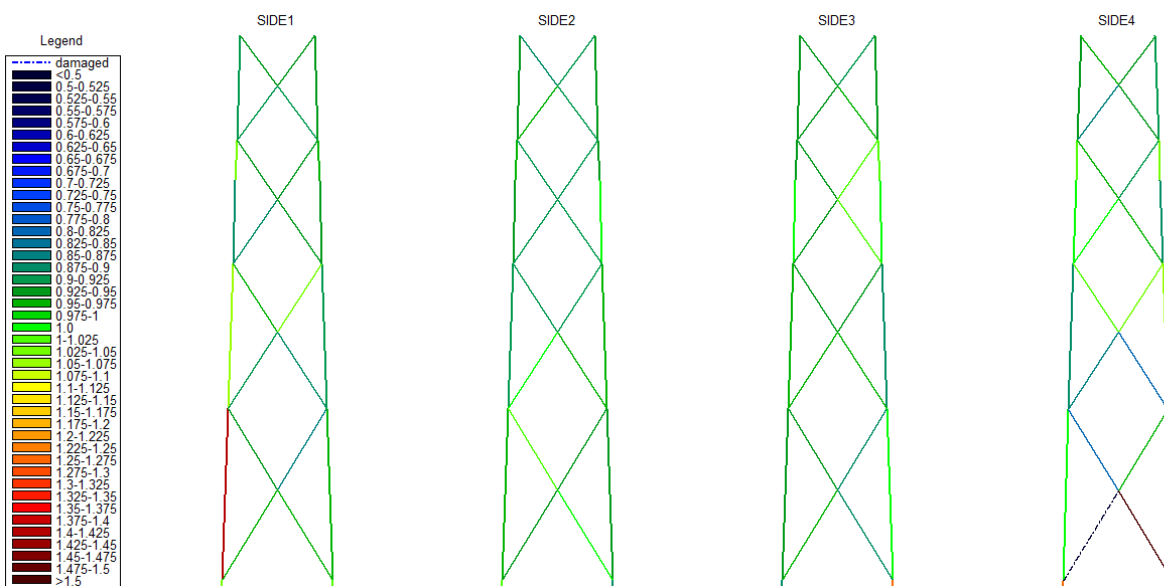
Design situation	DLC	Wind condition	Waves	Wind and wave directionality	Water level	Type of analysis	Type of EFL	Damaged element	Type of damage
Power Production	1.2	NTM 3<Vhub<25 4:2:24 m/s	NSS Hs=E[Hs Vhub]	COD,UNI	MSL	FATIGUE	FORCE	X-Brace 45 Level I-II	E=0.3E0



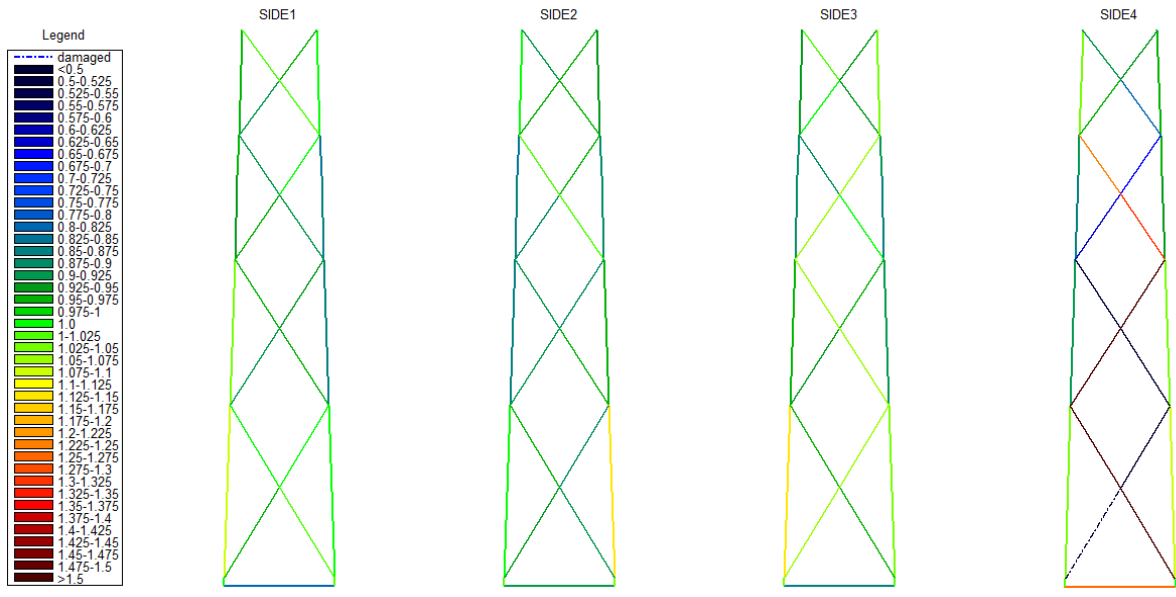
Design situation	DLC	Wind condition	Waves	Wind and wave directionality	Water level	Type of analysis	Type of EFL	Damaged element	Type of damage
Power Production	1.2	NTM 3<Vhub<25 4:2:24 m/s	NSS Hs=E[Hs Vhub]	COD,UNI	MSL	FATIGUE	MOMENT	X-Brace 45 Level I-II	E=0.3E0



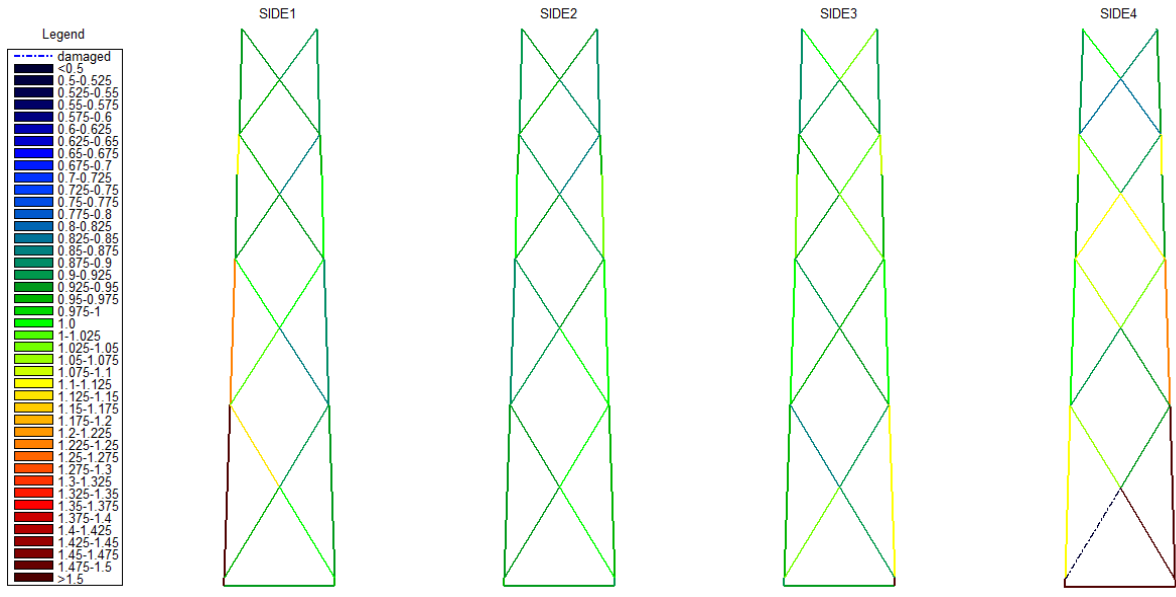
Design situation	DLC	Wind condition	Waves	Wind and wave directionality	Water level	Type of analysis	Type of EFL	Damaged element	Type of damage
Power Production	1.2	NTM $3 < V_{hub} < 25$ 4:2:24 m/s	NSS $H_s = E[H_s V_{hub}]$	COD,UNI	MSL	FATIGUE	FORCE	X-Brace 45 Level I-II	$E = 0.1E0$



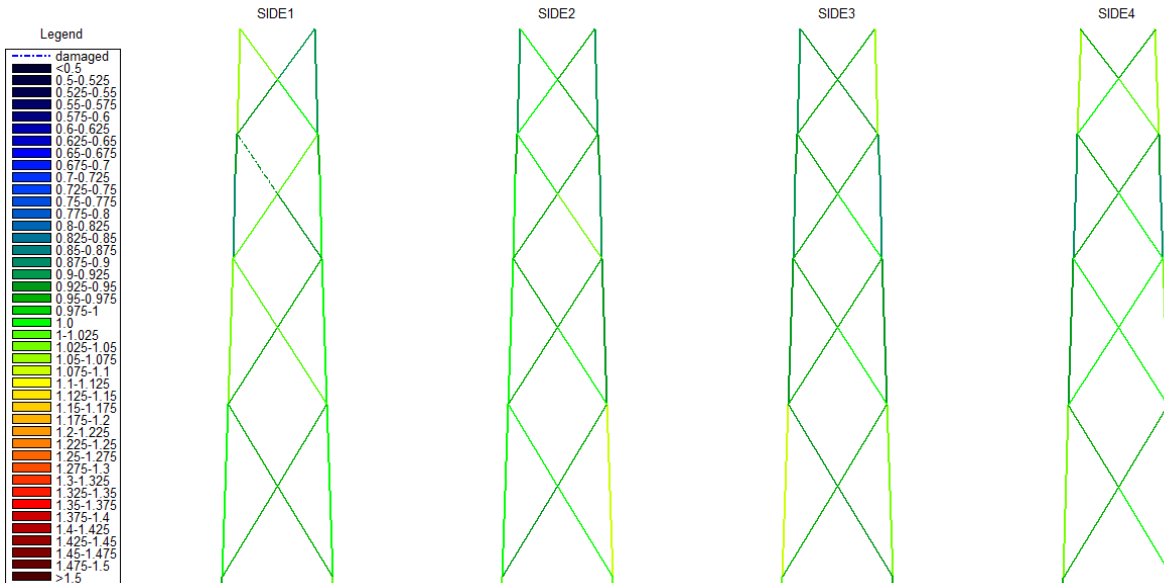
Design situation	DLC	Wind condition	Waves	Wind and wave directionality	Water level	Type of analysis	Type of EFL	Damaged element	Type of damage
Power Production	1.2	NTM $3 < V_{hub} < 25$ 4:2:24 m/s	NSS $H_s = E[H_s V_{hub}]$	COD,UNI	MSL	FATIGUE	MOMENT	X-Brace 45 Level I-II	$E = 0.1E0$



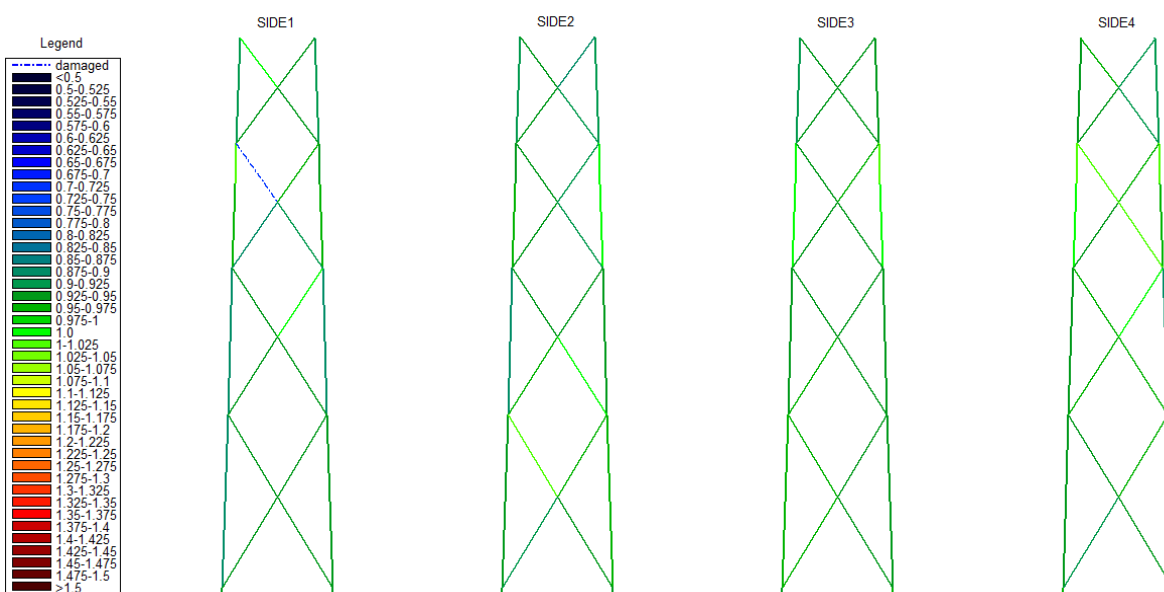
Design situation	DLC	Wind condition	Waves	Wind and wave directionality	Water level	Type of analysis	Type of EFL	Damaged element	Type of damage
Power Production	1.2	NTM 3<Vhub<25 4:2:24 m/s	NSS Hs=E[Hs Vhub]	COD,UNI	MSL	FATIGUE	FORCE	X-Brace 45 Level I-II	FREE-JOINT



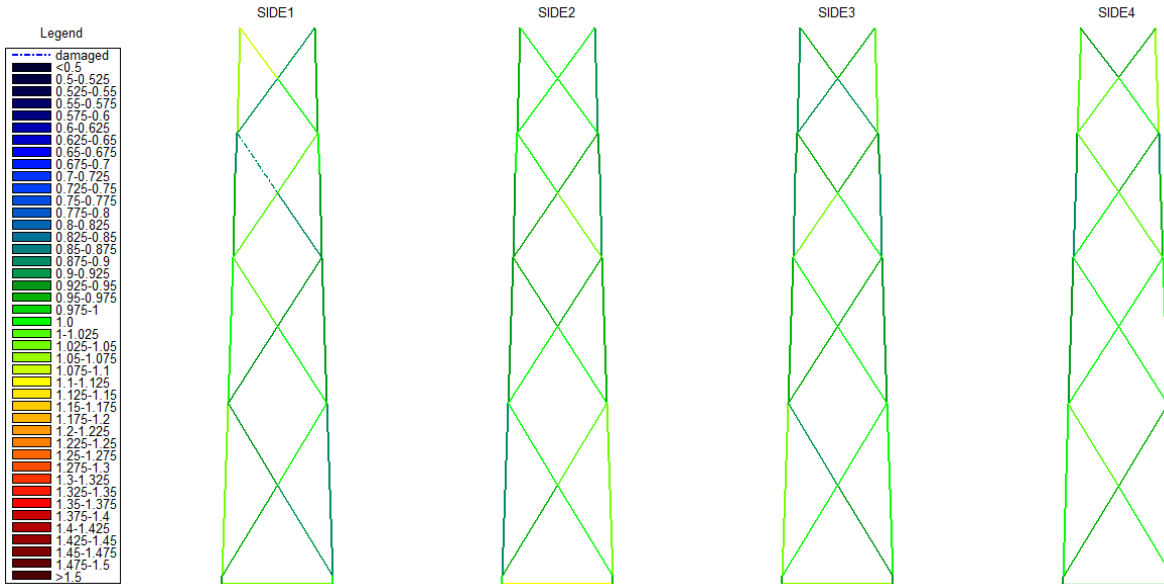
Design situation	DLC	Wind condition	Waves	Wind and wave directionality	Water level	Type of analysis	Type of EFL	Damaged element	Type of damage
Power Production	1.2	NTM 3<Vhub<25 4:2:24 m/s	NSS Hs=E[Hs Vhub]	COD,UNI	MSL	FATIGUE	MOMENT	X-Brace 45 Level I-II	FREE-JOINT



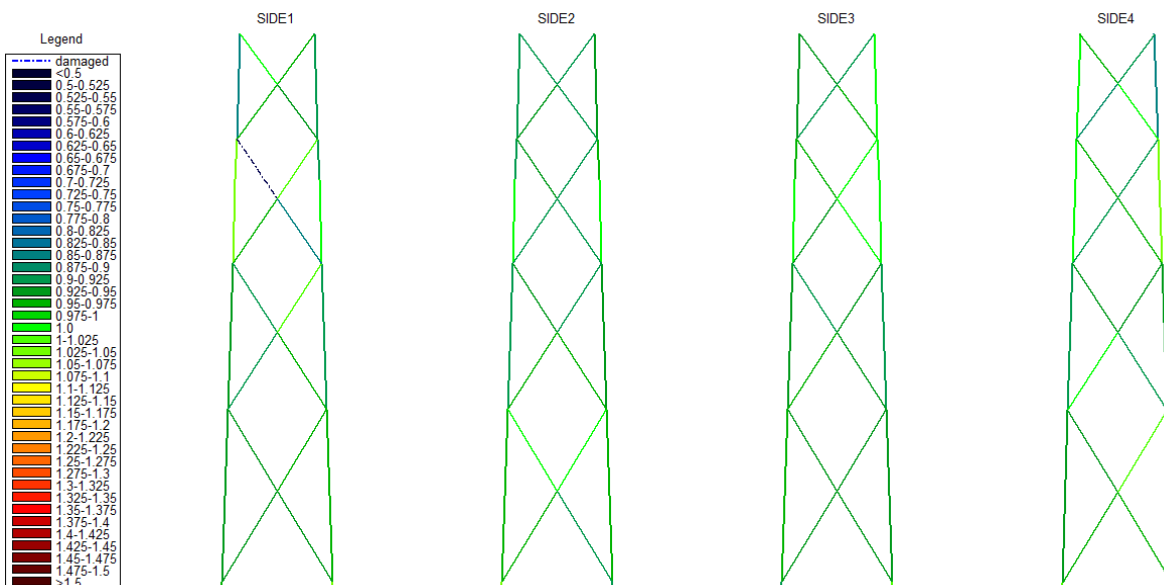
Design situation	DLC	Wind condition	Waves	Wind and wave directionality	Water level	Type of analysis	Type of EFL	Damaged element	Type of damage
Power Production	1.2	NTM 3<Vhub<25 4:2:24 m/s	NSS Hs=E[Hs Vhub]	COD,UNI	MSL	FATIGUE	FORCE	X-Brace 86 Level III-IV	E=0.7E0



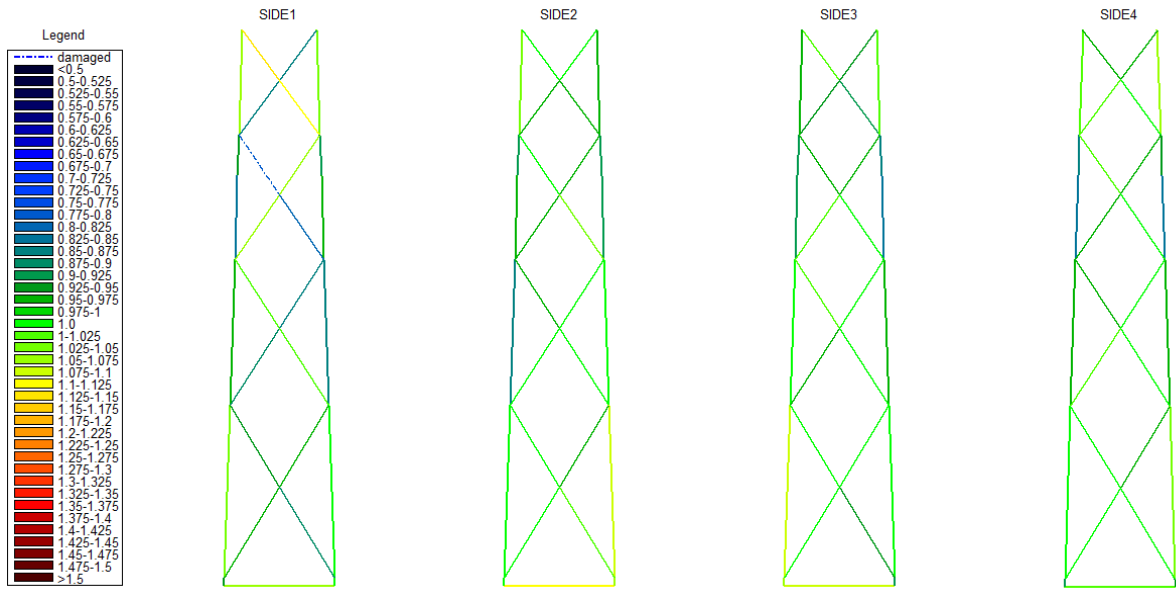
Design situation	DLC	Wind condition	Waves	Wind and wave directionality	Water level	Type of analysis	Type of EFL	Damaged element	Type of damage
Power Production	1.2	NTM 3<Vhub<25 4:2:24 m/s	NSS Hs=E[Hs Vhub]	COD,UNI	MSL	FATIGUE	MOMENT	X-Brace 86 Level III-IV	E=0.7E0



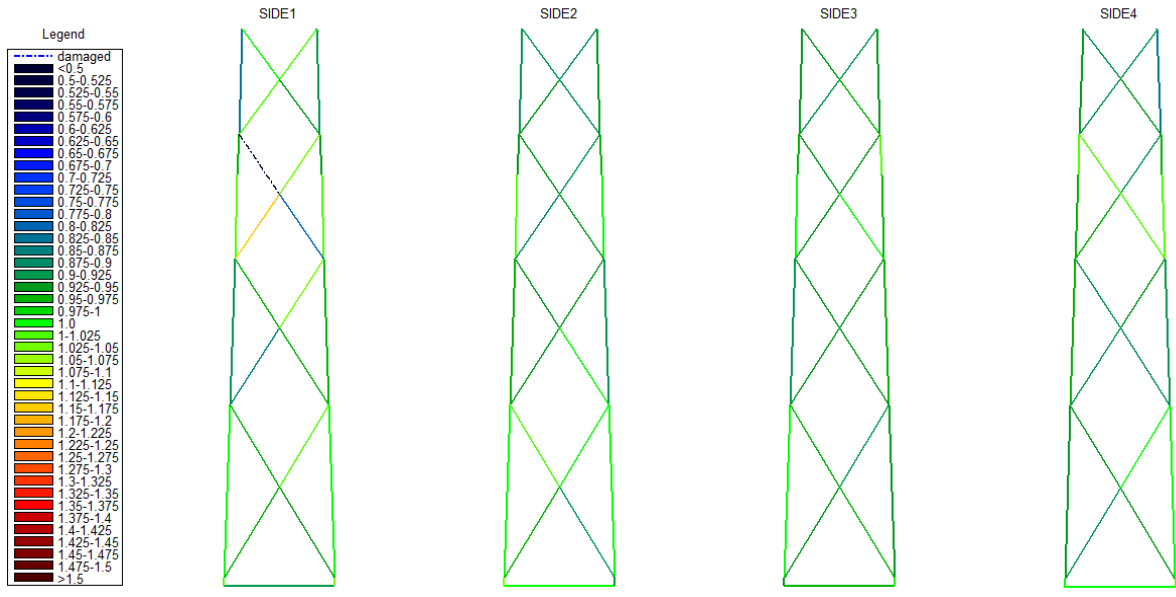
Design situation	DLC	Wind condition	Waves	Wind and wave directionality	Water level	Type of analysis	Type of EFL	Damaged element	Type of damage
Power Production	1.2	NTM 3V_{hub}<math><25</math> 4:2:24 m/s	NSS $H_s=E[H_s V_{hub}]$	COD,UNI	MSL	FATIGUE	FORCE	X-Brace 86 Level III-IV	E=0.5E0



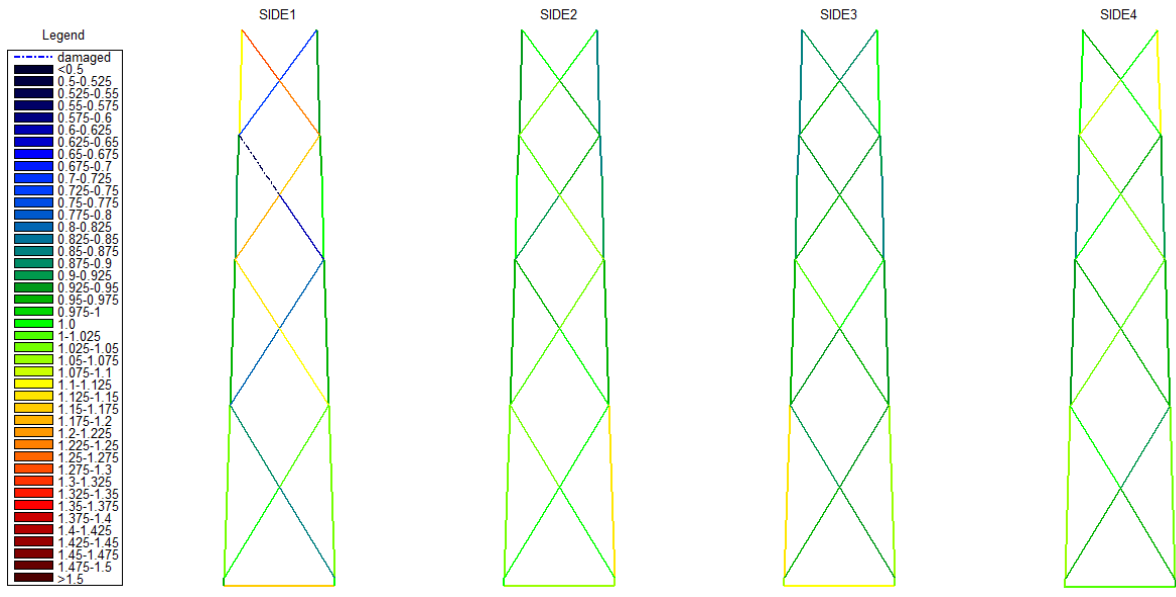
Design situation	DLC	Wind condition	Waves	Wind and wave directionality	Water level	Type of analysis	Type of EFL	Damaged element	Type of damage
Power Production	1.2	NTM 3V_{hub}<math><25</math> 4:2:24 m/s	NSS $H_s=E[H_s V_{hub}]$	COD,UNI	MSL	FATIGUE	MOMENT	X-Brace 86 Level III-IV	E=0.5E0



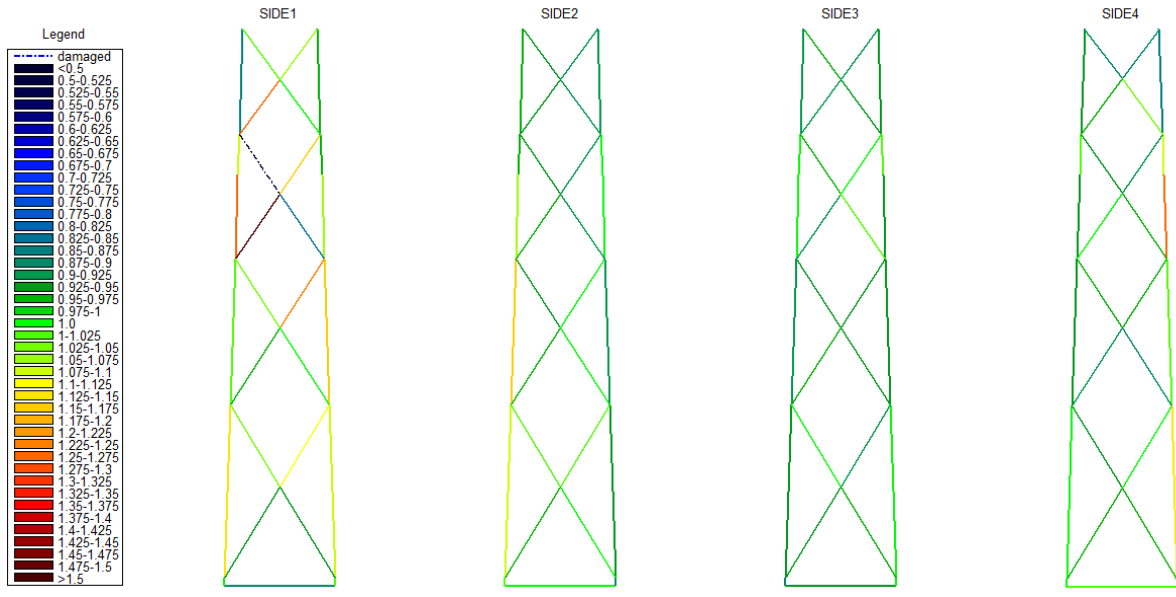
Design situation	DLC	Wind condition	Waves	Wind and wave directionality	Water level	Type of analysis	Type of EFL	Damaged element	Type of damage
Power Production	1.2	NTM 3<Vhub<25 4:2:24 m/s	NSS Hs=E[Hs Vhub]	COD,UNI	MSL	FATIGUE	FORCE	X-Brace 86 Level III-IV	E=0.3E0



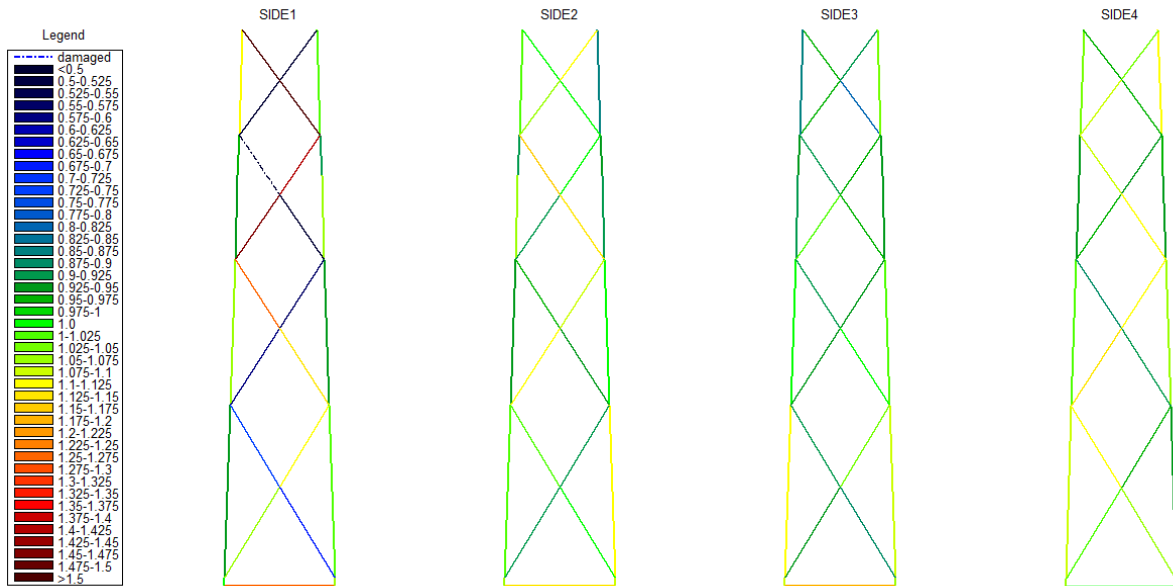
Design situation	DLC	Wind condition	Waves	Wind and wave directionality	Water level	Type of analysis	Type of EFL	Damaged element	Type of damage
Power Production	1.2	NTM 3<Vhub<25 4:2:24 m/s	NSS Hs=E[Hs Vhub]	COD,UNI	MSL	FATIGUE	MOMENT	X-Brace 86 Level III-IV	E=0.3E0



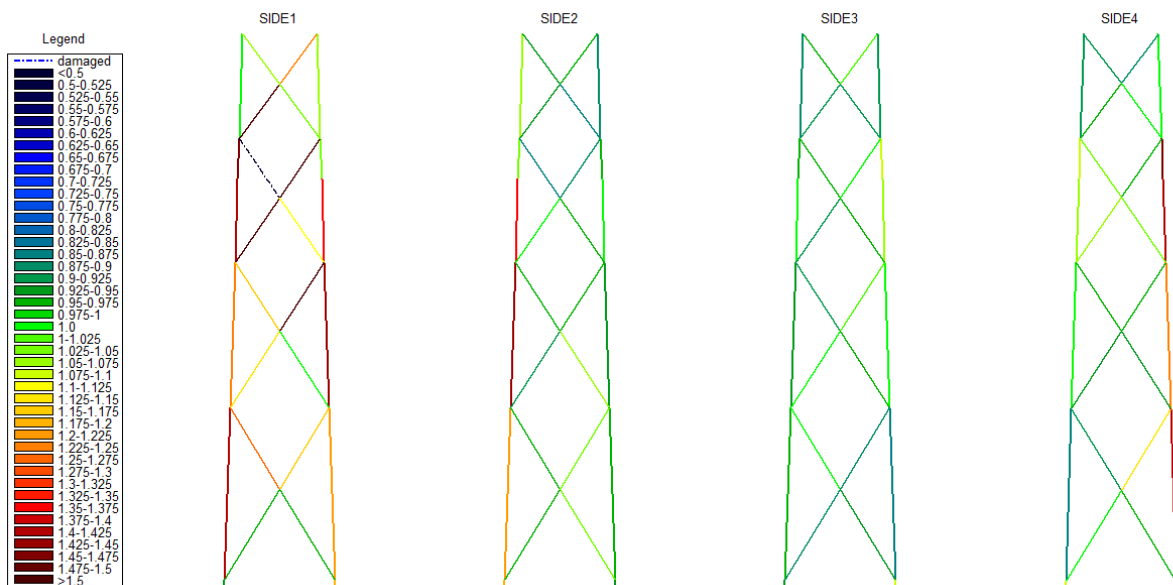
Design situation	DLC	Wind condition	Waves	Wind and wave directionality	Water level	Type of analysis	Type of EFL	Damaged element	Type of damage
Power Production	1.2	NTM 3<Vhub<25 4:2:24 m/s	NSS Hs=E[Hs Vhub]	COD,UNI	MSL	FATIGUE	FORCE	X-Brace 86 Level III-IV	E=0.1E0



Design situation	DLC	Wind condition	Waves	Wind and wave directionality	Water level	Type of analysis	Type of EFL	Damaged element	Type of damage
Power Production	1.2	NTM 3<Vhub<25 4:2:24 m/s	NSS Hs=E[Hs Vhub]	COD,UNI	MSL	FATIGUE	MOMENT	X-Brace 86 Level III-IV	E=0.1E0



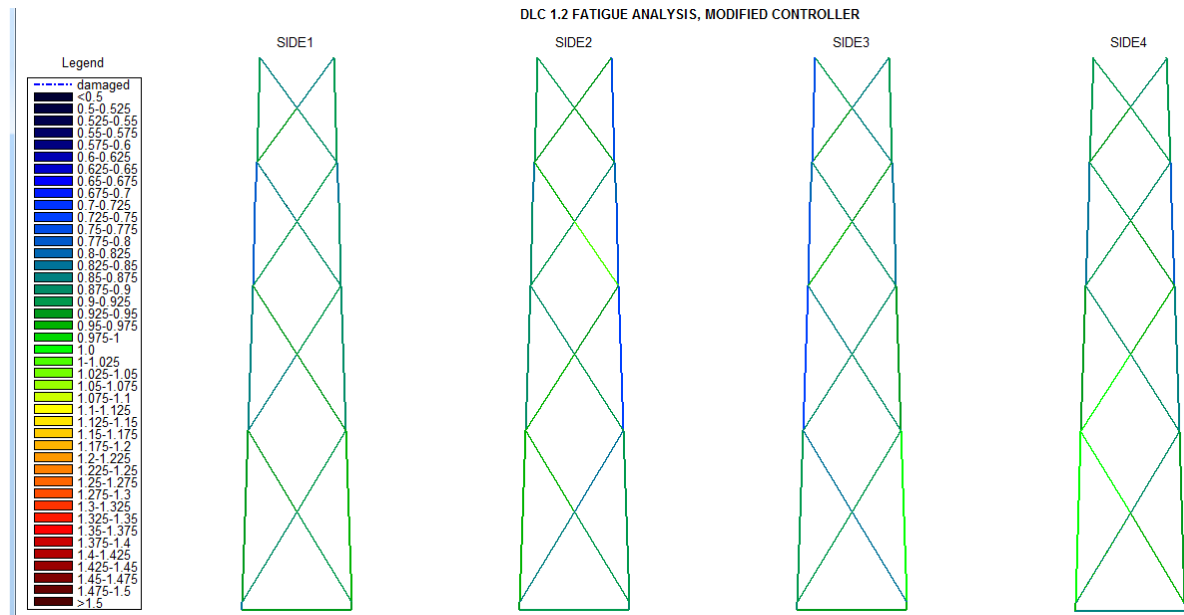
Design situation	DLC	Wind condition	Waves	Wind and wave directionality	Water level	Type of analysis	Type of EFL	Damaged element	Type of damage
Power Production	1.2	NTM 3<Vhub<25 4:2:24 m/s	NSS Hs=E[Hs Vhub]	COD,UNI	MSL	FATIGUE	FORCE	X-Brace 86 Level III-IV	FREE-JOINT



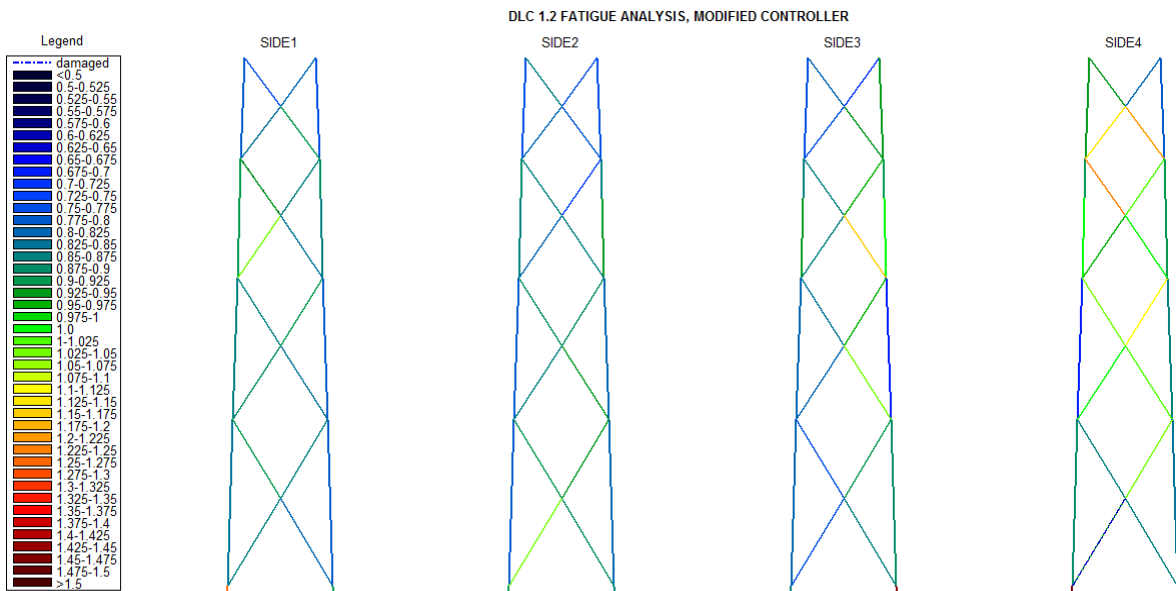
Design situation	DLC	Wind condition	Waves	Wind and wave directionality	Water level	Type of analysis	Type of EFL	Damaged element	Type of damage
Power Production	1.2	NTM 3<Vhub<25 4:2:24 m/s	NSS Hs=E[Hs Vhub]	COD,UNI	MSL	FATIGUE	MOMENT	X-Brace 86 Level III-IV	FREE-JOINT

APPENDIX C

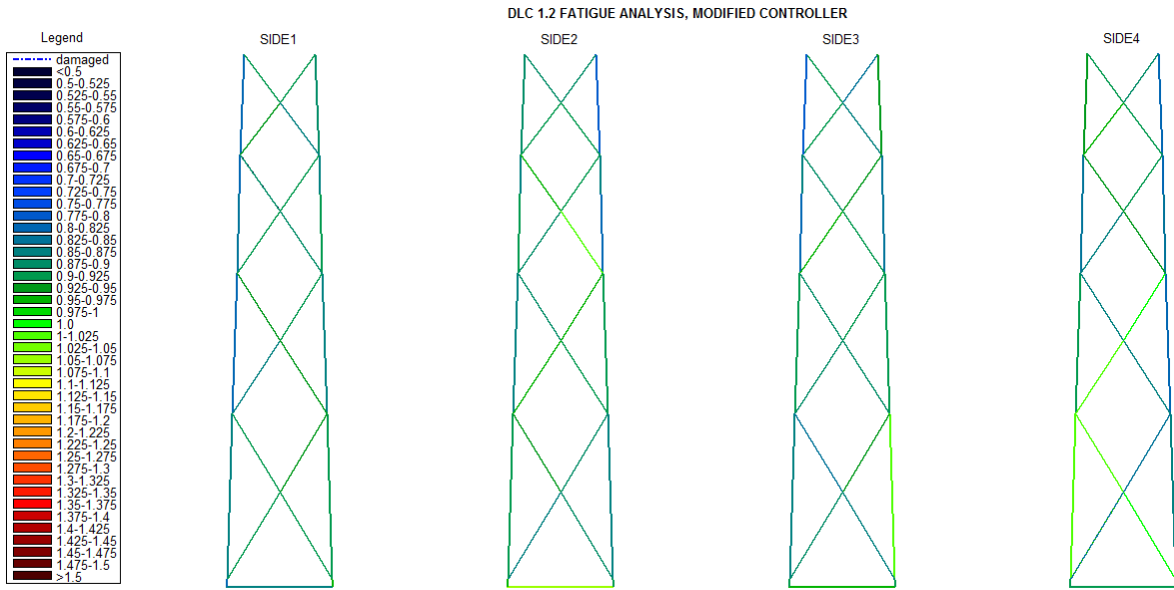
Results of fatigue analysis. Turbine operating with modified controller.



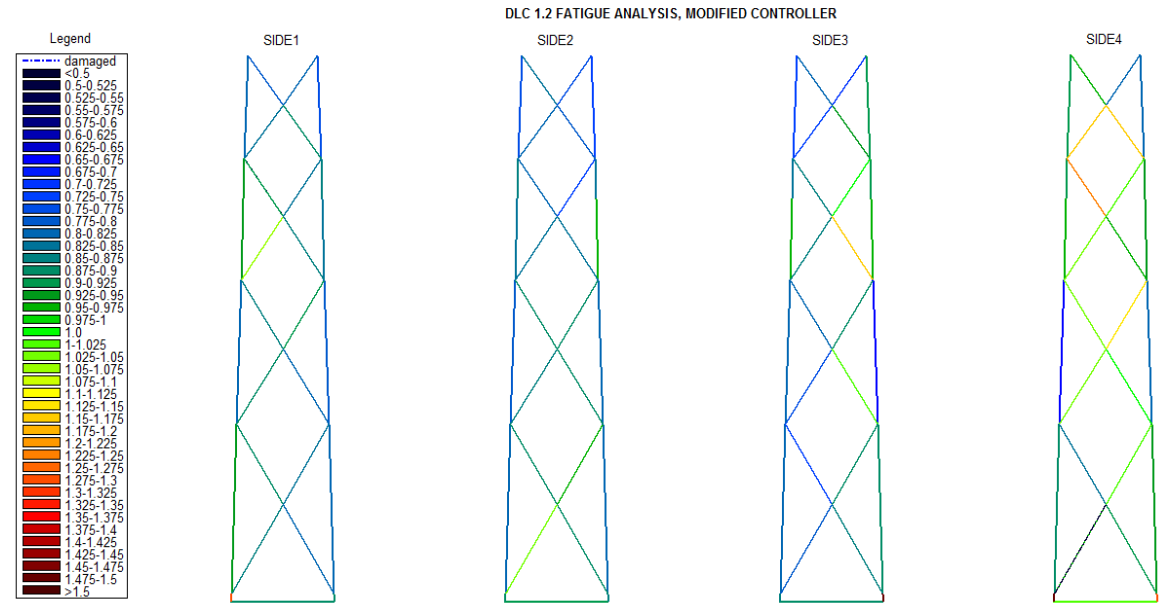
Design situation	DLC	Wind condition	Waves	Wind and wave directionality	Water level	Type of analysis	Type of EFL	Damaged element	Type of damage
Power Production	1.2	NTM 3<Vhub<25 4:2:24 m/s	NSS Hs=E[Hs Vhub]	COD,UNI	MSL	FATIGUE	FORCE	X-Brace 45 Level I-II	E=0.7E0



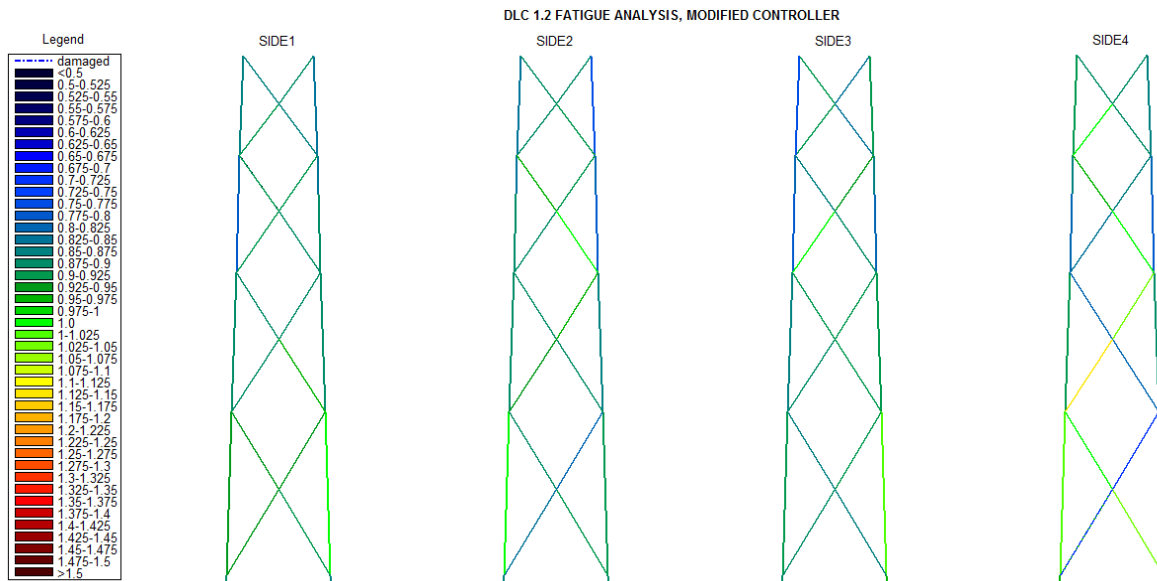
Design situation	DLC	Wind condition	Waves	Wind and wave directionality	Water level	Type of analysis	Type of EFL	Damaged element	Type of damage
Power Production	1.2	NTM 3<Vhub<25 4:2:24 m/s	NSS Hs=E[Hs Vhub]	COD,UNI	MSL	FATIGUE	MOMENT	X-Brace 45 Level I-II	E=0.7E0



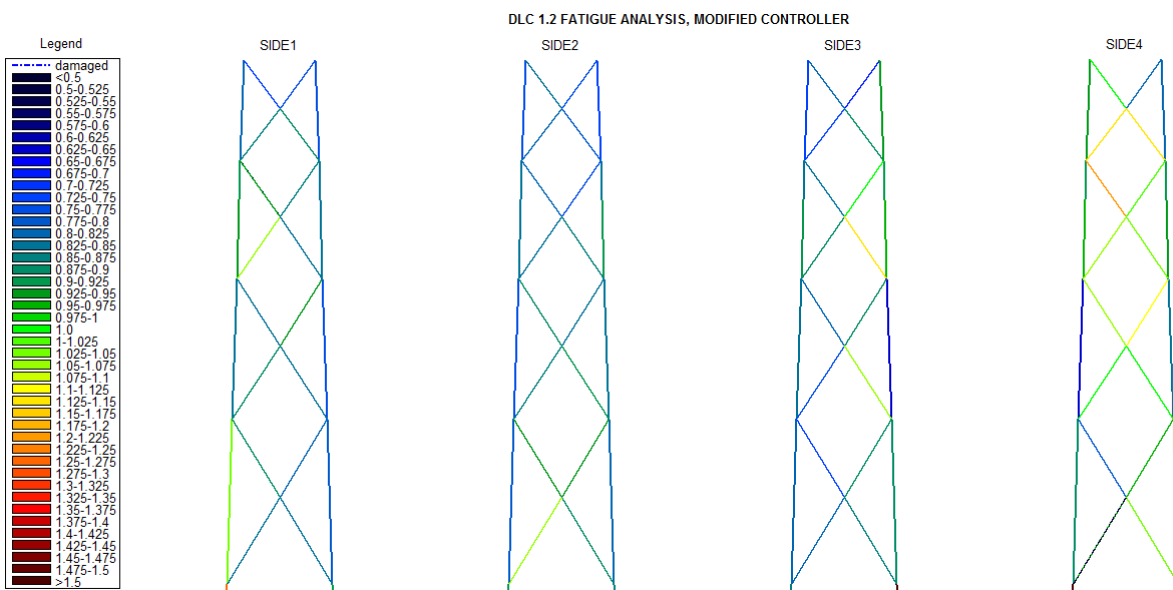
Design situation	DLC	Wind condition	Waves	Wind and wave directionality	Water level	Type of analysis	Type of EFL	Damaged element	Type of damage
Power Production	1.2	NTM 3<Vhub<25 4:2:24 m/s	NSS Hs=E[Hs Vhub]	COD,UNI	MSL	FATIGUE	FORCE	X-Brace 45 Level I-II	E=0.5E0



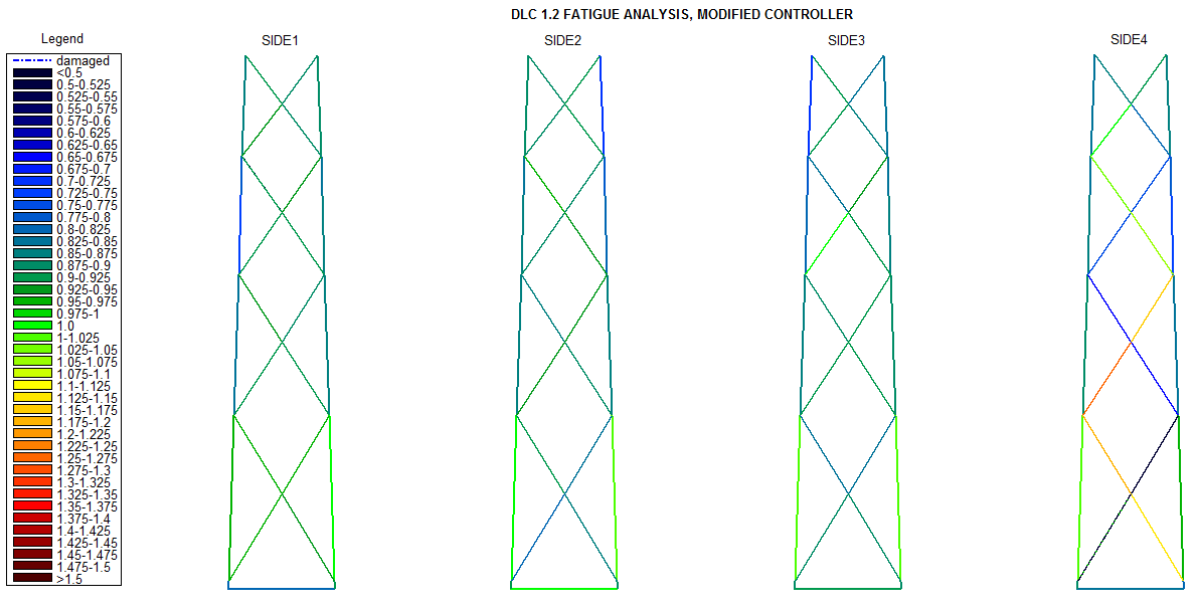
Design situation	DLC	Wind condition	Waves	Wind and wave directionality	Water level	Type of analysis	Type of EFL	Damaged element	Type of damage
Power Production	1.2	NTM 3<Vhub<25 4:2:24 m/s	NSS Hs=E[Hs Vhub]	COD,UNI	MSL	FATIGUE	MOMENT	X-Brace 45 Level I-II	E=0.5E0



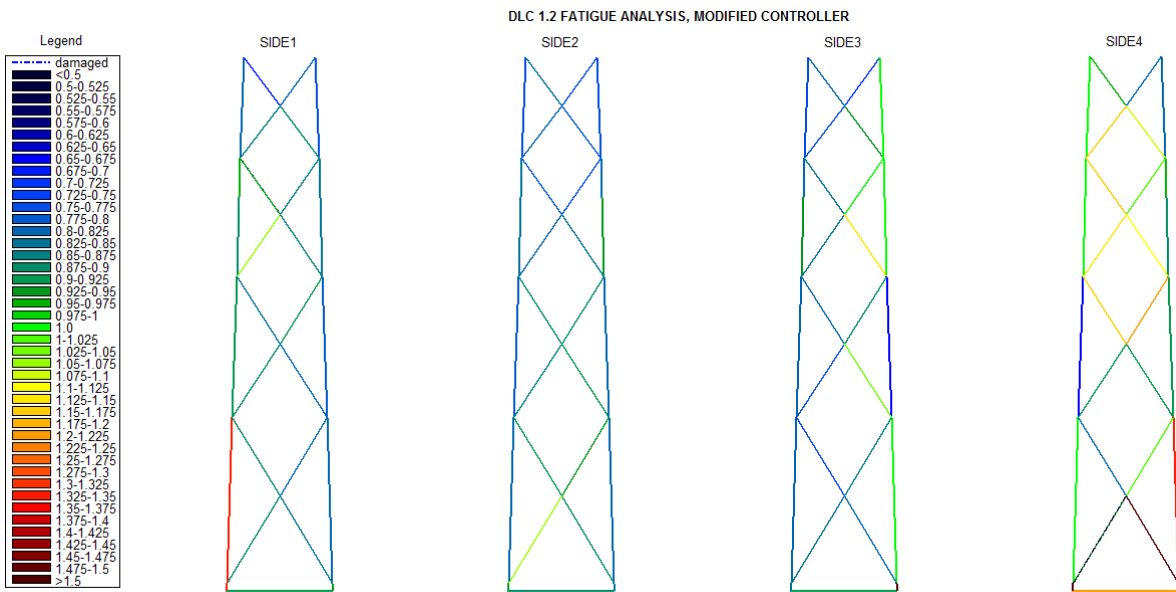
Design situation	DLC	Wind condition	Waves	Wind and wave directionality	Water level	Type of analysis	Type of EFL	Damaged element	Type of damage
Power Production	1.2	NTM 3<Vhub<25 4:2:24 m/s	NSS $H_s=E[H_s V_{hub}]$	COD,UNI	MSL	FATIGUE	FORCE	X-Brace 45 Level I-II	E=0.3E0



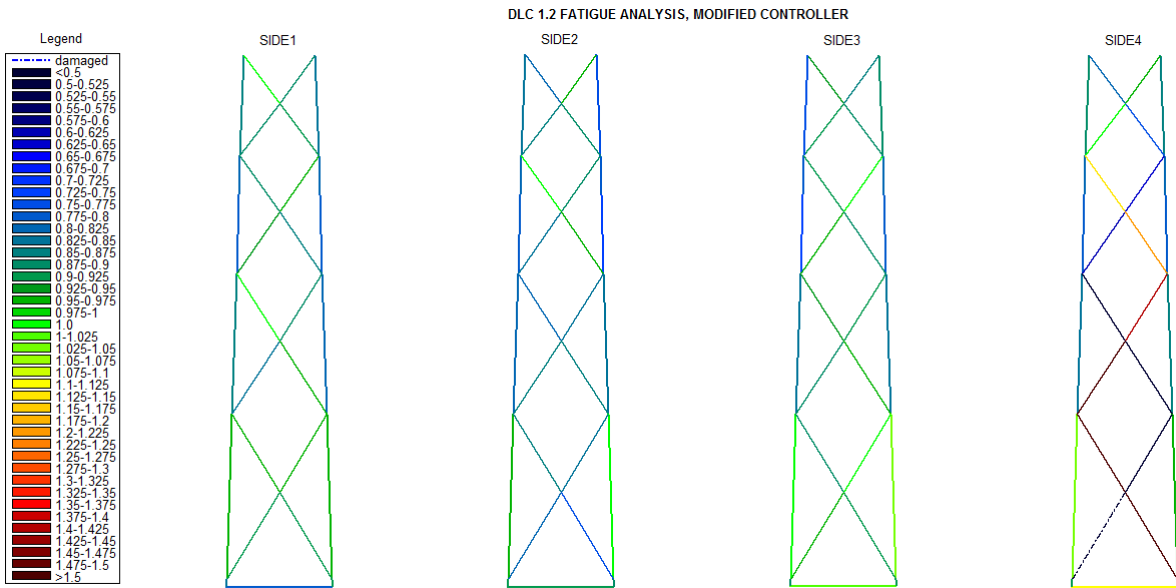
Design situation	DLC	Wind condition	Waves	Wind and wave directionality	Water level	Type of analysis	Type of EFL	Damaged element	Type of damage
Power Production	1.2	NTM 3<Vhub<25 4:2:24 m/s	NSS $H_s=E[H_s V_{hub}]$	COD,UNI	MSL	FATIGUE	MOMENT	X-Brace 45 Level I-II	E=0.3E0



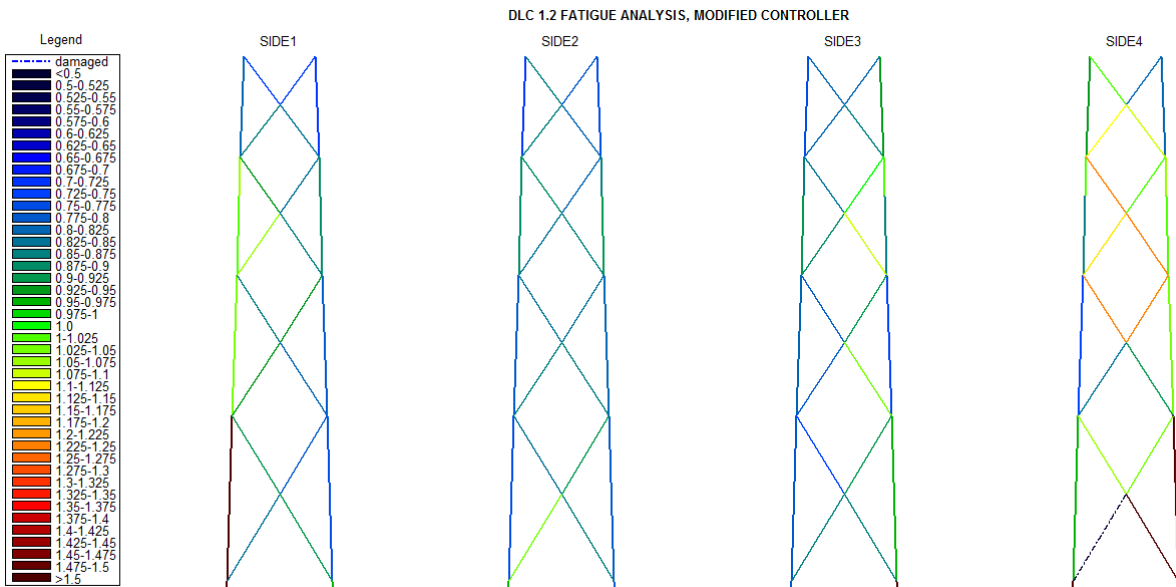
Design situation	DLC	Wind condition	Waves	Wind and wave directionality	Water level	Type of analysis	Type of EFL	Damaged element	Type of damage
Power Production	1.2	NTM 3<Vhub<25 4:2:24 m/s	NSS Hs=E[Hs Vhub]	COD,UNI	MSL	FATIGUE	FORCE	X-Brace 45 Level I-II	E=0.1E0



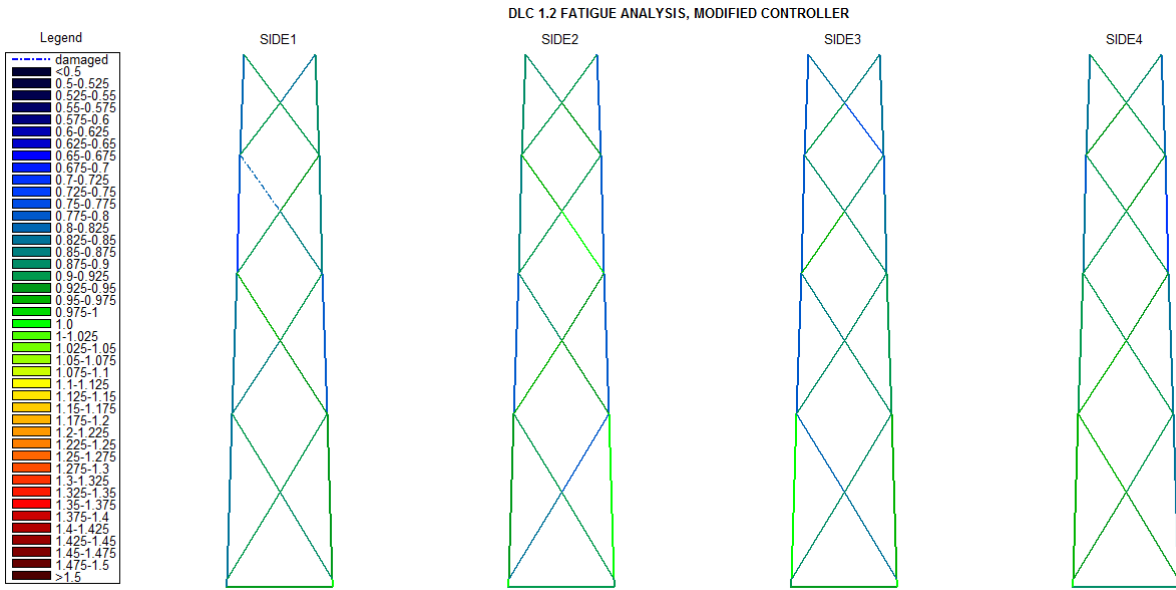
Design situation	DLC	Wind condition	Waves	Wind and wave directionality	Water level	Type of analysis	Type of EFL	Damaged element	Type of damage
Power Production	1.2	NTM 3<Vhub<25 4:2:24 m/s	NSS Hs=E[Hs Vhub]	COD,UNI	MSL	FATIGUE	MOMENT	X-Brace 45 Level I-II	E=0.1E0



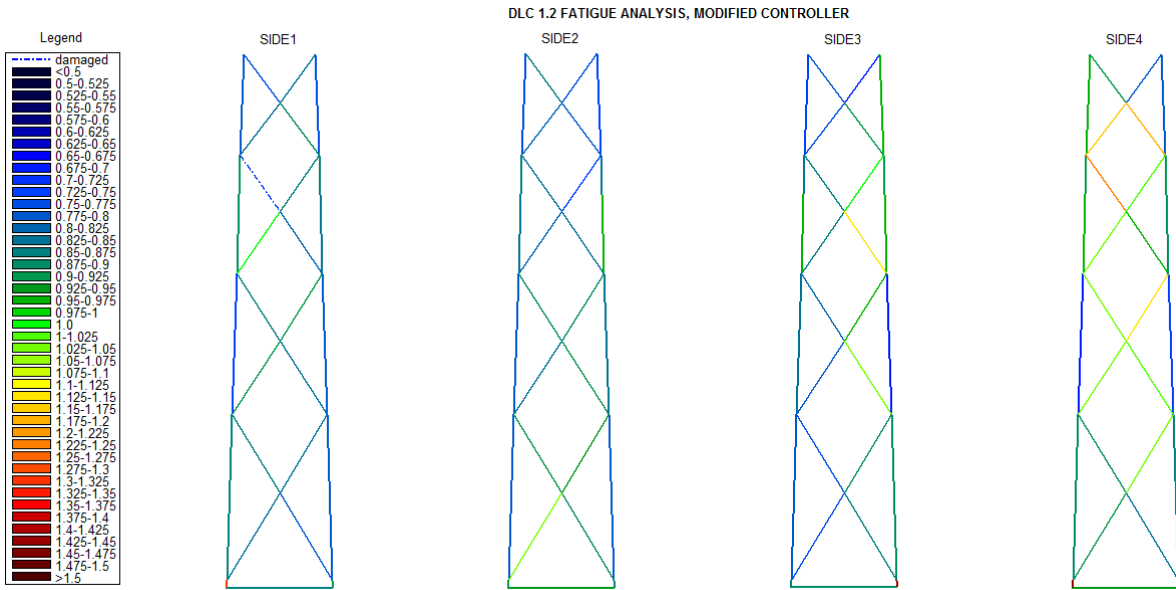
Design situation	DLC	Wind condition	Waves	Wind and wave directionality	Water level	Type of analysis	Type of EFL	Damaged element	Type of damage
Power Production	1.2	NTM 3<Vhub<25 4:2:24 m/s	NSS Hs=E[Hs Vhub]	COD,UNI	MSL	FATIGUE	FORCE	X-Brace 45 Level I-II	FREE-JOINT



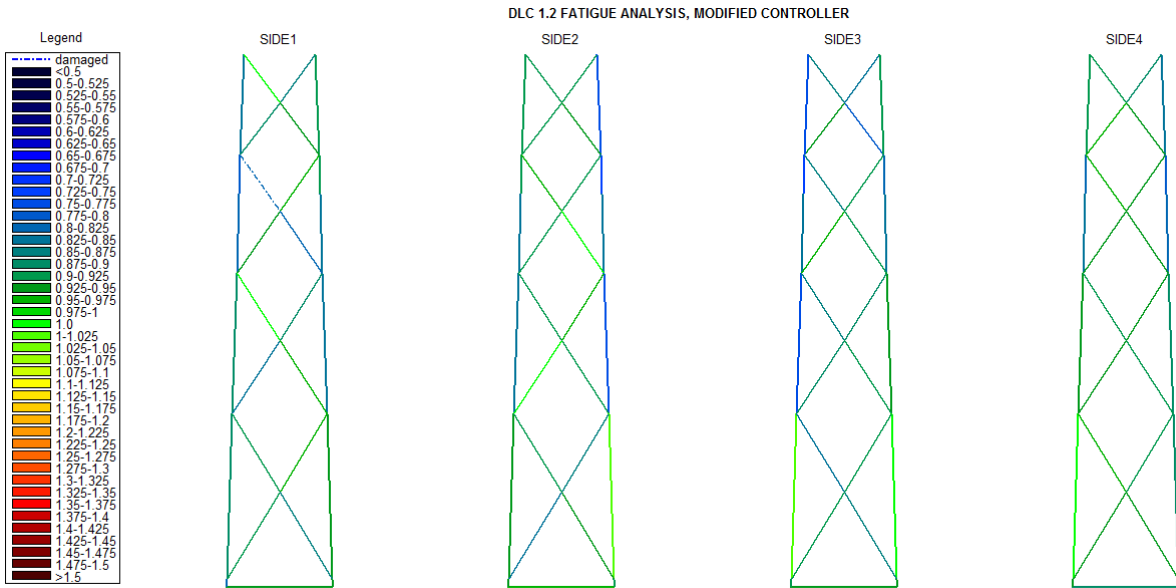
Design situation	DLC	Wind condition	Waves	Wind and wave directionality	Water level	Type of analysis	Type of EFL	Damaged element	Type of damage
Power Production	1.2	NTM 3<Vhub<25 4:2:24 m/s	NSS Hs=E[Hs Vhub]	COD,UNI	MSL	FATIGUE	MOMENT	X-Brace 45 Level I-II	FREE-JOINT



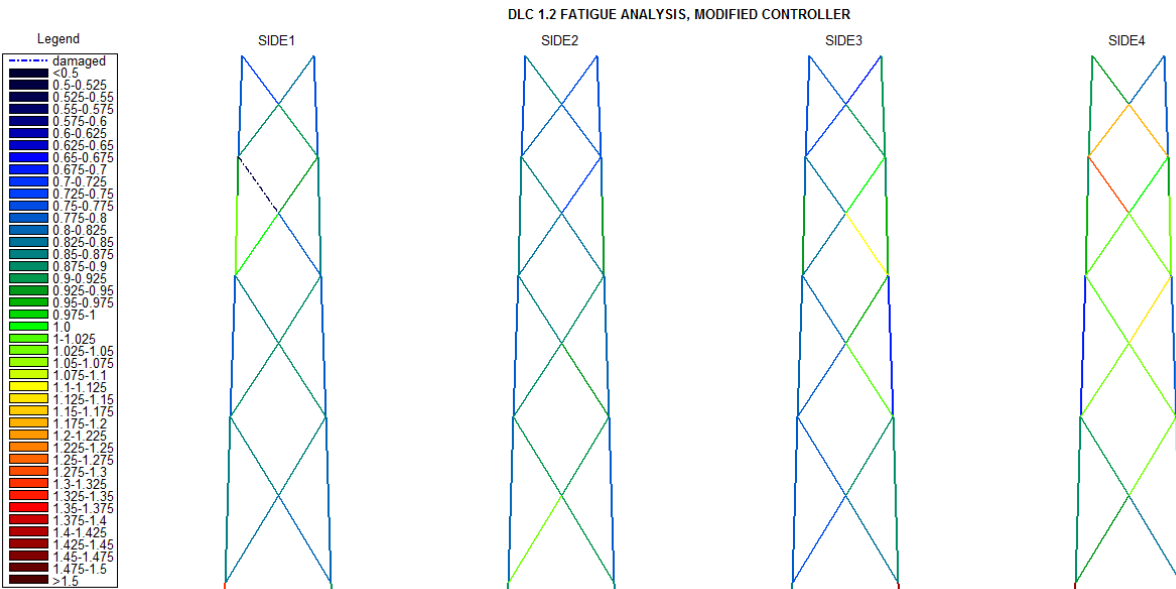
Design situation	DLC	Wind condition	Waves	Wind and wave directionality	Water level	Type of analysis	Type of EFL	Damaged element	Type of damage
Power Production	1.2	NTM $3 < V_{hub} < 25$ 4:2:24 m/s	NSS $H_s = E[H_s V_{hub}]$	COD,UNI	MSL	FATIGUE	FORCE	X-Brace 86 Level III-IV	$E=0.7E0$



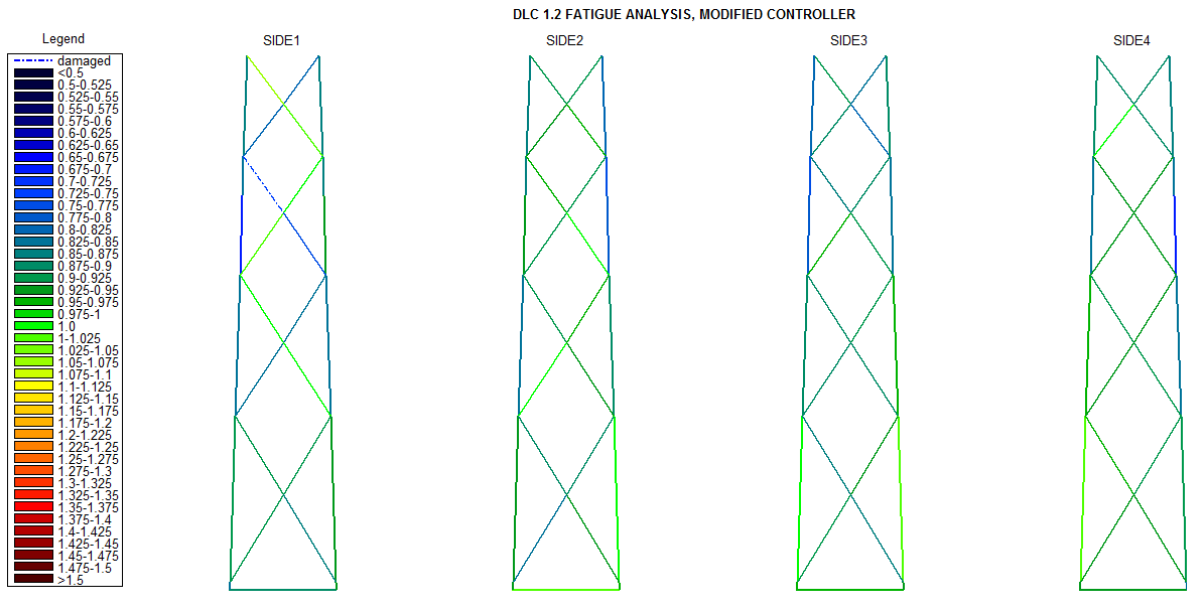
Design situation	DLC	Wind condition	Waves	Wind and wave directionality	Water level	Type of analysis	Type of EFL	Damaged element	Type of damage
Power Production	1.2	NTM $3 < V_{hub} < 25$ 4:2:24 m/s	NSS $H_s = E[H_s V_{hub}]$	COD,UNI	MSL	FATIGUE	MOMENT	X-Brace 86 Level III-IV	$E=0.7E0$



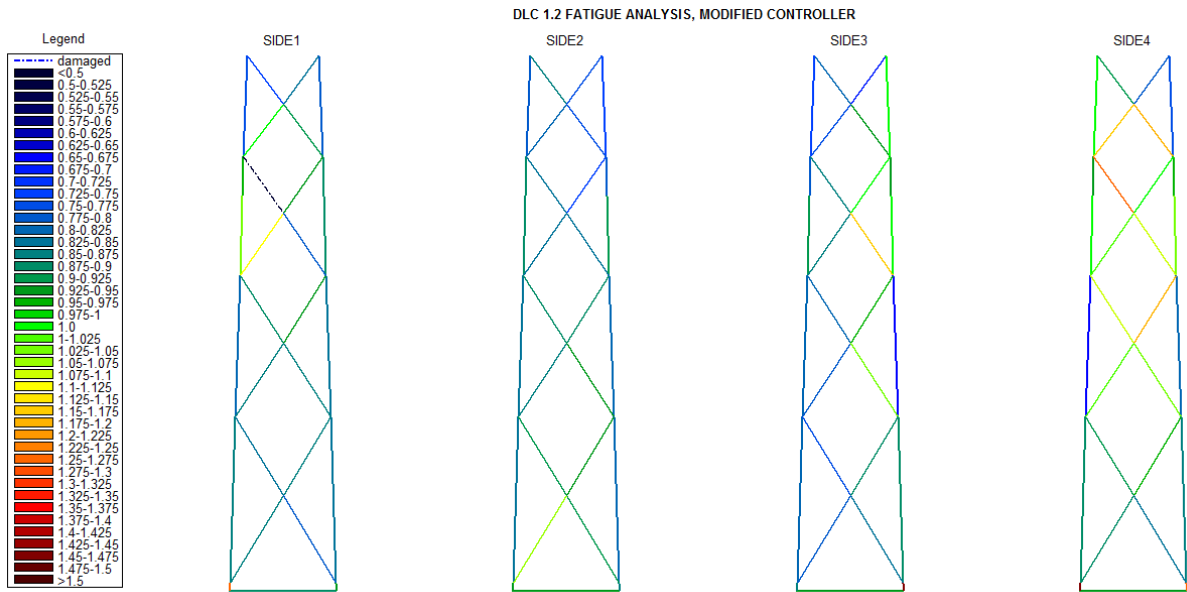
Design situation	DLC	Wind condition	Waves	Wind and wave directionality	Water level	Type of analysis	Type of EFL	Damaged element	Type of damage
Power Production	1.2	NTM 3<Vhub<25 4:2:24 m/s	NSS Hs=E[Hs Vhub]	COD,UNI	MSL	FATIGUE	FORCE	X-Brace 86 Level III-IV	E=0.5E0



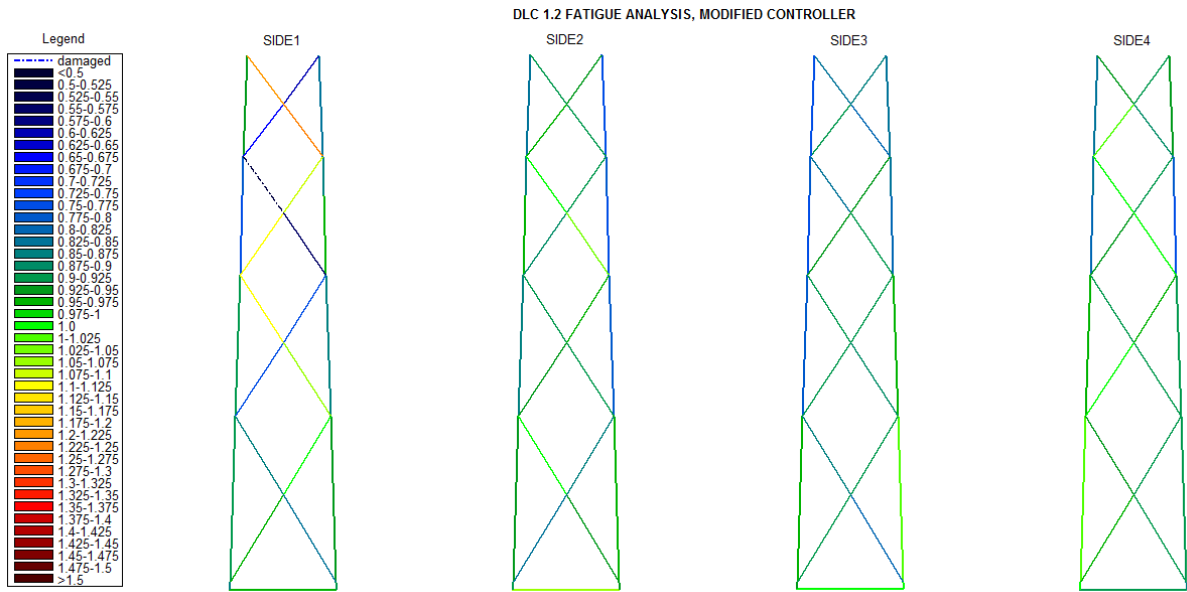
Design situation	DLC	Wind condition	Waves	Wind and wave directionality	Water level	Type of analysis	Type of EFL	Damaged element	Type of damage
Power Production	1.2	NTM 3<Vhub<25 4:2:24 m/s	NSS Hs=E[Hs Vhub]	COD,UNI	MSL	FATIGUE	MOMENT	X-Brace 86 Level III-IV	E=0.5E0



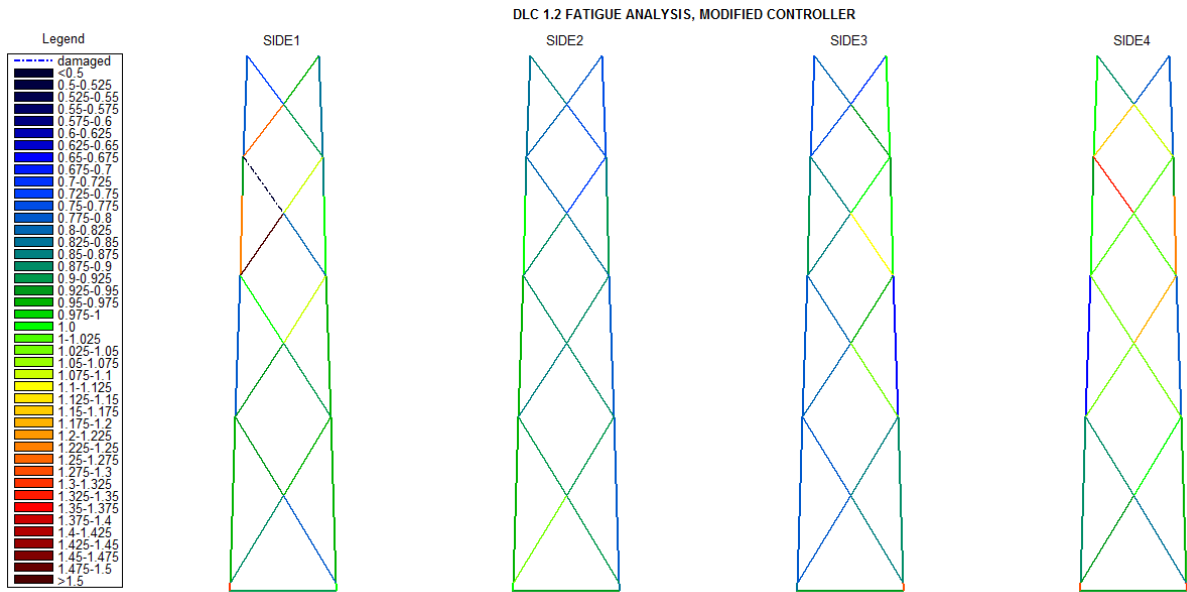
Design situation	DLC	Wind condition	Waves	Wind and wave directionality	Water level	Type of analysis	Type of EFL	Damaged element	Type of damage
Power Production	1.2	NTM 3<Vhub<25 4:2:24 m/s	NSS Hs=E[Hs Vhub]	COD,UNI	MSL	FATIGUE	FORCE	X-Brace 86 Level III-IV	E=0.3E0



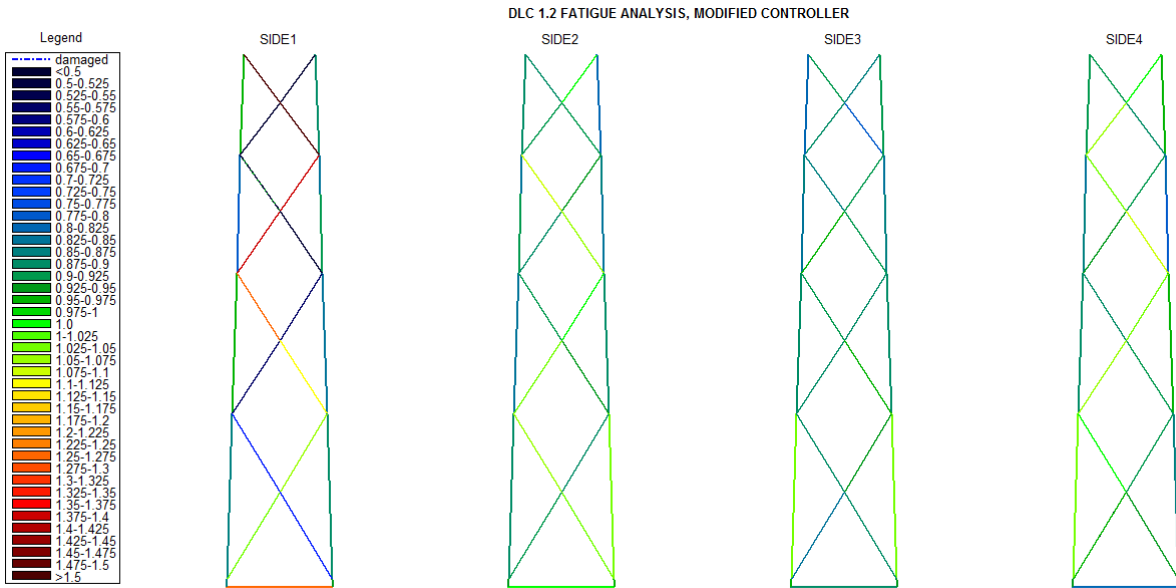
Design situation	DLC	Wind condition	Waves	Wind and wave directionality	Water level	Type of analysis	Type of EFL	Damaged element	Type of damage
Power Production	1.2	NTM 3<Vhub<25 4:2:24 m/s	NSS Hs=E[Hs Vhub]	COD,UNI	MSL	FATIGUE	MOMENT	X-Brace 86 Level III-IV	E=0.3E0



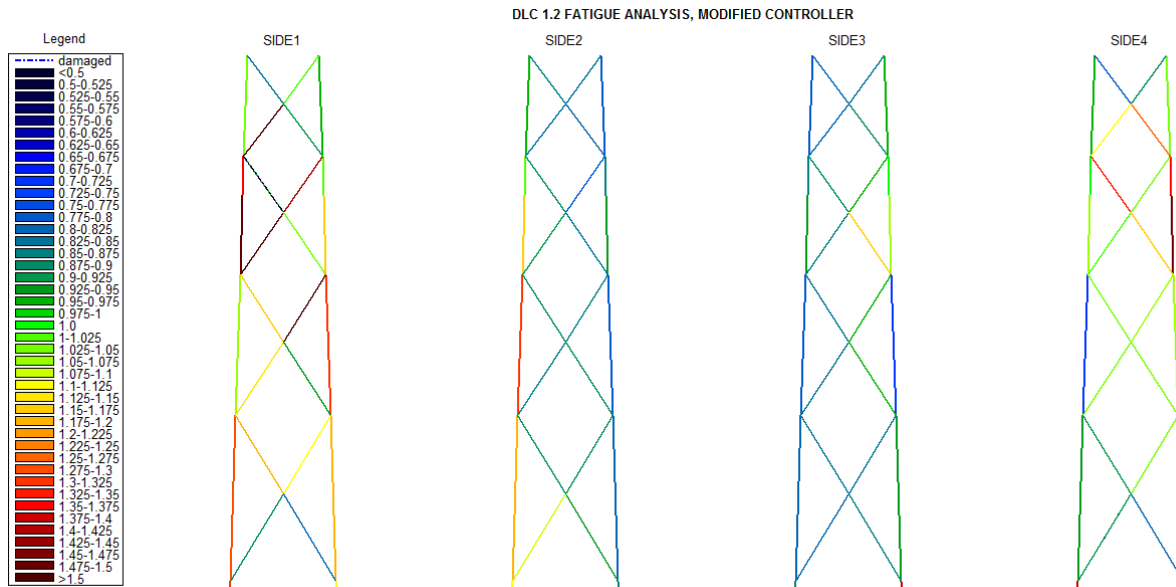
Design situation	DLC	Wind condition	Waves	Wind and wave directionality	Water level	Type of analysis	Type of EFL	Damaged element	Type of damage
Power Production	1.2	NTM 3<Vhub<25 4:2:24 m/s	NSS Hs=E[Hs Vhub]	COD,UNI	MSL	FATIGUE	FORCE	X-Brace 86 Level III-IV	E=0.1E0



Design situation	DLC	Wind condition	Waves	Wind and wave directionality	Water level	Type of analysis	Type of EFL	Damaged element	Type of damage
Power Production	1.2	NTM 3<Vhub<25 4:2:24 m/s	NSS Hs=E[Hs Vhub]	COD,UNI	MSL	FATIGUE	MOMENT	X-Brace 86 Level III-IV	E=0.1E0



Design situation	DLC	Wind condition	Waves	Wind and wave directionality	Water level	Type of analysis	Type of EFL	Damaged element	Type of damage
Power Production	1.2	NTM 3<Vhub<25 4:2:24 m/s	NSS Hs=E[Hs Vhub]	COD,UNI	MSL	FATIGUE	FORCE	X-Brace 86 Level III-IV	FREE-JOINT



Design situation	DLC	Wind condition	Waves	Wind and wave directionality	Water level	Type of analysis	Type of EFL	Damaged element	Type of damage
Power Production	1.2	NTM 3<Vhub<25 4:2:24 m/s	NSS Hs=E[Hs Vhub]	COD,UNI	MSL	FATIGUE	MOMENT	X-Brace 86 Level III-IV	FREE-JOINT

APPENDIX D

A rainflow counting algorithm was extracted from educational website [42] and adapted for the fatigue analysis.

```
clear all;
close all;
clc;
tic
%%%%%%%%%%%%%%%%%%%%%%%%%%%%%%%%%%%%%%%%%%%%%%%%%%%%%%%%%%%%%%%%%%%%%%%%
%OPEN ALSO PROGRESSBAR!

DLC=1.2 ;
%CHANGE path of ascii files and namefile!
path='D:\Users\Konrad\Desktop\Praca magisterska\resultsrotor\curve\';

if DLC==1.2;
Nofascii=121;
namefile='OC4-model_NTM_event_';
elseif DLC==1.3;
Nofascii=121;
namefile='OC4_modelintact_ETM_event_';
elseif DLC==6.1;
Nofascii=11;
end;

for XXX=3:Nofascii;
clear XAW;
clear DXC;
clear fid;
if DLC==1.2;
if XXX>=1 && XXX<=11;
namecase='1_2I';
COL=686;
elseif XXX>=12 && XXX<=22;
namecase='1_2_45_E07';
COL=686;
elseif XXX>=23 && XXX<=33;
namecase='1_2_45_E05';
COL=686;
elseif XXX>=34 && XXX<=44;
namecase='1_2_45_E03';
COL=686;
elseif XXX>=45 && XXX<=55;
namecase='1_2_45_E01';
COL=686;
elseif XXX>=56 && XXX<=66;
namecase='1_2_86_E07';
COL=686;
elseif XXX>=67 && XXX<=77;
namecase='1_2_86_E05';
COL=686;
elseif XXX>=78 && XXX<=88;
namecase='1_2_86_E03';
COL=686;
elseif XXX>=89 && XXX<=99;
namecase='1_2_86_E01';
COL=686;
elseif XXX>=100 && XXX<=110;
namecase='1_2_45_F';
COL=692;
elseif XXX>=111 && XXX<=121;
namecase='1_2_86_F';
COL=692;
end;
elseif DLC==1.3;
if XXX>=1 && XXX<=11;
namecase='1_3I';
COL=686;
elseif XXX>=12 && XXX<=22;
namecase='1_3_45_E07';
COL=686;
```

```

elseif XXX>=23 && XXX<=33;
namecase='1_3_45_E05';
COL=686;
elseif XXX>=34 && XXX<=44;
namecase='1_3_45_E03';
COL=686;
elseif XXX>=45 && XXX<=55;
namecase='1_3_45_E01';
COL=686;
elseif XXX>=56 && XXX<=66;
namecase='1_3_86_E07';
COL=686;
elseif XXX>=67 && XXX<=77;
namecase='1_3_86_E05';
COL=686;
elseif XXX>=78 && XXX<=88;
namecase='1_3_86_E03';
COL=686;
elseif XXX>=89 && XXX<=99;
namecase='1_3_86_E01';
COL=686;
elseif XXX>=100 && XXX<=110;
namecase='1_3_45_F';
COL=692;
elseif XXX>=111 && XXX<=121;
namecase='1_3_86_F';
COL=692;
end;
elseif DLC==6.1;
if XXX==1 ;
namecase='6_1I';
COL=686;
elseif XXX==2;
namecase='6_1_45_E07';
COL=686;
elseif XXX==3;
namecase='6_1_45_E05';
COL=686;
elseif XXX==4;
namecase='6_1_45_E03';
COL=686;
elseif XXX==5;
namecase='6_1_45_E01';
COL=686;
elseif XXX==6;
namecase='6_1_86_E07';
COL=686;
elseif XXX==7;
namecase='6_1_86_E05';
COL=686;
elseif XXX==8;
namecase='6_1_86_E03';
COL=686;
elseif XXX==9;
namecase='6_1_86_E01';
COL=686;
elseif XXX==10;
namecase='6_1_45_F';
COL=692;
elseif XXX==11;
namecase='6_1_86_F';
COL=692;
end;
end;
%Main part of the name of final variable
zmienna='var_';

savevariable= horzcat(strcat(path,zmienna,namecase,'_',num2str(XXX),'.mat'));
for i=XXX;
    sss(i) = horzcat(strcat(namefile,num2str(i),'.asc'));
end;

filename{1} = fullfile(path,sss{1,XXX});

for i=1:COL;
    str{i} = strcat('%s');
end;

```

```

str2=cell2mat(str);
for i=1:COL;
    ftr(i) = strcat('%f');
end;
ftr2=cell2mat(ftr);
fid = fopen(filename{1},'r');
XAW=textscan(fid, str2, 'HeaderLines',6);
fclose(fid);
fid = fopen(filename{1},'r');
DXC=textscan(fid, ftr2, 'HeaderLines',8002);
fclose(fid);
ZZZ=COL-1;
    for nnn=2:ZZZ
%       nnn=5;
        clear B;
clear a;
clear aa;
clear cc;
clear THM;
clear THM1;
clear THM_hold;
clear t;
clear C;
clear y;
clear L;
clear max;
clear size;
clear m;
clear k;
clear iscale;
clear length;
clear slopel;
clear slope2;
clear BIG;
clear dat;
clear data_s;

clear THM1;
clear IndexD;
clear IndexE;
clear IndexF;
clear IndexG;

Name=[XAW{nnn}{1,1}];
IndexD = strfind(Name, 'mom');
Name2=[XAW{nnn+1}{1,1}];
IndexE = strfind(Name2, 'mom');
inD=isempty(IndexD);
inE=isempty(IndexE);
IndexF = strfind(Name, 'Triad');
inF=isempty(IndexF);
IndexG = strfind(Name, 'Revolute');
inG=isempty(IndexG);
IndexH = strfind(Name, 'Curve');
inH=isempty(IndexH);
Final2(1,nnn)={Name};
    THM=[DXC{1} DXC{nnn}];
    THM1=[DXC{1} DXC{nnn+1}];
if inF==1;
    THM=THM ;
else
    continue
end;
if inG==1;
    THM=THM ;
else
    continue
end;
if inH==1;
    THM=THM ;
else
    continue
end;
if inD==0 && inE==0 ;
    THM(:,2)=sqrt(THM(:,2).^2+THM1(:,2).^2) ;

```

```

        max2=max(THM(:,2));
        min2=min(THM(:,2));
        max3=max(THM1(:,2));
        min3=min(THM1(:,2));
    elseif inD==0 && inE==1 ;
        continue
    end;

    close all;
    fig_num=1;

y=double(THM(:,2));
%
THM1=[THM(:,1),THM(:,2)];
max1=max(THM(:,2));
min1=min(THM(:,2));

fig_num=fig_num+1;

% if(ic==1)
%     plot(y);
% else
    plot(THM(:,1),THM(:,2));
% end
grid on;
THM_hold=THM;
clear THM;
%
m=length(y)-1;
a=zeros(m,1);
t=zeros(m,1);
a(1)=y(1);
t(1)=1;
k=2;
%
out1=sprintf(' total input points =%d ',m);
%s disp(out1)
%
%s disp(' Begin slope calculation ')
%
slope1=( y(2)-y(1));
for i=2:m
    slope2=(y(i+1)-y(i));
    if((slope1*slope2)<=0)
        a(k)=y(i);
        t(k)=i;
        k=k+1;
    end
    slope1=slope2;
end
%
a(k)=y(m+1);
t(k)=t(k-1)+1;
k=k+1;
%
%s disp(' End slope calculation ')
%
clear temp;
temp(1:k-1)=a(1:k-1);
clear a;
a=temp;
%
clear temp;
temp(1:k-1)=t(1:k-1);
clear t;
t=temp;
%
clear aa;
sza=size(a);
if(sza(2)>sza(1))
    a=a';
end
szt=size(t);
if(szt(2)>szt(1))
    t=t';

```

```

end
%
aa=[t a];
%
cc=a;
%
% num=round(max(a)-min(a))+1;
%
n=1;
i=1;
j=2;
%
%%%%%%%%%%%%%%%%%%%%%%%%%%%%%%%%%%%%%%%%%%%%%%%%%%%%%%%%%%%%%%%%%%%%%%%%
%
% Rules for this method are as follows: let X denote
% range under consideration; Y, previous range adjacent to X; and
% S, starting point in the history.
%
%%%%%%%%%%%%%%%%%%%%%%%%%%%%%%%%%%%%%%%%%%%%%%%%%%%%%%%%%%%%%%%%%%%%%%%%
%
%s progressbar % Create figure and set starting time
%
close figure 1
clear B;
aamax=0;
B=zeros(m,4);
a_mean=zeros(m,2);
kv=1;
msa_orig=max(size(aa));
while(1)
    msa=max(size(aa));
    %s progressbar(1-msa/msa_orig) % Update figure
%
    if((j+1)>msa)
        break;
    end
    if((i+1)>=msa)
        break;
    end
%
    Y=(abs(aa(i,2)-aa(i+1,2)));
    X=(abs(aa(j,2)-aa(j+1,2)));
%
    if(X>=Y && Y>0)
        if(i==1)
            B(kv,2)=0.5;
            am=[aa(i,2) aa(i+1,2)];
            B(kv,3)=am(1);
            B(kv,4)=am(2);
            aa(1,:)=[];
        else
            B(kv,2)=1;
            am=[aa(i,2) aa(i+1,2)];
            B(kv,3)=am(1);
            B(kv,4)=am(2);
            aa(i+1,:)=[];
            aa(i,:)=[];
        end
        B(kv,1)=Y;
%%
%%     out1=sprintf(' %8.4g %8.4g %8.4g %8.4g ',B(kv,1),B(kv,2),B(kv,3),B(kv,4));
%%     disp(out1);
%%
        if(Y>aamax)
            p1=aa(i,2);
            p2=aa(i+1,2);
            tp1=aa(i,1);
            tp2=aa(i+1,1);
            aamax=Y;
        end
        kv=kv+1;
        i=1;
        j=2;
    else
        i=i+1;
        j=j+1;
    end
end

```

```

%
end
%s progressbar(1);
%
%%%%%%%%%%%%%%%%%%%%%%%%%%%%%%%%%%%%%%%%%%%%%%%%%%%%%%%%%%%%%%%%%%%%%%%%
%
% Count each range that has not been previously counted
% as one-half cycle.
%
N=max(size(aa));
%s disp(' ');
for i=1:N-1
    Y=(abs(aa(i,2)-aa(i+1,2)));
%
    if(Y>0)
        B(kv,1)=Y;
        B(kv,2)=0.5;
        am=[aa(i,2) aa(i+1,2)];
        B(kv,3)=am(1);
        B(kv,4)=am(2);
%%
        out1=sprintf('* %8.4g %8.4g %8.4g %8.4g ',B(kv,1),B(kv,2),B(kv,3),B(kv,4));
        disp(out1);
%%
        if(Y>aamax)
            p1=aa(i,2);
            p2=aa(i+1,2);
            tp1=aa(i,1);
            tp2=aa(i+1,1);
            aamax=Y;
        end
        kv=kv+1;
    end
end
end
%
amax=max(y)-min(y);

% disp(' Begin bin sorting ');
%
amax=max(B(:,1));
L(1)=5;
L(2)=7;
L(3)=10;
L(4)=15;
L(5)=20;
L(6)=25;
L(7)=30;
L(8)=35;
L(9)=40;
L(10)=45;
L(11)=50;
L(12)=55;
L(13)=60;
L(14)=65;
L(15)=70;
L(16)=75;
L(17)=80;
L(18)=85;
L(19)=95;
L(20)=100;
L(21)=101;
L(22)=105;
L(23)=110;
L(24)=115;
L(25)=120;
L(26)=125;
L(27)=130;
L(28)=135;
L(29)=140;
L(30)=145;
L(31)=150;
L(32)=155;
L(33)=160;
L(34)=165;
L(35)=170;
L(36)=175;
L(37)=180;

```

```

L(38)=185;
L(39)=195;
L(40)=200;
L(41)=201;
L(42)=205;
L(43)=210;
L(44)=215;
L(45)=220;
L(46)=225;
L(47)=230;
L(48)=235;
L(49)=240;
L(50)=245;
L(51)=250;
L(52)=255;
L(53)=260;
L(54)=265;
L(55)=270;
L(56)=275;
L(57)=280;
L(58)=285;
L(59)=295;
L(60)=300;
L(61)=301;
L(62)=305;
L(63)=310;
L(64)=315;
L(65)=320;
L(66)=325;
L(67)=330;
L(68)=335;
L(69)=340;
L(70)=345;
L(71)=350;
L(72)=355;
L(73)=360;
L(74)=365;
L(75)=370;
L(76)=375;
L(77)=380;
L(78)=385;
L(79)=395;
L(80)=400;
L(81)=401;
L(82)=405;
L(83)=410;
L(84)=415;
L(85)=420;
L(86)=425;
L(87)=430;
L(88)=435;
L(89)=440;
L(90)=445;
L(91)=450;
L(92)=455;
L(93)=460;
L(94)=465;
L(95)=470;
L(96)=475;
L(97)=480;
L(98)=485;
L(99)=495;
L(100)=500;
L=L*amax/500;
%
clear AverageMean;
clear MaxMean;
clear MinMean;
%
clear MaxAmp;
clear AverageAmp;
%
clear MinValley;
clear MaxPeak;
%
num=max(size(L))-1;
C=zeros(num,1);

```

```

%
AverageMean=zeros(num,1);
MaxMean=-1.0e+09*ones(num,1);
MinMean= 1.0e+09*ones(num,1);
%
MaxPeak=-1.0e+09*ones(num,1);
MinValley= 1.0e+09*ones(num,1);
%
MaxAmp=zeros(num,1);
AverageAmp=zeros(num,1);
%
kvn=kv-1;
%
clear range_cycles;
clear amp_cycles;
%
range_cycles=[B(1:kvn,1) B(1:kvn,2)];
amp_cycles=[0.5*B(1:kvn,1) B(1:kvn,2)];
%
for i=1:kvn
    for ijk=1:num
        Y=B(i,1);
        if(Y>=L(ijk) && Y<=L(ijk+1))
            C(ijk)=C(ijk)+B(i,2);
            bm=(B(i,3)+B(i,4))/2;
            if(B(i,3)>MaxPeak(ijk))
                MaxPeak(ijk)=B(i,3);
            end
            if(B(i,4)>MaxPeak(ijk))
                MaxPeak(ijk)=B(i,4);
            end
            if(B(i,3)<MinValley(ijk))
                MinValley(ijk)=B(i,3);
            end
            if(B(i,4)<MinValley(ijk))
                MinValley(ijk)=B(i,4);
            end
        end
        %
        AverageAmp(ijk)=AverageAmp(ijk)+B(i,1)*B(i,2);
        AverageMean(ijk)=AverageMean(ijk)+bm*B(i,2);
        %
        if( bm > MaxMean(ijk))
            MaxMean(ijk)=bm;
        end
        if( bm < MinMean(ijk))
            MinMean(ijk)=bm;
        end
        %
        if(B(i,1)>MaxAmp(ijk))
            MaxAmp(ijk)=B(i,1);
        end
        break;
    end
end
end
for ijk=1:num
    if( C(ijk)>0)
        AverageAmp(ijk)=AverageAmp(ijk)/C(ijk);
        AverageMean(ijk)=AverageMean(ijk)/C(ijk);
    end
end
%%%%%%%%%%%%%%%%%%%%%%%%%%%%%%%%%%%%%%%%%%%%%%%%%%%%%%%%%%%%%%%%%%%%%%%%
%
% disp(' ');
% disp(' Round the cycle and amplitude values to nearest integer ? ');
% disp(' 1=yes 2=no');
% rv=input(' ');
%
clear BIG;
N=max(size(C));
BIG=zeros(N,10);
% disp(' ');
% disp(' Range = (peak-valley) ');
% disp(' Amplitude = (peak-valley)/2 ');
% disp(' ');
% disp(' Range Limits Cycle Average Max Min Average Max
Min Max ');

```



```

% % disp('          (units)          Counts          Amp          Amp          Mean          Mean
Mean Valley Peak');
%
MaxAmp=MaxAmp/2;
AverageAmp=AverageAmp/2;
%
for i=1:N
    j=N+1-i;
%
    if(C(j)==0)
        AverageAmp(j)=0.;
        MaxAmp(j)=0.;
        MinMean(j)=0.;
        AverageMean(j)=0.;
        MaxMean(j)=0.;
        MinValley(j)=0.;
        MaxPeak(j)=0.;
%
        out1=sprintf('\t %7.4g to %7.4g \t %g \t %6.3g \t %6.3g \t %6.3g\t %6.3g\t %6.3g\t
%6.3g\t
%6.3g',L(j),L(j+1),C(j),AverageAmp(j),MaxAmp(j),MinMean(j),AverageMean(j),MaxMean(j),MinValley
(j),MaxPeak(j));

        end
        %s disp(out1);
        BIG(i,1)=L(j);
        BIG(i,2)=L(j+1);
        BIG(i,3)=C(j);
        BIG(i,4)=AverageAmp(j);
        BIG(i,5)=MaxAmp(j);
        BIG(i,6)=MinMean(j);
        BIG(i,7)=AverageMean(j);
        BIG(i,8)=MaxMean(j);
        BIG(i,9)=MinValley(j);
        BIG(i,10)=MaxPeak(j);
    end
%
out1=sprintf('\n Max filename{6}=%6.3g ',aamax);
%s disp(out1);
%
TC=sum(C);

    out1=sprintf('\n Total Cycles =%g \n',TC);

%s disp(out1);
%
%%%%%%%%%%%%%%%%%%%%%%%%%%%%%%%%%%%%%%%%%%%%%%%%%%%%%%%%%%%%%%%%%%%%%%%%
%
close all hidden;
%

%
%
table1 = uitable;
set(table1,'ColumnWidth',{26})
f = figure('Position',[100 100 900 350]);
dat = BIG(:,1:10);
columnname = {'Lower Range','Upper Range','Cycles','Ave Amp',...
'Max Amp','Min Mean','Ave Mean','Max Mean','Min Valley','Max Peak' };
columnformat = {'numeric','numeric','numeric','numeric','numeric',...
'numeric','numeric','numeric','numeric','numeric'};
columneditable = [false false false false false false false false false];
%
sz=size(BIG);
%
for i = 1:sz(1)
    for j=1:sz(2)
        if(j==3)
            tempStr = sprintf('%10.1f', dat(i,j));
        else
            tempStr = sprintf('%8.4g', dat(i,j));
        end
        data_s{i,j} = tempStr;
    end
end
end

```

```

%
table1 = uitable('Units','normalized','Position',...
    [0.1 0.1 0.9 0.9], 'Data', data_s,...
    'ColumnName', columnname,...
    'ColumnFormat', columnformat,...
    'ColumnEditable', columneditable,...
    'RowName', []);
%

%%%%%%%%%%%%%%%%%%%%%%%%%%%%%%%%%%%%%%%%%%%%%%%%%%%%%%%%%%%%%%%%%%%%%%%%
%
%%%%%%%%%%%%%%%%%%%%%%%%%%%%%%%%%%%%%%%%%%%%%%%%%%%%%%%%%%%%%%%%%%%%%%%%
%
fig_num=3;
figure(fig_num);
fig_num=fig_num+1;

    plot(THM_hold(:,1),THM_hold(:,2));

grid on;
%
    figure(fig_num);
    fig_num=fig_num+1;
    h1=bar(C);
    grid on;
    title('Rainflow');
    ylabel('Cycle Counts');
    xlabel('Range');
%
%
RB=BIG(:,1:3);
aaB=aa;
%
% % disp(' ');
% % disp(' Output arrays: ');
% % disp(' range_cycles (range & cycles)');
% % disp(' amp_cycles (amplitude & cycles)');

close figure 1
for i=1:N
    j=N+1-i;
    C(j);

        smalla(i,1)=C(j);
        smalla(i,2)=AverageAmp(j);

    end
    smalla;
    close all hidden;

    duzy=zeros(99,2);
duzy(1:99,1:2)=smalla;

mmm=length(duzy(:,2));

DD=0;
maxx=length(duzy(:,2));

num=maxx;
BIG=zeros(num,3);
C=duzy(:,1);
cycles=zeros(num,1);
LARGE=zeros(num,2);
AverageAmp=zeros(num,1);
YY=zeros(num,1);
%CYCLES
for i=1:mmm
    for ijk=1:num
        YY=duzy(i,2);

            if(YY>=L(ijk) && YY<=L(ijk+1));
                cycles(ijk)=cycles(ijk)+C(i);
                AverageAmp(ijk)=AverageAmp(ijk)+duzy(i,2);
            end
        end
    end
end
end

```

```

b=5;
YYY=zeros(num,1);
SN=zeros(num,1);
for ijk=1:num
    if cycles(ijk)>0;
        AverageAmp(ijk)=AverageAmp(ijk)/cycles(ijk);
        if AverageAmp(ijk)>0;
            SN(ijk)=10.^(14.576-b*log10(AverageAmp(ijk).*10^-6));
            YYY(ijk)=cycles(ijk)/SN(ijk);
        end
        else
            YYY(ijk)=0;
        end
    end
end

%DAMAGE EQUIVALENT LOAD
DD=0;
sscycles=0;
for i=2:num
    j=num+1-i;

    DD(1)= YYY(1);
    DD(i)=[YYY(i)]+DD(i-1);
    sscycles(1)=cycles(num);
    sscycles(num+1-j)=[cycles(j)]+sscycles(num-j);
end

% EQUIVALENT FATIGUE LOAD
niSib=0;
for i=2:num
    j=num+1-i;
    NN=sscycles(num);

    AverageAmp(j);
    cycles(j);
    niSib(1)=cycles(num)*((AverageAmp(num)*10.^-6)^b);
    niSib(num+1-j)=cycles(j)*((AverageAmp(j)*10.^-6)^b)+niSib(num-j);

end
EFL=(niSib(num)/NN).^(1/b);
% EFL1= sprintf('%f', EFL);
ROK=20*365*24;
D= DD(num)*ROK;
D2=1/(10^14.576).*niSib(num)*ROK;
D3=NN.*(EFL.^b)/(10^14.576)*ROK;
% DD3=sprintf('%f', D3);

maxXX=max1*10.^-6;
minXX=min1*10.^-6;
Final2(1,1)={'Name'};
Final2(2,1)={'EFL'};
Final2(3,1)={'DEL'};
Final2(4,1)={'MaxLoadF'};
Final2(5,1)={'MinLoadF'};
Final2(6,1)={'MaxLoadMy*'};
Final2(7,1)={'MinLoadMy*'};
Final2(8,1)={'MaxLoadMz*'};
Final2(9,1)={'MinLoadMz*'};
Final2(2,nnn)={EFL};
Final2(3,nnn)={D3};

if inD==0 && inE==0 ;
maxXX2=max2*10.^-6;
minXX2=min2*10.^-6;
maxXX3=max3*10.^-6;
minXX3=min3*10.^-6;
Final2(6,nnn)={maxXX2};
Final2(7,nnn)={minXX2};
Final2(8,nnn)={maxXX3};
Final2(9,nnn)={minXX3};
else
Final2(4,nnn)={maxXX};
Final2(5,nnn)={minXX};
end;

```

```
if nnn==ZZZ;
    %save(['savevariable_' num2str(nnn)], 'Final2');
    save(['savevariable_' num2str(nnn)], 'Final2');
else
    continue;
end;
end;
end;
save([namecase num2str(XXX)], 'Final2');
end;

toc
```

APPENDIX E

Matlab code *tpabaqus4side.m* adapted for presenting the results.

```
% clear all

clc
tic

%load=0 FORCE load=1 MOMENT
DLC=1.2;
Load1=0;
%%%%% side 1,2,3,4 or 5(all)
side=5;
%Find name of mode
presentation=1;
DEL=0;
path='D:\Users\Konrad\Desktop\sebastian\';
pathtables='D:\Users\Konrad\Desktop\Praca magisterska\resultsmode\tabele\';
pathplot='D:\Users\Konrad\Desktop\Praca magisterska\FatigueDLC1_2\';
namecases={'1_2_45_E07' '1_2_45_E05' '1_2_45_E03' '1_2_45_E01' '1_2_86_E07' '1_2_86_E05'
'1_2_86_E03' '1_2_86_E01' '1_2_45_F' '1_2_86_F'};
cs=10;
ile=87:116;
for Event=1:11;

clear Final2;
clear Final2int;
E=1;
ext=horzcat(strcat('var_',namecases{1,cs},'_',num2str(cs*11+Event)));
zmienna=what(path);
cellsize = cellfun(@size,zmienna.mat,'uni',false);
Value= length(cellsize);
for i=1:Value;
nzw(i,1)=zmienna.mat{i,1};
end;
if DLC==1.2;
intr='var_1_2I_';
intact=horzcat(strcat(intr,num2str(Event),'.mat'));
filenamein = fullfile(path,intact);
end
load(filenamein);
Final2int=Final2;
clear Final2;

mode=horzcat(strcat(ext, '.mat'));

filenamestiff = fullfile(path,mode);
load(filenamestiff);
if cs==1 || cs==2 || cs==3 || cs==4 || cs==9 ;
dbrace=45;
elseif cs==5 || cs==6 || cs==7 || cs==8 || cs==10 ;
dbrace=86;
end;

Final2size1 = cellfun(@size,Final2,'uni',false);
lFinal2= length(Final2size1);
Final2intsize1 = cellfun(@size,Final2int,'uni',false);
lFinal2int= length(Final2intsize1);
%SIZE FINAL2
for i=1:lFinal2;
IndexF = strfind(Final2{1,i}, 'Triad');
inF=isempty(IndexF);
IndexG = strfind(Final2{1,i}, 'Revolute');
inG=isempty(IndexG);
IndexH = strfind(Final2{1,i}, 'Curve');
inH=isempty(IndexH);
IndexQ = Final2{3,i};
inQ=isempty(IndexQ);
if inQ==1
Final2{1,i}=[] ;
end
if inF==0
```

```

Final2{1,i}=[] ;

elseif inG==0;
    Final2{1,i}=[] ;

elseif inH==0;
    Final2{1,i}=[] ;

else;
    continue ;
end;
end;

%SIZE FINAL2INT
for i=1:lFinal2int;
    IndexF = strfind(Final2int{1,i}, 'Triad');
inF=isempty(IndexF);
IndexG = strfind(Final2int{1,i}, 'Revo');
inG=isempty(IndexG);
IndexH = strfind(Final2int{1,i}, 'Curve');
inH=isempty(IndexH);
IndexQ = Final2int{3,i};
inQ=isempty(IndexQ);
if inQ==1
    Final2int{1,i}=[] ;
end

if inF==0
    Final2int{1,i}=[] ;

elseif inG==0;
    Final2int{1,i}=[] ;

elseif inH==0;
    Final2int{1,i}=[] ;

else
    continue ;
end;
end;
clear lFinal2;

Final2size1 = cellfun(@size,Final2,'uni',false);
lFinal2= length(Final2size1);
Final2( : , all(cellfun(@isempty,Final2),1)) = [];
cellsz = cellfun(@size,Final2,'uni',false);

nodsds= length(cellsz);

nods= length(cellsz);
Final2int( : , all(cellfun(@isempty,Final2int),1)) = [];

cellszint = cellfun(@size,Final2int,'uni',false);
nodsint= length(cellszint);
nods1{1,1}={27 30 31 1.9393 58.778 1.554 47.505 };
nods1{2,1}={2600 30 2900 1.554 47.505 1.4108 43.127};
nods1{3,1}={3000 34 3300 10.324 47.505 10.4673 43.127};
nods1{4,1}={26 29 2900 1.4108 43.127 1.119 34.205};
nods1{5,1}={25 15 29 1.119 34.205 0.606 18.513 };
nods1{6,1}={12 14 15 0 0 0.606 18.531 };
nods1{7,1}={31 34 35 9.9387 58.778 10.324 47.505 };
nods1{8,1}={30 33 3300 10.4673 43.127 10.759 34.205};
nods1{9,1}={29 20 33 10.759 34.205 11.272 18.513 };
nods1{10,1}={16 20 19 11.272 18.513 11.878 0 };
nods1{11,1}={104 35 56 9.955 58.778 5.939 53.3891};
nods1{12,1}={103 30 56 1.554 47.505 5.939 53.3891 };
nods1{13,1}={102 31 56 1.923 58.778 5.939 53.3891 };
nods1{14,1}={101 34 56 5.939 53.3891 10.324 47.505 };
nods1{15,1}={86 30 52 1.554 47.505 5.939 41.1693};
nods1{16,1}={88 34 52 10.324 47.505 5.939 41.1693};
nods1{17,1}={87 29 52 5.939 41.1693 1.119 34.205 };
nods1{18,1}={85 33 52 5.939 41.1693 10.759 34.205};
nods1{19,1}={70 29 48 1.119 34.205 5.939 26.7554 };

```

```

nods1{20,1}={72 33 48 5.939 26.7554 10.759 34.205 };
nods1{21,1}={71 15 48 5.939 26.7554 0.606 18.513};
nods1{22,1}={69 20 48 5.939 26.7554 11.272 18.513};
nods1{23,1}={54 15 44 5.939 9.7541 0.606 18.513};
nods1{24,1}={56 20 44 11.272 18.513 5.939 9.7541};
nods1{25,1}={55 14 44 0 0 5.939 9.7541};
nods1{26,1}={53 19 44 5.939 9.7541 11.878 0};
nods1{27,1}={39 13 18 11.906 -0.834 -0.028 -0.834 };
nods1{28,1}={11 13 14 0 0 -0.028 -0.834 };
nods1{29,1}={15 18 19 11.878 0 11.906 -0.834 };
nods2{1,1}={31 34 35 1.9393 58.778 1.554 47.505 };
nods2{2,1}={3000 34 3300 1.554 47.505 1.4108 43.127};
nods2{3,1}={30 33 3300 1.4108 43.127 1.119 34.205};
nods2{4,1}={29 20 33 1.119 34.205 0.606 18.513};
nods2{5,1}={16 19 20 0 0 0.606 18.531 };
nods2{6,1}={4 4 5 11.272 18.513 11.878 0 };
nods2{7,1}={17 5 21 10.759 34.205 11.272 18.513 };
nods2{8,1}={18 21 2100 10.4673 43.127 10.759 34.205};
nods2{9,1}={1800 22 2100 10.324 47.505 10.4673 43.127};
nods2{10,1}={19 22 23 9.9387 58.778 10.324 47.505 };
nods2{11,1}={90 35 53 1.923 58.778 5.939 53.3891 };
nods2{12,1}={92 23 53 9.955 58.778 5.939 53.3891};
nods2{13,1}={89 22 53 5.939 53.3891 10.324 47.505};
nods2{14,1}={91 34 53 1.554 47.505 5.939 53.3891 };
nods2{15,1}={74 34 49 1.554 47.505 5.939 41.1693};
nods2{16,1}={76 22 49 10.324 47.505 5.939 41.1693};
nods2{17,1}={75 33 49 5.939 41.1693 1.119 34.205 };
nods2{18,1}={73 21 49 5.939 41.1693 10.759 34.205};
nods2{19,1}={58 33 45 1.119 34.205 5.939 26.7554 };
nods2{20,1}={60 21 45 5.939 26.7554 10.759 34.205 };
nods2{21,1}={57 5 45 5.939 26.7554 11.272 18.513};
nods2{22,1}={59 20 45 5.939 26.7554 0.606 18.513};
nods2{23,1}={42 41 20 5.939 9.7541 0.606 18.513};
nods2{24,1}={44 41 5 11.272 18.513 5.939 9.7541};
nods2{25,1}={41 4 41 5.939 9.7541 11.878 0};
nods2{26,1}={43 19 41 0 0 5.939 9.7541};
nods2{27,1}={40 18 3 11.906 -0.834 -0.028 -0.834};
nods2{28,1}={15 18 19 0 0 -0.028 -0.834 };
nods2{29,1}={3 3 4 11.878 0 11.906 -0.834 };
snods3{1,1}={100 23 55 1.923 58.778 5.939 53.3891 };
snods3{2,1}={98 27 55 9.955 58.778 5.939 53.3891};
snods3{3,1}={99 26 55 5.939 53.3891 10.324 47.505};
snods3{4,1}={97 22 55 1.554 47.505 5.939 53.3891};
snods3{5,1}={4 4 5 0 0 0.606 18.531};
snods3{6,1}={17 5 21 1.119 34.205 0.606 18.513};
snods3{7,1}={18 21 2100 1.4108 43.127 1.119 34.205 };
snods3{8,1}={1800 22 2100 1.554 47.505 1.4108 43.127};
snods3{9,1}={19 22 23 1.9393 58.778 1.554 47.505 };
snods3{10,1}={8 9 10 11.272 18.513 11.878 0 };
snods3{11,1}={21 10 25 10.759 34.205 11.272 18.513 };
snods3{12,1}={22 25 2500 10.4673 43.127 10.759 34.205};
snods3{13,1}={2200 26 2500 10.324 47.505 10.4673 43.127};
snods3{14,1}={23 26 27 9.9387 58.778 10.324 47.505 };
snods3{15,1}={84 22 51 1.554 47.505 5.939 41.1693};
snods3{16,1}={82 26 51 10.324 47.505 5.939 41.1693};
snods3{17,1}={81 21 51 5.939 41.1693 1.119 34.205 };
snods3{18,1}={83 25 51 5.939 41.1693 10.759 34.205};
snods3{19,1}={65 5 47 5.939 26.7554 0.606 18.513};
snods3{20,1}={68 21 47 1.119 34.205 5.939 26.7554 };
snods3{21,1}={66 25 47 5.939 26.7554 10.759 34.205 };
snods3{22,1}={67 10 47 5.939 26.7554 11.272 18.513};
snods3{23,1}={52 5 43 5.939 9.7541 0.606 18.513};
snods3{24,1}={50 10 43 11.272 18.513 5.939 9.7541};
snods3{25,1}={51 9 43 5.939 9.7541 11.878 0};
snods3{26,1}={49 4 43 0 0 5.939 9.7541};
snods3{27,1}={37 3 8 11.906 -0.834 -0.028 -0.834};
snods3{28,1}={3 3 4 0 0 -0.028 -0.834 };
snods3{29,1}={7 8 9 11.878 0 11.906 -0.834 };
nods4{1,1}={8 9 10 0 0 0.606 18.531};
nods4{2,1}={21 10 25 1.119 34.205 0.606 18.513};
nods4{3,1}={22 25 2500 1.4108 43.127 1.119 34.205};
nods4{4,1}={2200 26 2500 1.554 47.505 1.4108 43.127};
nods4{5,1}={23 26 27 1.9393 58.778 1.554 47.505 };
nods4{6,1}={27 30 31 9.9387 58.778 10.324 47.505 };
nods4{7,1}={2600 30 2900 10.324 47.505 10.4673 43.127};
nods4{8,1}={12 14 15 11.272 18.513 11.878 0 };
nods4{9,1}={26 29 2900 10.4673 43.127 10.759 34.205};

```

```

nods4{10,1}={25 15 29 10.759 34.205 11.272 18.513 };
nods4{11,1}={96 27 54 1.923 58.778 5.939 53.3891 };
nods4{12,1}={94 31 54 9.955 58.778 5.939 53.3891 };
nods4{13,1}={95 30 54 5.939 53.3891 10.324 47.505};
nods4{14,1}={93 26 54 1.554 47.505 5.939 53.3891 };
nods4{15,1}={80 26 50 1.554 47.505 5.939 41.1693 };
nods4{16,1}={78 30 50 10.324 47.505 5.939 41.1693};
nods4{17,1}={77 23 50 5.939 41.1693 1.119 34.205 };
nods4{18,1}={79 29 50 5.939 41.1693 10.759 34.205};
nods4{19,1}={64 25 46 1.119 34.205 5.939 26.7554 };
nods4{20,1}={62 29 46 5.939 26.7554 10.759 34.205 };
nods4{21,1}={63 15 46 5.939 26.7554 11.272 18.513};
nods4{22,1}={61 10 46 5.939 26.7554 0.606 18.513};
nods4{23,1}={48 10 42 5.939 9.7541 0.606 18.513};
nods4{24,1}={46 15 42 11.272 18.513 5.939 9.7541};
nods4{25,1}={47 14 42 5.939 9.7541 11.878 0 };
nods4{26,1}={45 9 42 0 0 5.939 9.7541};
nods4{27,1}={38 8 13 11.906 -0.834 -0.028 -0.834};
nods4{28,1}={7 8 9 0 0 -0.028 -0.834 };
nods4{29,1}={11 13 19 11.878 0 11.906 -0.834 };
cord=[nods1 ;nods2 ;snods3 ;nods4];
sls=length(cord);
%%%Lumped load cases table%%%
envcon{1,1}='V [m/s]';
envcon{1,2}='Hs [m]';
envcon{1,3}='Tp [m]';
envcon{1,4}='Peakness,Fatigue [-]';
envcon{1,5}='Peakness,Extreme [-]';
envcon{1,6}='f [%]';
envcon{1,7}='occ./year [hrs]';

en(4,2:8)=[1.1 5.88 1 3.3 0.08911 780 0.09621];
en(6,2:8)=[1.18 5.76 1 3.3 0.14048 1230.6 0.15115];
en(8,2:8)=[1.31 5.67 1 3.3 0.13923 1219.7 0.15032] ;
en(10,2:8)=[1.48 5.74 1 3.3 0.14440 1264.9 0.15590];
en(12,2:8)=[1.7 5.88 1 3.3 0.12806 1121.8 0.13826];
en(14,2:8)=[1.91 6.07 1 3.3 0.10061 881.3 0.10862];
en(16,2:8)=[2.19 6.37 1 3.3 0.07554 661.7 0.08155];
en(18,2:8)=[2.47 6.71 1 3.3 0.04878 427.3 0.05266];
en(20,2:8)=[2.76 6.99 1 3.3 0.03151 276.1 0.03402];
en(22,2:8)=[3.09 7.4 1 3.3 0.01924 168.6 0.02077];
en(24,2:8)=[3.42 7.8 1 3.3 0.00977 85.6 0.01055];

for i=2:12;
    for j=2:8;
        envcon2{i-1,1}=2*i;
        envcon2{i-1,j}=en(2*i,j);
    end;
end;
end;
% sumaprobability=sum(envcon2(2:7,8));
for i=6:nodsint;
    IndexZ1 = strfind(Final2{1,i}, 'for');
    inZ1=isempty(IndexZ1);
    %inZ1=0 FORCE inZ1=1 MOMENT
    if inZ1==Load1;
        NAME{1,i}=strsplit(Final2{1,i},'_');
        TableEFL{i,1}=horzcat(strcat(NAME{1,i}{1,2}));

        %table col 3 intact EFL
        TableEFL{i,3}=Final2int{2,i};
        TableEFL{i,4}=Final2{2,i};
        TableEFLi{i,2}=Final2int{2,i};
        TableEFLi{i,1}=Final2{2,i};
    %
        NN=Final2int{3,i}*
        %Ratio, Table EFL/EFL0
        TableEFLd(i,Event)=envcon2{Event,8}*TableEFLi{i,1}./TableEFLi{i,2};
    %
        TableEFLi(i,Event)=Final2int{3,i};
        TableEFL{i,5}=TableEFL{i,4}./TableEFL{i,3};
        TableEFL{i,6}=envcon2{Event,8}*TableEFL{i,4}./TableEFL{i,3};
        TableEFL{i,6+Event}=TableEFL{i,6};
        TableEFLload{i,Event}=TableEFL{i,4};
    %
        TableEFL{i,3}=sprintf('%0.5f',Final2int{2,i});
    %
        TableEFL{i,4}=sprintf('%0.5f',Final2{2,i});
        TableEFL{i,2}=1;
    end;
end;

```



```

        end;

    end;

end;

end;
TableEFLd( ~any(TableEFLd,2), : ) = [];
% TableEFLi( ~any(TableEFLi,2), : ) = [];
gfg=length(TableEFLd);

DELd=sum(TableEFLd,2);
% DELi=sum(TableEFLi,2);
% DELratio=DELd./DELi;

TableEFLload(all(cellfun(@isempty,TableEFLload),2),: ) = [];
TableEFL(all(cellfun(@isempty,TableEFL),2),: ) = [];

cSorted = sortrows(TableEFL,1);
cellsz3 = cellfun(@size,TableEFL,'uni',false);
nods3= length(cellsz3);
for i=1:nods3;

    if i>1;
        name1=str2num(TableEFL{i,1});
        name2=str2num(TableEFL{i-1,1});
        if name1==name2;
            TableEFL{i,2}=2 ;
        else
            TableEFL{i,2}=1 ;
        end;
    end;
end;
dlq=length(nods1);

for k=1:nods3;
    Change1(k,1)=sum(cellfun(@double,TableEFL(k,7:17)));
    Change1(k,3)=max(cellfun(@double,TableEFLload(k,1:11)));
    Change1(k,4)=min(cellfun(@double,TableEFLload(k,1:11)));
    Change1(k,2)=str2num(TableEFL{k,1});
end;

for hj=1:sls;
    for gh=1:nods3;

        np1=str2num(TableEFL{gh,1});
        np2=cord{hj,1}{1,1};
        nbv(hj)=cord{hj,1}{1,1};
        if np1==np2;
            if gh==nods3;
                gf=gh;
            else;
                gf=gh+1;
            end;
        if gh==1;
            gd=gh;
        else;
            gd=gh-1;
        end;
        TableEFL1{2*hj-1,1}=TableEFL{gh,1};
        TableEFL1{2*hj,1}=TableEFL{gh,1};
        TableEFL1{2*hj-1,2}=cord{hj,1}{1,2};
        TableEFL1{2*hj,2}=cord{hj,1}{1,3};
        % TableEFL{2*hj-1,2}=cord{hj,1}{1,2};
        % TableEFL{2*hj,2}=cord{hj,1}{1,3};
        TableEFL1{2*hj-1,3}=1;
        TableEFL1{2*hj,3}=2;

        np3=str2num(TableEFL{gf,1});

        np4=str2num(TableEFL{gd,1});
        nb(hj,1)=np1;
        nb(hj,2)=np3;
        nb(hj,3)=np4;
        endl(hj,1)=TableEFL1{2*hj-1,3};
    end;
end;

```

```

end1(hj,2)=TableEFL1{2*hj,3};
end2(hj,1)=TableEFL{gh,2};
end2(hj,2)=TableEFL{gf,2};
end2(hj,3)=TableEFL{gd,2};

if np1==np3 && end1(hj,1)==end2(hj,1);
TableEFL1{2*hj-1,4}=Change1(gh,1);
TableEFL1{2*hj-1,5}=Change1(gh,3);
TableEFL1{2*hj-1,6}=Change1(gh,4);
end;

if np1==np4 && end1(hj,2)==end2(hj,3);
TableEFL1{2*hj,4}=Change1(gd,1);
TableEFL1{2*hj,5}=Change1(gd,3);
TableEFL1{2*hj,6}=Change1(gd,4);
elseif np1==np3 && end1(hj,2)==end2(hj,2);
TableEFL1{2*hj,4}=Change1(gf,1);
TableEFL1{2*hj,5}=Change1(gf,3);
TableEFL1{2*hj,6}=Change1(gf,4);
end;
% Change(hj,1)=np1;

else;
continue;
end;
end;
end;
for b=1:232;
if dbrace==45;
keep(b,cs)=TableEFL1{b,4};
keepx= keepx;
elseif dbrace==86;
keep2(b,cs)=TableEFL1{b,4};
keepx= keepx2;
end;
end;
for hjj=1:sls;

Change2(hjj,1)=(TableEFL1{2*hjj-1,4})+(TableEFL1{2*hjj,4})*0.5;

m(hjj)=Change2(hjj,1);

end;

for i=ile;
if Load1==0;

loads(i,1)=Change2(i,1);

xc(i,1)=Change2(i,1);
xc(~any(xc,2),:)=[];
sredniaF(1,cs)=mean(xc);

else

loads(i,2)=Change2(i,1);

xc(i,1)=Change2(i,1);
xc(~any(xc,2),:)=[];
sredniaM(1,cs)=mean(xc);
end

end

if DEL==1;
for i=1:58;
if Load1==0;
loads(i,1)=Change1(i,1);
elseif Load1==1;
loads(i,2)=Change1(i,1);
end;
MINUS1{i}=1;

```

```

MNOZNIK{i}=100;
BB(i,2)=(loads(i,1));
BB(i,3)=(loads(i,2));
BB(i,1)=Changel(2*i,2);
end
vcv=max(BB(:,2));
if vcv<=5;
vcv
else
vcv=5;
end;

gw = 0.7; % almost touching, 1 is touching
gx=20;
hg=58;
x = 1:hg ;
fig(1) = bar((x-1)+10*gw/gx, BB(:,2), gw/2, 'b') ;
hold on ;
fig(2) = bar((x-1)+20*gw/gx, BB(:,3), gw/2, 'r') ;
hold off ;
grid on;
Xl = [0 hg];
Yl=[0 1.5*vcv];
Xt=0.5:2:57.5;
set(fig(1), 'FaceColor', [1 0 1]) ;
set(fig(2), 'FaceColor', [0 0 1]) ;
set(gca, 'XLim', Xl, 'XTick', Xt, 'YLim', Yl);
set(gca, 'XTickLabel', ([BB(:,1)]));
set(gcf, 'color', 'w');
legend('DEL ratio refered to axial force', 'DEL ratio refered to equivalent moment');
B1=[0.926 0.88 0.8 0.5312 0.0018];
B1x=[0.702 0.507 0.391 0.151 0.0009];
B2=[1.01 1.032 1.073 1.192 1.454];
B2x=[1.01 1.175 1.388 2.197 2.953];

else

diagram=0;
if diagram==1

MINUS1{i}=1;
MNOZNIK{i}=100;
BB(i,2)=(loads(i,1)-MINUS1{i});
BB(i,3)=(loads(i,2)-MINUS1{i});
BB(i,1)=cord{i,1}{1,1};
end

AA1=(BB);

save(['bar name', num2str(cs), num2str(Load1)], 'AA1')

%
gw = 0.7; % almost touching, 1 is touching
gx=20;
hg=ile;
x = 1:hg ;
fig(1) = bar((x-1)+10*gw/gx, (AA1(:,2)), gw/2, 'b') ;
hold on ;
fig(2) = bar((x-1)+20*gw/gx, (AA1(:,3)), gw/2, 'r') ;
hold off ;
grid on;
Yl=[-1 1];
Yt=-1:0.25:2;

Xt=0:0.5:2;
Xl = [0 hg];
Xt=0.5:1:57.5;
set(fig(1), 'FaceColor', [1 0 1]) ;
set(fig(2), 'FaceColor', [0 0.2 1]) ;
set(gca, 'XLim', Xl, 'XTick', Xt, 'YLim', Yl, 'YTick', Yt);
set(gca, 'XTickLabel', ([AA(:,1)]), 'YTickLabel', [0 0.25 0.5 0.75 1 1.25 1.5 1.75 2]);

set(gcf, 'color', 'w');
legend('EFL ratio refered to axial force', 'EFL ratio refered to equivalent moment', 'Location', 'northwest');
end

```

```

save(['bar comparison',num2str(cs),num2str(Load1)],'loads');
;
[EFLM(1,1) EFLM(1,2)]=max(cell2mat(TableEFL1(:,4)));
[EFLM(2,1) EFLM(2,2)]=min(cell2mat(TableEFL1(:,4)));
end;
EFLc{1,4}=EFLM(1,1);
EFLc{1,3}=TableEFL1{EFLM(1,2),5}*10^3;
EFLc{1,2}=TableEFL1{EFLM(1,2),2};
EFLc{1,1}=TableEFL1{EFLM(1,2),1};

EFLc{2,4}=EFLM(2,1);
EFLc{2,3}=TableEFL1{EFLM(2,2),5}*10^3;
EFLc{2,2}=TableEFL1{EFLM(2,2),2};
EFLc{2,1}=TableEFL1{EFLM(2,2),1};
%
for i=1:nods3;
    TABLE{i+1,1}=i;
    TABLE{i+1,2}=TableEFL{i,1};
    TABLE{i+1,3}=TableEFL{i,2};
    TABLE{i+1,4}=TableEFL{i,3};
    TABLE{i+1,5}=TableEFL{i,4};
    TableEFL{i,5}=sprintf('% .3f',TableEFL{i,5});
    TABLE{i+1,6}=TableEFL{i,5};
    TABLE{i+1,7}=TableEFL{i,6};
end;
TABLE{1,1}='No';
TABLE{1,2}='Element';
TABLE{1,3}='Nod ';
TABLE{1,4}='EFL0 [MPa]';
TABLE{1,5}='EFL [MPa] ';
TABLE{1,6}='EFL atio';
TABLE{1,7}='Scaled EFL ratio';
KOLOR0=[0,0,0.2];
KOLOR1=[0,0,0.25];
KOLOR2=[0,0,0.3];
KOLOR3=[0,0,0.4];
KOLOR4=[0,0,0.5];
KOLOR5=[0,0,0.7];
KOLOR6=[0,0,0.8];
KOLOR7=[0,0,1];
KOLOR8=[0,0.1,1];
KOLOR9=[0,0.2,1];
KOLOR10=[0,0.25,1];
KOLOR11=[0,0.3,0.9];
KOLOR12=[0,0.35,0.8];
KOLOR13=[0,0.4,0.7];
KOLOR14=[0,0.45,0.6];
KOLOR15=[0,0.5,0.5];
KOLOR16=[0,0.55,0.4];
KOLOR17=[0,0.6,0.3];
KOLOR18=[0,0.6,0.1];
KOLOR19=[0,0.7,0];
KOLOR20=[0,0.85,0];
KOLOR20x=[0,1,0];
KOLOR21=[0.3,1,0];
KOLOR22=[0.45,1,0];
KOLOR23=[0.6,1,0];
KOLOR24=[0.8,1,0];
KOLOR25=[1,1,0];
KOLOR26=[1,0.9,0];
KOLOR27=[1,0.8,0];
KOLOR28=[1,0.7,0];
KOLOR29=[1,0.6,0];
KOLOR30=[1,0.5,0];
KOLOR31=[1,0.4,0];
KOLOR32=[1,0.3,0];
KOLOR33=[1,0.2,0];
KOLOR34=[1,0.1,0];
KOLOR35=[1,0,0];
KOLOR36=[0.8,0,0];
KOLOR37=[0.7,0,0];
KOLOR38=[0.6,0,0];
KOLOR39=[0.5,0,0];
KOLOR40=[0.4,0,0];
KOLOR41=[0.3,0,0];

```

```

        for i=1:nods3
MINUS1{i}=1;
MNOZNIK{i}=100;
    BAR{i,2}=(TableEFL{i,5}-MINUS1{i})*100;
    BAR{i,1}=i;
end
asd=1:dlq;
m(1,85)=(m(1,56)+m(1,27))/2;
    for ngf=1:41;
        ngv(ngf)=0.5+(ngf-1)*0.025;
end;
for i=[2:21];
    sss{1}= horzcat(strcat('<0.5'));
    sss{i} = horzcat(strcat(num2str(ngv(i-1)),'-',num2str(ngv(i))));
    sss{22}='1.0';

end;
for i=[23:42];
    sss{1}= horzcat(strcat('<0.5'));
    sss{22}='1.0';
    sss{i} = horzcat(strcat(num2str(ngv(i-2)),'-',num2str(ngv(i-1))));
    sss{43}=horzcat(strcat('>1.5'));
end;

    shape='-.';
%
% ALL SIDES
if side==1;
sides=side;

dff=nods1;
for i=asd;
    n=1.5

n=m(i+(sides-1)*dlq);
if n<= ngv(1,1) ;

    KOLOR=KOLOR0;

elseif (n > ngv(1,1)) && (n <= ngv(1,2)) ;
KOLOR=KOLOR1;

elseif (n > ngv(1,2)) &&(n <= ngv(1,3));
KOLOR=KOLOR2;

elseif (n > ngv(1,3)) && (n <= ngv(1,4)) ;
KOLOR=KOLOR3;

elseif (n > ngv(1,4)) && (n <= ngv(1,5)) ;
KOLOR=KOLOR4;

elseif (n > ngv(1,5)) && (n <= ngv(1,6)) ;
KOLOR=KOLOR5;

elseif (n > ngv(1,6)) && (n <= ngv(1,7)) ;
KOLOR=KOLOR6;

elseif (n > ngv(1,7)) && (n<= ngv(1,8)) ;
KOLOR=KOLOR7;

elseif (n > ngv(1,8)) && (n<=ngv(1,9) );
KOLOR=KOLOR8;

elseif (n > ngv(1,9)) && (n<=ngv(1,10) );
KOLOR=KOLOR9;

elseif (n > ngv(1,10)) && (n<=ngv(1,11) );
KOLOR=KOLOR10;
elseif (n > ngv(1,11)) && (n<=ngv(1,12) );
KOLOR=KOLOR11;

elseif (n > ngv(1,12)) && (n<=ngv(1,13) );
    KOLOR=KOLOR12;

```

```

elseif (n > ngv(1,13)) && (n<=ngv(1,14) );
    KOLOR=KOLOR13;

elseif (n > ngv(1,14)) && (n<=ngv(1,15) );
    KOLOR=KOLOR14;
elseif (n > ngv(1,15)) && (n<=ngv(1,16) );
    KOLOR=KOLOR15;

elseif (n > ngv(1,16)) && (n<=ngv(1,17) );
    KOLOR=KOLOR16;

elseif (n > ngv(1,17)) && (n<=ngv(1,18) );
    KOLOR=KOLOR17;
elseif (n > ngv(1,18)) && (n<=ngv(1,19) );
    KOLOR=KOLOR18;
elseif (n > ngv(1,19)) && (n<=ngv(1,20) );
    KOLOR=KOLOR19;
elseif (n ==ngv(1,20))
    KOLOR=KOLOR20;
elseif (n > ngv(1,20)) && (n <=ngv(1,21) );
    KOLOR=KOLOR20x;
elseif (n > ngv(1,21)) && (n <=ngv(1,22) );
    KOLOR=KOLOR21;
elseif (n > ngv(1,22)) && (n <=ngv(1,23) );
    KOLOR=KOLOR22;
elseif (n > ngv(1,23)) && (n <=ngv(1,24) );
    KOLOR=KOLOR23;
elseif (n > ngv(1,24)) && (n <=ngv(1,25) );
    KOLOR=KOLOR24;
elseif (n > ngv(1,25)) && (n <=ngv(1,26) );
    KOLOR=KOLOR25;
elseif (n > ngv(1,26)) && (n <=ngv(1,27) );
    KOLOR=KOLOR26;
elseif (n > ngv(1,27)) && (n <=ngv(1,28) );
    KOLOR=KOLOR27;
elseif (n > ngv(1,28)) && (n <=ngv(1,29) );
    KOLOR=KOLOR28;
elseif (n > ngv(1,29)) && (n <=ngv(1,30) );
    KOLOR=KOLOR29;
elseif (n > ngv(1,30)) && (n <=ngv(1,31) );
    KOLOR=KOLOR30;
elseif (n > ngv(1,31)) && (n <=ngv(1,32) );
    KOLOR=KOLOR31;
elseif (n > ngv(1,32)) && (n <=ngv(1,33) );
    KOLOR=KOLOR32;
elseif (n > ngv(1,33)) && (n <=ngv(1,34) );
    KOLOR=KOLOR33;
elseif (n > ngv(1,34)) && (n <=ngv(1,35) );
    KOLOR=KOLOR34;
elseif (n > ngv(1,35)) && (n <=ngv(1,36) );
    KOLOR=KOLOR35;
elseif (n > ngv(1,36)) && (n <=ngv(1,37) );
    KOLOR=KOLOR36;
elseif (n > ngv(1,37)) && (n <=ngv(1,38) );
    KOLOR=KOLOR37;
elseif (n > ngv(1,38)) && (n <=ngv(1,39) );
    KOLOR=KOLOR38;
elseif (n > ngv(1,39)) && (n <=ngv(1,40) );
    KOLOR=KOLOR39;
elseif (n > ngv(1,40)) && (n <=ngv(1,41) );
    KOLOR=KOLOR40;
elseif (n > 1.5) ;
    KOLOR=KOLOR41;
end;
dvc{i}=(dff{i,1}{1,1});

if dvc{i}==dbrace && E~=0
    plot([dff{i,1}{1,4} dff{i,1}{1,6}], [dff{i,1}{1,5}, dff{i,1}{1,7}],shape,'Color',
    KOLOR,'LineWidth',2 );
else;
    blc=plot([dff{i,1}{1,4} dff{i,1}{1,6}], [dff{i,1}{1,5}, dff{i,1}{1,7}], 'Color',
    KOLOR,'LineWidth',2 );
    titleside=horzcat(strcat('SIDE',num2str(side)));
    title(titleside)
end;

```

```

        hold on;
        axis equal;
        axis off;

end;

elseif side==5;

for xkl=1:4
    if xkl==1;
sides=xkl;

dff=nods1;
elseif xkl==2;
sides=xkl;
dff=nods2;

elseif xkl==3;
sides=xkl;
dff=sods3;
elseif xkl==4;
sides=xkl;
dff=nods4;

end;
for i=asd;

n=m(i+(sides-1)*dlq);

if n<= ngv(1,1) ;

    KOLOR=KOLOR0;

elseif (n > ngv(1,1)) && (n <= ngv(1,2)) ;
KOLOR=KOLOR1;

elseif (n > ngv(1,2)) &&(n <= ngv(1,3));
KOLOR=KOLOR2;

elseif (n > ngv(1,3)) && (n <= ngv(1,4)) ;
KOLOR=KOLOR3;

elseif (n > ngv(1,4)) && (n <= ngv(1,5)) ;
KOLOR=KOLOR4;

elseif (n > ngv(1,5)) && (n <= ngv(1,6)) ;
KOLOR=KOLOR5;

elseif (n > ngv(1,6)) && (n <= ngv(1,7)) ;
KOLOR=KOLOR6;

elseif (n > ngv(1,7)) && (n<= ngv(1,8)) ;
KOLOR=KOLOR7;

elseif (n > ngv(1,8)) && (n<=ngv(1,9) );
KOLOR=KOLOR8;

elseif (n > ngv(1,9)) && (n<=ngv(1,10) );
KOLOR=KOLOR9;

elseif (n > ngv(1,10)) && (n<=ngv(1,11) );
KOLOR=KOLOR10;
elseif (n > ngv(1,11)) && (n<=ngv(1,12) );
KOLOR=KOLOR11;

elseif (n > ngv(1,12)) && (n<=ngv(1,13) );
    KOLOR=KOLOR12;

elseif (n > ngv(1,13)) && (n<=ngv(1,14) );
    KOLOR=KOLOR13;

elseif (n > ngv(1,14)) && (n<=ngv(1,15) );
    KOLOR=KOLOR14;

```

```

elseif (n > ngv(1,15)) && (n<=ngv(1,16) );
KOLOR=KOLOR15;

elseif (n > ngv(1,16)) && (n<=ngv(1,17) );
KOLOR=KOLOR16;

elseif (n > ngv(1,17)) && (n<=ngv(1,18) );
KOLOR=KOLOR17;
elseif (n > ngv(1,18)) && (n<=ngv(1,19) );
KOLOR=KOLOR18;
elseif (n > ngv(1,19)) && (n<=ngv(1,20) );
KOLOR=KOLOR19;
elseif (n ==ngv(1,20))
KOLOR=KOLOR20;
elseif (n > ngv(1,20)) && (n <=ngv(1,21) );
KOLOR=KOLOR20x;
elseif (n > ngv(1,21)) && (n <=ngv(1,22) );
KOLOR=KOLOR21;
elseif (n > ngv(1,22)) && (n <=ngv(1,23) );
KOLOR=KOLOR22;
elseif (n > ngv(1,23)) && (n <=ngv(1,24) );
KOLOR=KOLOR23;
elseif (n > ngv(1,24)) && (n <=ngv(1,25) );
KOLOR=KOLOR24;
elseif (n > ngv(1,25)) && (n <=ngv(1,26) );
KOLOR=KOLOR25;
elseif (n > ngv(1,26)) && (n <=ngv(1,27) );
KOLOR=KOLOR26;
elseif (n > ngv(1,27)) && (n <=ngv(1,28) );
KOLOR=KOLOR27;
elseif (n > ngv(1,28)) && (n <=ngv(1,29) );
KOLOR=KOLOR28;
elseif (n > ngv(1,29)) && (n <=ngv(1,30) );
KOLOR=KOLOR29;
elseif (n > ngv(1,30)) && (n <=ngv(1,31) );
KOLOR=KOLOR30;
elseif (n > ngv(1,31)) && (n <=ngv(1,32) );
KOLOR=KOLOR31;
elseif (n > ngv(1,32)) && (n <=ngv(1,33) );
KOLOR=KOLOR32;
elseif (n > ngv(1,33)) && (n <=ngv(1,34) );
KOLOR=KOLOR33;
elseif (n > ngv(1,34)) && (n <=ngv(1,35) );
KOLOR=KOLOR34;
elseif (n > ngv(1,35)) && (n <=ngv(1,36) );
KOLOR=KOLOR35;
elseif (n > ngv(1,36)) && (n <=ngv(1,37) );
KOLOR=KOLOR36;
elseif (n > ngv(1,37)) && (n <=ngv(1,38) );
KOLOR=KOLOR37;
elseif (n > ngv(1,38)) && (n <=ngv(1,39) );
KOLOR=KOLOR38;
elseif (n > ngv(1,39)) && (n <=ngv(1,40) );
KOLOR=KOLOR39;
elseif (n > ngv(1,40)) && (n <=ngv(1,41) );
KOLOR=KOLOR40;
elseif (n > 1.5) ;
KOLOR=KOLOR41;
end;
dvc{i}=(dff{i,1}{1,1});

shape='-.';
if presentation==1;

if dvc{i}==dbrace
    subplot(1,4,xkl);

    plot([dff{i,1}{1,4} dff{i,1}{1,6}], [dff{i,1}{1,5}, dff{i,1}{1,7}],shape,'Color',
KOLOR,'LineWidth',2);
else;

    subplot(1,4,xkl);
    blc=plot([dff{i,1}{1,4} dff{i,1}{1,6}], [dff{i,1}{1,5}, dff{i,1}{1,7}], 'Color',
KOLOR,'LineWidth',2 );
    titleside=horzcat(strcat('SIDE',num2str(xkl)));
    title(titleside)

```



```

end;
elseif presentation==0;

if dvc{i}==dbrace && E~=0
    subplot(1,4,xkl);
    plot([dff{i,1}{1,4} dff{i,1}{1,6}], [dff{i,1}{1,5}, dff{i,1}{1,7}], '-.','Color',
KOLOR,'LineWidth',2.5 );
else;
    blc=plot([dff{i,1}{1,4} dff{i,1}{1,6}], [dff{i,1}{1,5}, dff{i,1}{1,7}], 'Color',
KOLOR,'LineWidth',2.5 );
    x0=0.3;y0=0.3;width=1;height=5;
    if i==sls;
set(gcf,'units','normalized','outerposition',[0 0 1 1]);
set(gcf,'PaperPositionMode','auto');
set(gcf,'color','w');
savenameplot3= horzcat(strcat('D:\Users\Konrad\Desktop\Praca magisterska\resultsrotor\rys
kratownicy\','kratownica',num2str(xkl)));

print(savenameplot3,'-djpeg','-r1000');
end;
end;
end;
hold on;
axis equal;
axis off;

end;
end;
end;
set(gcf,'units','normalized','outerposition',[0 0 1 1]);
set(gcf,'PaperPositionMode','auto');
set(gcf,'color','w');

if Load1==0;
    TABLE{1,7}='Max Force [MN]';
    nametab='for';
elseif Load1==1;
    TABLE{1,7}='Max Moment [MNm]';
    nametab='mom';
end

% ramka
if side==5
hold on;
cordx=[0 0.00000001];
cordy=[0 0.0000000000000001];

p=plot(cordx,cordy,shape,'Color',[0 0 1],'LineWidth',2);

set(p, 'visible', 'off');
hold on;
p0=bar(cordy,'FaceColor',KOLOR0);
set(p0, 'visible', 'off');
hold on
p1=bar(cordy,'FaceColor',KOLOR1);
set(p1, 'visible', 'off');
hold on
p2=bar(cordy,'FaceColor',KOLOR2);

set(p2, 'visible', 'off');
hold on
p3=bar(cordy,'FaceColor',KOLOR3);

set(p3, 'visible', 'off');
hold on
p4=bar(cordy,'FaceColor',KOLOR4);

set(p4, 'visible', 'off');
hold on
p5=bar(cordy,'FaceColor',KOLOR5);

set(p5, 'visible', 'off');
hold on

p6=bar(cordy,'FaceColor',KOLOR6);

```

```

set(p6, 'visible', 'off');
hold on
p7=bar(cordy,'FaceColor',KOLOR7);

set(p7, 'visible', 'off');
hold on

p8=bar(cordy,'FaceColor',KOLOR8);

set(p8, 'visible', 'off');
hold on
p9=bar(cordy,'FaceColor',KOLOR9);

set(p9, 'visible', 'off');
hold on
p10=bar(cordy,'FaceColor',KOLOR10);

set(p10, 'visible', 'off');
hold on
p11=bar(cordy,'FaceColor',KOLOR11);

set(p11, 'visible', 'off');
hold on
p12=bar(cordy,'FaceColor',KOLOR12);

set(p12, 'visible', 'off');
hold on
p13=bar(cordy,'FaceColor',KOLOR13);
set(p13, 'visible', 'off');
hold on
p14=bar(cordy,'FaceColor',KOLOR14);
set(p14, 'visible', 'off');
hold on
p15=bar(cordy,'FaceColor',KOLOR15);
set(p15, 'visible', 'off');
hold on
p16=bar(cordy,'FaceColor',KOLOR16);
set(p16, 'visible', 'off');
hold on
p17=bar(cordy,'FaceColor',KOLOR17);
set(p17, 'visible', 'off');
hold on;
p18=bar(cordy,'FaceColor',KOLOR18);
set(p18, 'visible', 'off');
hold on;
p19=bar(cordy,'FaceColor',KOLOR19);
set(p19, 'visible', 'off');
hold on;
p20=bar(cordy,'FaceColor',KOLOR20);
set(p20, 'visible', 'off');
hold on;
p21=bar(cordy,'FaceColor',KOLOR21);
set(p21, 'visible', 'off');
hold on;
p22=bar(cordy,'FaceColor',KOLOR22);
set(p22, 'visible', 'off');
hold on;
set(p1, 'visible', 'off');
hold on
hold on
p23=bar(cordy,'FaceColor',KOLOR23);

set(p23, 'visible', 'off');
hold on
p24=bar(cordy,'FaceColor',KOLOR24);

set(p24, 'visible', 'off');
hold on
p25=bar(cordy,'FaceColor',KOLOR25);

set(p25, 'visible', 'off');
hold on

p26=bar(cordy,'FaceColor',KOLOR26);

set(p26, 'visible', 'off');
hold on

```

```

p27=bar(cordy,'FaceColor',KOLOR27);
set(p27, 'visible', 'off');
hold on

p28=bar(cordy,'FaceColor',KOLOR28);
set(p28, 'visible', 'off');
hold on
p29=bar(cordy,'FaceColor',KOLOR29);
set(p29, 'visible', 'off');
hold on
p30=bar(cordy,'FaceColor',KOLOR30);
set(p30, 'visible', 'off');
hold on
p31=bar(cordy,'FaceColor',KOLOR31);
set(p31, 'visible', 'off');
hold on
p32=bar(cordy,'FaceColor',KOLOR32);
set(p32, 'visible', 'off');
hold on
p33=bar(cordy,'FaceColor',KOLOR33);
set(p33, 'visible', 'off');
hold on
p34=bar(cordy,'FaceColor',KOLOR34);
set(p34, 'visible', 'off');
hold on
p35=bar(cordy,'FaceColor',KOLOR35);
set(p35, 'visible', 'off');
hold on
p36=bar(cordy,'FaceColor',KOLOR36);
set(p36, 'visible', 'off');
hold on
p37=bar(cordy,'FaceColor',KOLOR37);
set(p37, 'visible', 'off');
hold on;
p38=bar(cordy,'FaceColor',KOLOR38);
set(p38, 'visible', 'off');
hold on;
p39=bar(cordy,'FaceColor',KOLOR39);
set(p39, 'visible', 'off');
hold on;
p40=bar(cordy,'FaceColor',KOLOR40);
set(p40, 'visible', 'off');
hold on;
p41=bar(cordy,'FaceColor',KOLOR41);
set(p41, 'visible', 'off');
hold on;
p20x=bar(cordy,'FaceColor',KOLOR20x);
set(p20x, 'visible', 'off');
hold on;

pl13=legend([p p0 p1 p2 p3 p4 p5 p6 p7 p8 p9 p10 p11 p12 p13 p14 p15 p16 p17 p18 p19 p20
p20x p21 p22 p23 p24 p25 p26 p27 p28 p29 p30 p31 p32 p33 p34 p35 p36 p37 p38 p39 p40
p41], ['damaged' sss]);
v = get(pl13,'title');
set(v,'string','Legend');
x0=0.3 ;y0=2;width=3;height=14;
set(pl13,'units','centimeter','position',[x0,y0,width,height]);
else;
savenameplot3= horzcat(strcat(pathplot,num2str(cs),'\',namecases{1,cs},'for','side_1'));
print(savenameplot3,'-djpeg','-r1500');
end;
set(gcf,'color','w');

axis off;

ha = axes('Position',[0 0 1 1],'Xlim',[0 1],'Ylim',[0
1],'Box','off','Visible','off','Units','normalized','clipping','off');

```

```
text(0.5, 1, '\bf DLC 1.2 FATIGUE ANALYSIS  
, 'HorizontalAlignment', 'center', 'VerticalAlignment', 'top')
```

APPENDIX F

Offshore Wind Turbine natural frequencies extracted from FEDEM Windpower

considering different structure states

Case 0 Undamaged state structure

```
.....
EIGENVALUE ANALYSIS AT TIME (S): 0.00000E+00
.....

EIGENFREQUENCIES [Hz] (using SAM::SPRLAN) :

EIGFREQ 1    EIGFREQ 2    EIGFREQ 3    EIGFREQ 4    EIGFREQ 5    EIGFREQ 6    EIGFREQ 7    EIGFREQ 8    EIGFREQ 9    EIGFREQ10
3.11160E-01  3.12368E-01  6.22703E-01  6.52892E-01  6.65400E-01  7.15969E-01  1.06534E+00  1.07069E+00  1.15669E+00  1.18867E+00
1.61377E+00  1.86684E+00  1.94373E+00  2.59462E+00  2.86785E+00  3.37094E+00  3.49342E+00  3.55643E+00  3.91827E+00  4.02451E+00
4.20352E+00  4.46713E+00  4.47819E+00  4.64015E+00  4.68729E+00  4.74567E+00  4.75108E+00  4.92922E+00  5.11485E+00  5.21278E+00
5.26011E+00  5.51364E+00  5.56090E+00  5.56247E+00  5.56625E+00  6.23824E+00  6.47941E+00  6.51377E+00  6.99245E+00  7.01331E+00
7.48491E+00  7.69921E+00  7.87123E+00  7.89542E+00  7.90625E+00  8.01480E+00  8.06987E+00  8.56470E+00  8.57788E+00  8.87033E+00
.....
```

Case 1 Damaged state structure, X-brace 45 Young's modulus reduction $E=0.7E_0$

```
.....
EIGENVALUE ANALYSIS AT TIME (S): 0.00000E+00
.....

EIGENFREQUENCIES [Hz] (using SAM::SPRLAN) :

EIGFREQ 1    EIGFREQ 2    EIGFREQ 3    EIGFREQ 4    EIGFREQ 5    EIGFREQ 6    EIGFREQ 7    EIGFREQ 8    EIGFREQ 9    EIGFREQ10
3.11147E-01  3.12362E-01  6.22628E-01  6.52892E-01  6.65380E-01  7.15938E-01  1.06534E+00  1.07066E+00  1.15644E+00  1.18657E+00
1.61274E+00  1.86684E+00  1.94373E+00  2.58622E+00  2.86666E+00  3.36909E+00  3.48474E+00  3.52253E+00  3.91686E+00  4.02440E+00
4.19286E+00  4.42113E+00  4.46715E+00  4.62637E+00  4.64043E+00  4.72075E+00  4.73371E+00  4.92796E+00  5.09619E+00  5.20311E+00
5.25590E+00  5.51104E+00  5.56090E+00  5.56245E+00  5.56624E+00  6.23656E+00  6.47686E+00  6.50587E+00  6.99014E+00  6.99261E+00
7.45232E+00  7.69330E+00  7.80362E+00  7.88655E+00  7.89546E+00  8.01467E+00  8.06984E+00  8.53962E+00  8.57052E+00  8.85452E+00
.....
```

Case 2 Damaged state structure, X-brace 45 Young's modulus reduction $E=0.5E_0$

```
.....
EIGENVALUE ANALYSIS AT TIME (S): 0.00000E+00
.....

EIGENFREQUENCIES [Hz] (using SAM::SPRLAN) :

EIGFREQ 1    EIGFREQ 2    EIGFREQ 3    EIGFREQ 4    EIGFREQ 5    EIGFREQ 6    EIGFREQ 7    EIGFREQ 8    EIGFREQ 9    EIGFREQ10
3.11132E-01  3.12356E-01  6.22540E-01  6.52891E-01  6.65358E-01  7.15902E-01  1.06533E+00  1.07062E+00  1.15611E+00  1.18414E+00
1.61153E+00  1.86683E+00  1.94373E+00  2.57570E+00  2.86520E+00  3.36690E+00  3.45228E+00  3.50635E+00  3.91479E+00  4.02424E+00
4.17139E+00  4.35040E+00  4.46704E+00  4.59012E+00  4.63745E+00  4.69822E+00  4.72796E+00  4.92687E+00  5.08575E+00  5.19359E+00
5.25378E+00  5.50942E+00  5.56090E+00  5.56243E+00  5.56623E+00  6.23485E+00  6.47494E+00  6.49590E+00  6.96005E+00  6.99244E+00
7.41055E+00  7.67738E+00  7.74502E+00  7.88483E+00  7.89396E+00  8.01462E+00  8.06983E+00  8.51677E+00  8.56753E+00  8.84266E+00
.....
```

Case 3 Damaged state structure, X-brace 45 Young's modulus reduction $E=0.3E_0$

```

.....
EIGENVALUE ANALYSIS AT TIME (S): 0.00000E+00
.....

EIGENFREQUENCIES [Hz] (using SAM::SPRLAN) :

EIGFREQ 1    EIGFREQ 2    EIGFREQ 3    EIGFREQ 4    EIGFREQ 5    EIGFREQ 6    EIGFREQ 7    EIGFREQ 8    EIGFREQ 9    EIGFREQ10
3.11105E-01  3.12346E-01  6.22374E-01  6.52889E-01  6.65316E-01  7.15833E-01  1.06533E+00  1.07055E+00  1.15530E+00  1.17970E+00
1.60921E+00  1.86682E+00  1.94373E+00  2.55382E+00  2.86224E+00  3.35975E+00  3.37432E+00  3.50168E+00  3.90886E+00  4.02372E+00
4.10063E+00  4.27928E+00  4.46680E+00  4.55783E+00  4.63091E+00  4.66601E+00  4.72538E+00  4.92545E+00  5.07680E+00  5.17975E+00
5.25203E+00  5.50786E+00  5.56090E+00  5.56242E+00  5.56621E+00  6.23183E+00  6.47111E+00  6.47637E+00  6.89738E+00  6.99242E+00
7.33636E+00  7.63036E+00  7.71702E+00  7.88390E+00  7.89242E+00  8.01456E+00  8.06981E+00  8.49047E+00  8.56463E+00  8.82984E+00
.....

```

Case 4 Damaged state structure, X-brace 45 Young's modulus reduction $E=0.1E_0$

```

.....
EIGENVALUE ANALYSIS AT TIME (S): 0.00000E+00
.....

EIGENFREQUENCIES [Hz] (using SAM::SPRLAN) :

EIGFREQ 1    EIGFREQ 2    EIGFREQ 3    EIGFREQ 4    EIGFREQ 5    EIGFREQ 6    EIGFREQ 7    EIGFREQ 8    EIGFREQ 9    EIGFREQ10
3.11039E-01  3.12323E-01  6.21936E-01  6.52886E-01  6.65207E-01  7.15655E-01  1.06530E+00  1.07032E+00  1.15120E+00  1.17005E+00
1.60306E+00  1.86680E+00  1.94373E+00  2.48526E+00  2.85344E+00  3.19572E+00  3.35586E+00  3.49998E+00  3.86093E+00  3.96594E+00
4.02506E+00  4.24718E+00  4.46497E+00  4.50041E+00  4.60399E+00  4.64648E+00  4.72385E+00  4.92355E+00  5.06911E+00  5.15855E+00
5.25057E+00  5.50629E+00  5.56089E+00  5.56241E+00  5.56617E+00  6.22276E+00  6.40990E+00  6.47100E+00  6.76644E+00  6.99240E+00
7.23872E+00  7.58071E+00  7.70975E+00  7.88323E+00  7.89071E+00  8.01451E+00  8.06980E+00  8.46138E+00  8.56155E+00  8.81623E+00
.....

```

Case 5 Damaged state structure, X-brace 45 Free-joint insertion

```

.....
EIGENVALUE ANALYSIS AT TIME (S): 0.00000E+00
.....

EIGENFREQUENCIES [Hz] (using SAM::SPRLAN) :

EIGFREQ 1    EIGFREQ 2    EIGFREQ 3    EIGFREQ 4    EIGFREQ 5    EIGFREQ 6    EIGFREQ 7    EIGFREQ 8    EIGFREQ 9    EIGFREQ10
3.10941E-01  3.12293E-01  6.21265E-01  6.52881E-01  6.65045E-01  7.15384E-01  1.06523E+00  1.06983E+00  1.13682E+00  1.16352E+00
1.59363E+00  1.86676E+00  1.94373E+00  2.36375E+00  2.83794E+00  3.05096E+00  3.21497E+00  3.45243E+00  3.50072E+00  3.92634E+00
4.02424E+00  4.22983E+00  4.42845E+00  4.46970E+00  4.58088E+00  4.64163E+00  4.72150E+00  4.92207E+00  5.05235E+00  5.14220E+00
5.24705E+00  5.50075E+00  5.56089E+00  5.56238E+00  5.56613E+00  6.19867E+00  6.32882E+00  6.45875E+00  6.67784E+00  6.99213E+00
7.14191E+00  7.38760E+00  7.63127E+00  7.70680E+00  7.84145E+00  7.89710E+00  8.01372E+00  8.06931E+00  8.13277E+00  8.47182E+00
.....

```

Case 6 Damaged state structure, X-brace 86 Young's modulus reduction $E=0.7E_0$

```

.....
EIGENVALUE ANALYSIS AT TIME (S): 0.00000E+00
.....

EIGENFREQUENCIES [Hz] (using SAM::SPRLAN) :

EIGFREQ 1    EIGFREQ 2    EIGFREQ 3    EIGFREQ 4    EIGFREQ 5    EIGFREQ 6    EIGFREQ 7    EIGFREQ 8    EIGFREQ 9    EIGFREQ10
3.11149E-01  3.12358E-01  6.22643E-01  6.52886E-01  6.65397E-01  7.15968E-01  1.06534E+00  1.07063E+00  1.15582E+00  1.18867E+00
1.61328E+00  1.86680E+00  1.94373E+00  2.59286E+00  2.86783E+00  3.37077E+00  3.49319E+00  3.55618E+00  3.91793E+00  4.02451E+00
4.20216E+00  4.46711E+00  4.47796E+00  4.64005E+00  4.68704E+00  4.74353E+00  4.74616E+00  4.92903E+00  5.11048E+00  5.21271E+00
5.25991E+00  5.51181E+00  5.56090E+00  5.56244E+00  5.56625E+00  6.23731E+00  6.47893E+00  6.51266E+00  6.98557E+00  6.99432E+00
7.47131E+00  7.69783E+00  7.82941E+00  7.88643E+00  7.90486E+00  8.01474E+00  8.06969E+00  8.50657E+00  8.56251E+00  8.83329E+00
.....

```

Case 7 Damaged state structure, X-brace 86 Young's modulus reduction $E=0.5E_0$

```

.....
EIGENVALUE ANALYSIS AT TIME (S): 0.00000E+00
.....

EIGENFREQUENCIES [Hz] (using SAM::SPRLAN) :

EIGFREQ 1    EIGFREQ 2    EIGFREQ 3    EIGFREQ 4    EIGFREQ 5    EIGFREQ 6    EIGFREQ 7    EIGFREQ 8    EIGFREQ 9    EIGFREQ10
3.11141E-01  3.12349E-01  6.22570E-01  6.52879E-01  6.65393E-01  7.15967E-01  1.06533E+00  1.07056E+00  1.15476E+00  1.18866E+00
1.61269E+00  1.86674E+00  1.94372E+00  2.59072E+00  2.86780E+00  3.37060E+00  3.49295E+00  3.55591E+00  3.91750E+00  4.02450E+00
4.20044E+00  4.46709E+00  4.47772E+00  4.63996E+00  4.68666E+00  4.73603E+00  4.74577E+00  4.92881E+00  5.10515E+00  5.21265E+00
5.25973E+00  5.51002E+00  5.56090E+00  5.56241E+00  5.56624E+00  6.23647E+00  6.47854E+00  6.51143E+00  6.95244E+00  6.99319E+00
7.45484E+00  7.69563E+00  7.77664E+00  7.88128E+00  7.90380E+00  8.01468E+00  8.06948E+00  8.41970E+00  8.55952E+00  8.80800E+00
.....

```

Case 8 Damaged state structure, X-brace 86 Young's modulus reduction $E=0.3E_0$

```

.....
EIGENVALUE ANALYSIS AT TIME (S): 0.00000E+00
.....

EIGENFREQUENCIES [Hz] (using SAM::SPRLAN) :

EIGFREQ 1    EIGFREQ 2    EIGFREQ 3    EIGFREQ 4    EIGFREQ 5    EIGFREQ 6    EIGFREQ 7    EIGFREQ 8    EIGFREQ 9    EIGFREQ10
3.11132E-01  3.12333E-01  6.22424E-01  6.52865E-01  6.65386E-01  7.15965E-01  1.06532E+00  1.07042E+00  1.15266E+00  1.18866E+00
1.61151E+00  1.86664E+00  1.94371E+00  2.58643E+00  2.86776E+00  3.37030E+00  3.49256E+00  3.55542E+00  3.91659E+00  4.02450E+00
4.19678E+00  4.46703E+00  4.47728E+00  4.63980E+00  4.68540E+00  4.72137E+00  4.74563E+00  4.92836E+00  5.09459E+00  5.21255E+00
5.25949E+00  5.50712E+00  5.56089E+00  5.56235E+00  5.56622E+00  6.23521E+00  6.47802E+00  6.50917E+00  6.87561E+00  6.99301E+00
7.42319E+00  7.66831E+00  7.70480E+00  7.87211E+00  7.90260E+00  8.01455E+00  8.06898E+00  8.27614E+00  8.55606E+00  8.78495E+00
.....

```

Case 9 Damaged state structure, X-brace 86 Young's modulus reduction $E=0.1E_0$

```

.....
EIGENVALUE ANALYSIS AT TIME (S): 0.00000E+00
.....

EIGENFREQUENCIES [Hz] (using SAM::SPRLAN) :

EIGFREQ 1    EIGFREQ 2    EIGFREQ 3    EIGFREQ 4    EIGFREQ 5    EIGFREQ 6    EIGFREQ 7    EIGFREQ 8    EIGFREQ 9    EIGFREQ10
3.11120E-01  3.12294E-01  6.21988E-01  6.52824E-01  6.65366E-01  7.15963E-01  1.06527E+00  1.06995E+00  1.14640E+00  1.18864E+00
1.60804E+00  1.86634E+00  1.94368E+00  2.57339E+00  2.86763E+00  3.36948E+00  3.49165E+00  3.55410E+00  3.91334E+00  4.02448E+00
4.18351E+00  4.46677E+00  4.47583E+00  4.63885E+00  4.66146E+00  4.69396E+00  4.74549E+00  4.92691E+00  5.06435E+00  5.21239E+00
5.25908E+00  5.50047E+00  5.56089E+00  5.56216E+00  5.56618E+00  6.23180E+00  6.47687E+00  6.50036E+00  6.61488E+00  6.99294E+00
7.34460E+00  7.47670E+00  7.69331E+00  7.84349E+00  7.90125E+00  8.01376E+00  8.05780E+00  8.08435E+00  8.55168E+00  8.76553E+00
.....

```

Case 10 Damaged state structure, X-brace 86 Free-joint insertion

```

.....
EIGENVALUE ANALYSIS AT TIME (S): 0.00000E+00
.....

EIGENFREQUENCIES [Hz] (using SAM::SPRLAN) :

EIGFREQ 1    EIGFREQ 2    EIGFREQ 3    EIGFREQ 4    EIGFREQ 5    EIGFREQ 6    EIGFREQ 7    EIGFREQ 8    EIGFREQ 9    EIGFREQ10
3.11115E-01  3.12225E-01  6.21109E-01  6.52744E-01  6.65330E-01  7.15964E-01  1.06509E+00  1.06882E+00  1.13437E+00  1.18870E+00
1.60144E+00  1.86575E+00  1.94362E+00  2.54782E+00  2.86741E+00  3.36747E+00  3.49031E+00  3.55129E+00  3.90291E+00  4.02446E+00
4.14207E+00  4.46234E+00  4.47031E+00  4.54724E+00  4.63998E+00  4.69011E+00  4.74545E+00  4.92350E+00  5.01711E+00  5.21236E+00
5.25858E+00  5.48682E+00  5.56088E+00  5.56178E+00  5.56610E+00  6.14842E+00  6.24801E+00  6.45733E+00  6.48336E+00  6.78638E+00
6.99292E+00  7.33925E+00  7.67989E+00  7.76895E+00  7.89843E+00  7.93899E+00  8.01503E+00  8.07032E+00  8.54982E+00  8.74158E+00
.....

```